Habitat Complexity and Functional Ecology of Shallow Glass Sponge Reefs in Howe Sound, British Columbia

by

Nikita Sergeenko

A thesis submitted in partial fulfillment of the requirements for the degree of

Master of Science

Department of Biological Sciences
University of Alberta

Abstract

The habitat complexity of an aquatic ecosystem plays an important role in niche partitioning and mediating the coexistence of numerous species within a given space. Studying the habitat complexity of glass sponge reefs along the British Columbia (BC) coast provides insight into how and why ecologically and commercially valuable species interact with the reefs. A first step is to establish a set of easily reproducible and accurate protocols for measuring the 3D habitat complexity of the reefs that can subsequently be related to the functional traits of the inhabiting community to determine which aspects of the physical complexity are important to the community. This thesis examines first methodology for quantifying structural complexity and second how structural complexity of sponge reefs influences community (species and traits) composition. The studies took place on several glass sponge reefs in Howe Sound, British Columbia.

Chapter 2 of this thesis evaluates the repeatability and reproducibility of two underwater techniques to measure structural complexity, 3D structure-from-motion (SfM) photogrammetry and microtopographic laser scanning (MiLS). The measurement error of both techniques was compared from SCUBA diver surveys of three reef plots on the Inshore (Western) East Defence Islands glass sponge reef, in Howe Sound, BC. The measurement error for both techniques was inconsistent across the three plots and was positively correlated with the habitat complexity metrics rugosity and the ratio of surface area-to-planar area (SAPA). While the coefficient of variation was lower for the metrics derived from 3D photogrammetry, the technique was not necessarily better than MiLS since both were inconsistent in measuring the physical complexity of a static reef plot over different days. These inconsistencies were likely due to the varying ambient light and turbidity conditions of the water, which affected the noise-to-signal ratio in images from which the 3D models (3D photogrammetry) and the 2D height profiles (MiLS) were constructed. Nonetheless, 3D photogrammetry had an advantage over MiLS in that it could

disseminate and measure more 3D habitat complexity metrics than MiLS could for the same survey effort.

Chapter 3 investigates the relationships between 3D habitat complexity metrics and the functional diversity and community composition of three reefs in Howe Sound, BC. Using a functional traits approach over the traditional biodiversity approach provides insight into which dietary and habitat use traits were linked to 3D complexity metrics for the reefs and enabled the development of hypotheses about the functional role habitat complexity plays in glass sponge reefs. Fifteen sites over three reefs were surveyed using the 3D photogrammetric technique outlined in Chapter 2, and species in the reef sites were counted by divers. The traits analyzed consisted of diet and position in the reef, both of which reflect the importance of trophic interactions in sustaining the productivity of an ecosystem and where those important trophic interactions occur. Surprisingly, functional diversity had a negative relationship with the structural metrics SAPA, relief, slope and curvature. This trend was driven primarily by the invertebrate community, due to the much higher abundances of invertebrate species relative to those of fish species. When individual traits were analyzed, abundance of benthic detritivores was driven by SAPA, while the presence of benthopelagic predators was driven by slope. This analysis provided insight about which structural components of the reefs influence individual traits and how reef structural complexity influences the functional community that inhabits within and over reef patches.

Preface

Chapter 2 will be submitted as a coauthored publication with Sally P. Leys (SPL; University of Alberta) and Jessica A. Schultz (JAS; formerly Ocean Wise). SPL and I designed the project's direction and analysis. JAS and I developed the survey protocols and collected the relevant data. I conducted the statistical analyses. SPL, JAS, and I contributed to the writing of the manuscript.

Chapter 3 is collaborative work involving SPL and JAS. SPL, JAS, and I designed the project's direction and analysis. JAS and I developed the survey protocols and collected the relevant data. I conducted the statistical analyses. SPL and I contributed to the writing of the manuscript.

Acknowledgments

I would like to thank my supervisor Sally Leys who agreed to take me under her wing three years ago. Without her guidance and support, this project would not have developed to fruition. As the representative for Ocean Wise and the Vancouver Aquarium, Jessica Schultz was instrumental in providing the inspiration for this research project as well as securing the necessary funding. I cannot thank both Sally and Jessica enough. I would also like to thank professors Stephanie Green and Rolf Vinebrooke for their role as my thesis committee. Their expert advice and guidance provided additional depth to this project. I really appreciated their questions, along with those from my arm's length examiner professor Viktoria Wagner, at my thesis defense as they really helped highlight the important implications of my research for the protection and long – term monitoring of glass sponge reefs.

Table of Contents

List of Tables

List of Figures

Glossary of Terms

Hexactinellida

A class of sponges, within the phylum Porifera, whose siliceous skeletons arise from six rayed spicules.

Habitat Complexity

The size, diversity, abundance, and distribution of habitat forming structures.

Structure from Motion (SfM) Photogrammetry

A range imaging technique used to estimate the structure of 3D objects from overlapping 2D images.

Repeatability

The variation of repeat measurements made under the same conditions.

Measurement Error (ME)

The random and systematic error that affects the absolute measurement, estimated in this thesis by the standard deviation (SD).

Microtopographic Laser Scanning (MiLS)

A laser imaging technique used to estimate the height variation of objects along a single plane.

Fractal Dimension

An index that characterizes the degree of complexity of an outline of an object as a function of the scale (resolution) of the straight line tangents which outline that object.

Surface Area to Planar Area (SAPA) Ratio

An estimate of surface heterogeneity, also known as surface complexity, across an area and which is equal to the surface area divided by the planar area.

Rugosity Ratio

An estimate of surface heterogeneity along a single plane and is equal to the profile length divided by the planar length.

Digital Elevation Map (DEM)

A digital 3D representation of a terrain's surface, commonly used in GIS as the basis for digitally produced relief maps.

Ground Control Point (GCP)

An object fixed to the ground/terrain with known geo-spatial reference coordinates.

Chapter 1. The Habitat and Ecosystem Roles of Glass Sponge Reefs in British Columbia

Sponges (phylum Porifera) are a diverse group of sessile aquatic animals that inhabit most marine and many freshwater habitats (Van Soest et al. 2012). As filter feeders, sponges draw environmental water through their perforated outer epithelium into a network of fine incurrent canals that terminate at flagellated chambers where gas exchange and feeding occurs (Leys and Hill 2012). Waste water is expelled from the chambers through excurrent canals into a central hollow atrium that opens to the environment at the osculum. Consequently, sponges have the ability to impact their surrounding water characteristics through bentho - pelagic coupling (Bell 2008). Additionally, sponges can alter their benthic environment, through bio - erosion (González-Rivero et al. 2013) as well as mineral deposition (Gutt, Boehmer, and Dimmler 2013; Bett and Rice 1992). Lastly, sponges can play an important role in mediating community structure through symbiosis (Sacristán-Soriano, Turon, and Hill 2020; Konstantinou et al. 2020), trophic interactions (Fitt 2020; Chu and Leys 2012; Yahel, Eerkes-Medrano, and Leys 2006), and habitat provision (Barthel 1992; Beaulieu 2001b; Beaulieu 2001a), the last of which is the focus of this thesis.

1.1. Glass Sponge Reef Discovery and Formation

Based on molecular evidence, sponges are believed to have evolved from the common ancestor to all other metazoans, making the group one of the oldest extant metazoan clades (Botting and Muir 2018; Telford, Moroz, and Halanych 2016; Wörheide et al. 2012). Their ecosystem role as habitat engineers has been well documented in the fossil record (Tian and Wang 2020; Bonuso, Stone, and Williamson 2020; Narbonne and Dixon 1984; Neuweiler, Mehdi, and Wilmsen 2001). Glass sponges (Hexactinellida), one of the four Porifera classes, characterized by their siliceous skeletons, formed prominent marine structures that discontinuously covered over 7000 km of seafloor along the Tethys Sea margin in the Late Jurassic period (Krautter et al. 2001). However, after the Cretaceous period, they disappeared from the fossil record, which led to the belief of their extinction, until their modern analogues were discovered in the late 1980s off of the central British Columbia (BC) coast of Canada (Conway et al. 1991). To date, while glass sponges are ubiquitous members of the deep-sea benthos, hexactinellid reefs as bioherms are only found in BC and Alaska coastal and shelf waters which makes these habitats globally unique (Krautter et al. 2001; Conway et al. 2001; Conway, Barrie, and Krautter 2005; Stone et al. 2014).

In addition to their unique siliceous skeletons, glass sponges are also characterized by their unique tissue composition (Leys, Mackie, and Reiswig 2007). Early embryonic cells fuse to form multinucleated strands of syncytial tissue that extends throughout the entire adult body; these strands form the trabecular reticulum which encompasses the flagellated chambers and houses the cytoplasm as well as the nuclei (Leys, Cheung, and Boury-Esnault 2006). The lack of borders between cells facilitates the conduction of electrical impulses throughout the body (Leys, Mackie, and Meech 1999; Leys and Meech 2006; Leys and Mackie 1997).

Skeletons are formed by the deposition of silicon dioxide within the sponge into unique six-rayed cubic spicules (Leys, Mackie, and Reiswig 2007). Spicules are either loosely held together by the trabecular reticulum (e.g., lyssacine hexactinellids), or fused by secondary deposition of silica to form a rigid scaffold (e.g., dictyonine hexactinellids), the latter of which are responsible for the formation of large extant reefs.

Modern glass sponge reefs are known to be formed by only three hexactinellid species: *Aphrocallistes vastus* (Schulze 1886), *Heterochone Calyx* (Schulze 1886), and *Farrea Occa* (Bowerbank 1862), whose siliceous skeletons are made of fused spicules and form a 3D scaffold that remains intact long after the animals die (Krautter, Conway, and Barrie 2006). Large quantities of dead skeletons baffle bottom currents, forcing suspended sediments to settle and burry the scaffolds. The rigid framework of scaffolds, cemented by sediments, forms the foundational substrate for larval settlement and growth. The subsequent successional layer-upon-layer of generational growth can form reefs in the form of mounds, biostromes (sheets) or ridges (Fig 1.1.). In Queen Charlotte Sound and Hecate Strait, where the reefs were first discovered, hexactinellid reefs discontinuously cover over 700 km^2 of seafloor and form mounds up to 21 m thick at depths between 150 – 250 m (Conway, Barrie, and Krautter 2005; Fig 1.2.). While the bulk of the reefs is buried under sediment, the top portions support a thriving 1 – 2 m tall reef-building sponge community that in turn supports a diverse megafaunal community. The modern reefs are estimated to be 12,000 years old with an annual growth rate of 3 - 9 cm (Krautter et al. 2001).

Since the initial discovery, subsequent exploration and mapping of the sea floor revealed eight smaller reefs in the Strait of Georgia at depths of 60 to 200 m (Krautter, Conway, and Barrie 2006; Dunham, Mossman, et al. 2018, DFO 2020b). Additionally, since 2011, a citizen science initiative in Howe Sound, a deep-water fjord adjacent to Vancouver, led to the discovery of eleven reefs between 24 and 96 m, the shallowest known to date (Clayton and Dennison 2017). Seven of the Howe Sound reefs: Dorman Point, Halkett Point, East Defence Islands, Lost Reef, Christie Islet, and Passage Island SW are all within air-gas depth limits for self- contained

underwater breathing apparatus (SCUBA) diving (DFO 2018; Dunham, Mossman, et al. 2018; Fig 1.3.). These reefs present a unique opportunity to advance our knowledge of glass sponge biology without the logistical and financial constraints associated with the use of autonomous, remotely operated or human occupied submersibles that are commonly used for deep-sea research.

1.2. Oceanographic Conditions

As sessile organisms, glass sponges rely on the stability of their environment for survival and growth. The confinement of glass sponge reefs to shelf waters of the BC coast has caused researchers to ask what environmental conditions drive reef distribution. Leys et al. (2004) first examined the vertical distribution of reef building sponges in the BC fjords and correlated it to nutrient concentrations and water chemistry. They found the highest sponge abundances between 20 and 260 m at sills with high silicate concentrations, low sediment loads, low ambient light levels, and low temperatures (9 – 10 °C). Conversely, low abundances were observed in parts of fjords with low oxygen conditions (< 2 mL L^{-1}).

In Hecate Strait and Queen Charlotte Sound, reefs are found on glacial till in canyons and troughs left behind by scouring icebergs during the Holocene (Conway et al. 2001; Conway, Barrie, and Krautter 2005). Conversely, reef building sponges do not grow on soft sediments. Furthermore, Whitney et al. (2005) determined that summer upwelling brings nutrient-rich water onto the continental shelf, from where it is funneled into the canyons that harbor the reefs. Bottom waters around sponge reefs contained 43 – 75 mM of silicates, 64 – 152 mM dissolved oxygen, and had temperatures of 5.5 – 7.3 °C. The canyons harboring the sponge reefs provided a means of concentrating particulate material that the sponges could use to enrich their habitat. Detrital rain also supplied particulates to the canyons. High tidal flow (25 cm s^{-1}) flushes sediments out of the canyons and carries waste products away from the sponges.

High sediment load has been identified as one of the stressors of reef-building sponges. The first experimental evidence of sediment smothering came from a study by Tompkins-McDonald and Leys (2008) who showed that sponge filtration (pumping) arrested in response to high concentrations (10 – 1,000 ml of 0.5 – 1 g L^{-1}) of fine (< 25 μm) sediment. This was further supported by in-situ experimental exposure of reef - building sponges to high suspended sediment loads in the Strait of Georgia, a marginal sea between Vancouver Island and the BC mainland (Grant et al. 2018; Grant et al. 2019). Grant et al. (2018) determined that 10 – 80 mg L^{-1} of suspended sediment concentrations (SSC) caused single arrests lasting several minutes in *Aphrocallistes vastus*. Ambient SSCs around the reefs in the Strait of Georgia were measured at

4.4 mg L^{-1}. Grant et al. (2019) also found a reduction in feeding currents in *Heterochone calyx* on the Hecate Strait reefs lasting several minutes after arrest in response to lower SSCs (5 - 10 mg L^{-1}). These coughing arrests showed a distinctive on/off pattern as sponge filtration returned to normal excurrent velocities after 30 - 60 minutes. Ambient SSCs were lower in the Hecate Strait (2.71 ± 0.09 mg L^{-1}, mean ± SD). While ambient SSCs are generally lower than the arrest thresholds, the implications of these arrests are that sediment disturbance to sponge filtration can occur from bottom-contact fishing gear. Modelling suggested that sponges would arrest their pumping up to 2.39 km from the source of the sediment plume (Grant et al. 2019).

1.3. Anthropogenic Stressors

In addition to the inadvertent sediment disturbance caused by bottom-contact fishing activities, reef-building glass sponges are susceptible to a suite of anthropogenic stressors. Unfortunately, humans have affected these reefs (knowingly or unknowingly) even before they were discovered. Mechanical damage from fishing gear was reported as early as the reefs' discovery (Krautter et al. 2001). Marks left by the trawl doors of bottom trawls were seen in side-scan sonar images and during multibeam bathymetry surveys as tracts kilometers long scouring the reef surface. Additionally, visual evidence of mechanical damage where whole portions of a reef were flattened by fishing gear were observed using submersibles, ROV's, and drop cameras (Clayton and Dennison 2017; Krautter et al. 2001). Unfortunately, recovery from mechanical damage in reef-building sponges rarely occurs and is followed by full body necrosis, however, the flattened reef rubble does provide new space for recruits to settle and grow on (Kahn et al. 2016). Settlement rates of recruits on dead reef-building sponges are highly variable.

1.4. Trophic Ecology

Reef - building sponges are efficient filter feeders and collectively (as reefs) filter vast volumes of water (Kahn et al 2015). Yahel, Eerkes-Medrano, and Leys (2006) found that reef - building sponges efficiently removed up to 99% of the most abundant bacterial cells, whereas clays, silt, and 'debris' particles were expelled into the excurrent water. The relatively scarce microbial cells were efficiently selected from a 'soup' of suspended clay and detritus particles. Filtration efficiencies were maximal for the relatively large and rare eukaryotic algae and for small non-photosynthetic bacteria. Intermediate sized non-photosynthetic bacteria characterized by higher nucleic acid content were efficiently removed in February when overall plankton concentration was low, but not in July. The intermediate sized photosynthetic

prokaryote *Synechococcus spp.* (1.1 to 1.5 µm) was also less preferred (Yahel et al. 2007). This evidence suggests that reef building sponges are selective feeders that can vary their feeding behavior seasonally. Removal of planktonic microorganisms (2.2 ± 1.3 µM C L^{-1} and 0.37 ± 0.17 µM N L^{-1}) accounted for the entire total organic C uptake and ammonium excretion. Despite the massive siliceous sponge skeleton, silica uptake was below detection levels (0.28 µM L^{-1}), supporting previous suggestions of low growth rates in glass sponges.

Kahn et al. (2015) also measured incurrent and excurrent nutrient concentrations and together with filtration rates, calculated the nutrient fluxes for all reefs in the Strait of Georgia, British Columbia. Sponges removed up to 90% of bacteria from the water and released ammonium. Because of the high density of sponges, high volumetric (oscula) flow rates, and the efficient extraction of bacteria, they calculated a grazing rate of $85 - 198$ m^3 m^{-2} d^{-1}. Consequently, reef-building sponges have the highest benthic grazing rate of any suspension-feeding community measured to date. However, reefs extract seven times more carbon than can be supported by vertical flux of total carbon alone and therefore require productive waters and steady currents to sustain their strong grazing. Reef building sponges have no microbial symbionts and remove little dissolved organic carbon. To determine how reef sponges therefore get enough food to sustain such substantial grazing Kahn, Chu, and Leys (2018) measured stable carbon and nitrogen isotope signatures of water, sediment and sponge tissues. Stable isotope analysis suggested that heterotrophic bacteria ingested by the sponges came from multiple trophic subsidies: from terrestrial and oceanic sources, and also potentially from sediment-borne bacteria resuspended by tidal currents.

1.5. Faunal Associations

Reef - building glass sponges have complex morphologies and their mittens and oscula can intertwine among individuals resulting in the formation of 3D mazes filled with channels, crevices, and tunnels for fauna to inhabit. Observations of reefs via human occupied and remotely operated submersibles, as well as diver observations of shallow reefs consistently reported high abundances and diversity of megafauna (Jamieson and Chew 2002; Krautter et al. 2001). Reef formations are not alone in attracting animals. Communities of reef-building sponges growing directly on bedrock, also known as sponge gardens, house high abundances of vertebrates and invertebrates (Jamieson and Chew 2002; Marliave et al. 2009). Both reefs and gardens house commercially valuable rockfishes (*Sebastes spp.*), Pacific cod (*Gadus macrocephalus*), Pacific halibut (*Hippoglossus stenolepis*), sea cucumbers (Holothuroidea), Pink shrimp (*Pandalus borealis*), Spot prawns (*Pandalus platyceros*), Dungeness crabs (*Cancer*

magister), along with a whole suite of other taxonomic groups, such as sea stars, tube worms, hydroids, cephalopods, and gastropods. The reefs also house non-reef-building sponges, including demosponges (Law et al. 2020) as well as a large suite of cryptic and micro-fauna (Guillas et al. 2019).

The first quantifiable measurements of species richness and abundances were reported in Cook, Conway, and Burd (2008) which was based on an MSc thesis by Cook (2005). Cook (2005) identified and counted species from ROV video footage of the reefs in Queen Charlotte Sound and related the counts to the physical appearance of the reefs. Cook (2005) observed higher taxonomic richness and abundances over reef patches with live, standing sponge bushes and lower richness and abundances over reef patches with dead and crumbled sponge bushes and even lower on flat off-reef patches. Cook's (2005) results suggested that the physical conditions and structural complexity of the sponge reefs played a role in driving faunal richness and abundance.

Subsequent studies that examined reef communities also related the species richness and/or abundances to an aspect of the reef's physical structure. For instance, Chu and Leys (2010) used a more quantitative approach by mapping the distribution of glass sponges on three reefs in the Strait of Georgia and relating the density of sponges to animal abundances. In general, more animals were found on reef areas with live sponges that had high oscula densities than those reef areas that were flat or had low oscula densities. In the case of Chu and Leys (2010), oscula density was a proxy for sponge density as it is hard to distinguish sponge individuals within dense sponge bushes.

Law (2018) quantified the area of reef patches occupied by live sponge bushes and related it to faunal abundances and biodiversity. While a positive relationship was observed between abundance and live reef area, there was no clear relationship between live reef area and biodiversity (Shannon-Winer index). Dunham, Archer, et al. (2018) also found no significant relationship between megafaunal biodiversity and reef substrate cover (i.e. live reef area, dead reef area, or flat reef), across all known reefs along the BC coast. Again, higher animal abundances and in some cases higher species richness were observed over reef patches with dense live sponge growth relative to flat areas or areas with dead sponge rubble; however, the effect of reef structure on biodiversity was inconclusive.

In general, there is a lack of consensus among the previously mentioned studies on the effect of reef structure on biodiversity. It is clear that biodiversity is higher over glass sponge reefs relative to the surrounding seascape (Dunham, Mossman, et al. 2018), however, it is unclear whether biodiversity is uniform within reefs. Part of the issue is that the studies that

investigated community – habitat associations within the reefs each used a slightly different technique to quantify the reef structure. Additionally, some studies related the overall reef structure to the epifaunal biodiversity at the whole - reef scale (Dunham, Archer, et al. 2018) while others related the reef structure at the reef - patch scale (Cook 2015; Law 2018). In both cases, no statistically significant relationships were observed between reef structure and biodiversity. Lastly, some studies did not report biodiversity and instead related reef structure only to animal abundances (Cook, Conway, and Burd 2008; Chu and Leys 2010).

1.6. Reef Habitat Complexity

Habitat complexity, defined as the size, diversity, abundance, and distribution of habitat forming structures, plays an important ecological role in many aquatic and marine ecosystems (Tokeshi and Arakaki 2012). Complex structures introduce spatial heterogeneity which in turn mediates habitat partitioning and allows for the coexistence of multiple species in a relatively small area (McNeely et al. 2001; Bell, McCoy, and Mushinsky 1991). This concept has been derived from the terrestrial setting in studies of forest bird biodiversity (MacArthur and MacArthur 1961). Marine species may use structures for refuge against predators or strong currents, for reproduction, and/or for enhanced productivity (Sueiro, Bortolus, and Schwindt 2011). Habitat complexity has been shown to affect post-settlement mortality and recruitment dynamics (Johnson 2007), mediate resource availability (Smith, Johnston, and Clark 2014), and structure fish assemblages in both tropical and temperate environments (Devine et al. 2020; Ferrari et al. 2018; Bracewell, Clark, and Johnston 2018; Kostylev et al. 2005; Gratwicke and Speight 2005). Habitat complexity has also been linked to fish behavioral patterns in some freshwater ecosystems (Shumway, Hofmann, and Dobberfuhl 2007). While the definition and consequently the measure of habitat complexity varies slightly from study to study (Carvalho and Barros 2017), generally, we can assume that an increase in habitat complexity is related to an increase in the structural (along the third dimension perpendicular to the benthos) and spatial (across the 2D benthos) heterogeneity of the physical habitat for a well-defined spatial scale. As such, it is not only important to define the spatial scale over which habitat complexity is measured, since it can vary at different spatial scales in the same ecosystem, but is also important to define the metric or set of metrics that are to be used to measure habitat complexity in a given study.

The previously mentioned glass sponge reef studies on megafaunal associations all used slightly different metrics of habitat complexity over different spatial scales. For example, Cook's (2005) approach was qualitative and reef patches were assigned complexity measure of high,

medium, or low based on the shape, size, and condition of sponges. Chu and Leys (2010) modelled sponge densities as a metric of habitat complexity and reported complexity at the reef level. Law (2018) and Dunham, Archer, et al. (2018) both used a similar approach for quantifying habitat complexity by measuring the live/dead reef area but reported their analyses at a different spatial scale. Law (2018) related complexity at the reef patch level to animal biodiversity and abundances whereas Dunham, Archer, et al. (2018) related complexity at the whole reef level.

In the last decade, new advances in underwater imaging technologies have allowed fine scale 3D modelling to be used to study reef habitat complexity. Structure-from-Motion (SfM) photogrammetry calculates the relative position and orientation of objects that appear in overlapping 2D photographs in 3D space (Micheletti, Chandler, and Lane 2013). The concept has been around for several decades and has been applied extensively in the geosciences via aerial photography (Granshaw 2018). However, the development of relatively inexpensive 3D modelling software, most notably Agisoft's Photoscan and Metashape applications (Agisoft LLC), as well as improved capture quality and optics of digital underwater cameras over the last decade, has enabled aquatic researchers who are not remote sensing experts to apply SfM photogrammetry with relative ease to their study environments. Essentially, researchers do not have to rely on expensive sonar mapping technology that provides up to 15 – 20 cm resolution (Pailhas, Petillot, and Capus 2010) when they can use SfM workflows to generate 3D models with < 1 cm spatial resolution (Lochhead and Hedley 2020).

The increased application of 3D modelling to underwater studies has allowed researchers to expand the scope of habitat complexity metrics that can be used to disentangle the drivers of community structure. For instance, Burns et al. (2015) characterized the physical structure of coral reefs using 3D metrics such as curvature, slope, and surface complexity (surface area of habitat forming structures). Others have related 3D structural metrics to kelp micro-faunal community composition (Orland et al. 2016) and have characterized macrofaunal community structures based on 3D surface complexity on deep-water coral reefs (Price et al. 2019; Prado et al. 2019). 3D photogrammetry has also been evaluated for repeat measurements on tropical coral reefs (Bryson et al. 2017) to determine its viability as a tool for monitoring changes in coral reef environments (Fukunaga et al. 2019). However, because of its newness, this technique has not yet been used to study the effects of varying 3D structural complexities of glass sponge reef patches on the megafaunal community composition.

1.7. Thesis Objectives and Rationale

The objectives of this thesis are two-fold: my first aim is to evaluate the effectiveness of using 3D photogrammetry to study glass sponge reef structure; the second is to determine which 3D reef structural characteristics correlate best with overall functional diversity and with individual dietary and habitat-use functional traits of the reefs communities.

Since 3D photogrammetry has never been used to quantify glass sponge reef structure, it is important to determine the accuracy (measured as error) of 3D models of glass sponge reef patches. While previous work has determined the measurement error of 3D models of coral reef patches (Bryson et al. 2017), that error cannot be applied to 3D models of glass sponge reefs since the sponge reefs are in cold temperate waters that typically contain high suspended sediment and organic particle loads which increase the turbidity of the water. Consequently, light attenuation is much higher in temperate waters which is further exacerbated by the relatively deep habitat of glass sponge reefs. Therefore, SfM photogrammetry in such environments must rely on the use of strobe lights which are more likely than not, affixed to the camera and consequently alter the contrast and shadows over the reef as the camera moves around to collect images. In a first study of this kind, Lochhead and Hedley (2020) characterized the measurement error of 3D models of glass sponges over a single small sponge individual, not over a reef patch. Their strobe lights were fixed around the sponge to eliminate the effects of moving shadows, an approach that would not be feasible over reef patches greater than a single sponge.

To determine whether 3D photogrammetry could be used as an effective tool for quantifying glass sponge reef habitat complexity, in Chapter 2 I evaluate the measurement error of 3D photogrammetry, its repeatability over time, and the sampling effort involved. This presented an opportunity to compare the efficacy of 3D photogrammetry with another remote sensing technique called microtopographic laser scanning (Du Preez and Tunnicliffe 2012) that has been previously used to measure the height variations of sponge bushes, but which has not yet been evaluated for measurement error in situ. Due to the laser's high accuracy and indifference to varying light conditions, I hypothesized that 3D photogrammetry would have a higher measurement error than microtopographic laser scanning (MiLS).

3D photogrammetry can quantify a whole suite of structural complexity metrics whose effects have not been investigated on the megafaunal community composition of reefs. It has been established that greater 'complexity', as measured by sponge density and percent live cover of the seafloor, drives species abundance, but these relationships have been reported as correlative and not causative effects. We do not know whether sponge density or percent cover

of the seafloor increases the sponge surface area, in turn providing more space for animals to live in/on. Additionally, the effect of habitat complexity on biodiversity was inconclusive in previous studies.

By using a functional traits approach, a different view of community complexity is gained which hints at the function of 3D structure in driving community composition. To determine which 3D habitat structural metrics were best correlated with the functional community composition, in Chapter 3 I characterize the functional communities of fifteen reef patches over 3 reefs in Howe Sound, British Columbia (BC). Using a functional traits approach rather than a classic biodiversity approach could provide insight into how the animals interact with their environment through habitat-use and resource partitioning. I hypothesized that functional diversity, measured by Rao's Q (Rao 1982), would increase with habitat complexity and this increase would be driven by structural metrics that directly increase the surface area of sponges for animals to live in/on. In particular, animals that would use the glass sponges as refuge, such as small invertebrates, would be numerous on complex reef patches and would in turn attract larger predators to feed on the small invertebrates.

Currently, widely accepted monitoring frameworks do not exist for the Hecate Strait – Queen Charlotte Sound glass sponge reef MPA or for the smaller protected reefs in the Strait of Georgia and Howe Sound. Previous studies have recommended tracking the percentage of area covered by live/dead sponges or the abundances of indicator species from ROV footage to monitor reef status (Dunham, Mossman, et al. 2018; Loh, Archer, and Dunham 2019). However, consistently deploying ROVs on all the known reefs would be financially costly. Additionally, the relationship between a glass sponge's 2D footprint and its overall 3D structure (including height and volume) is highly variable (Leys and Lauzon 1998), therefore tracking the percent cover of sponge on a reef is not a good indicator of the reef's overall habitat complexity. Lastly, the indicator species identified in previous studies (Dunham, Mossman, et al. 2018; Loh, Archer, and Dunham 2019) have positive relationships with sponge cover. However, the underlying mechanisms behind the interactions are not well understood. This thesis provides an alternative solution for monitoring glass sponge reefs. First, all of the data was collected by paid and volunteer SCUBA divers. SCUBA diving on the shallower glass sponge reefs provides a unique opportunity for researchers and citizen scientists to observe a reef's status first hand and to collect valuable data with high precision at high temporal and spatial resolutions, as is a common practice on many of the world's coral reefs (ReefLifeSurvey 2021; Gerovasileiou et al. 2016; Earp and Liconti 2020). Lessons learned in both parts of this thesis can help design and implement a SCUBA diver - based monitoring framework. Second, divers and ROV operators

can follow the protocols in Chapter 2 to measure a glass sponge reef's 3D structure over time with the reported level of certainty. Third, by using a functional traits approach, Chapter 3 provides insight into the relative importance of a reef's structural components to different animals and the interactions between the various functional traits. By monitoring the type and abundance of functional traits in addition to species, we can gain a better understanding of reef resilience and begin to predict the potential impacts of various disturbances on reef communities.
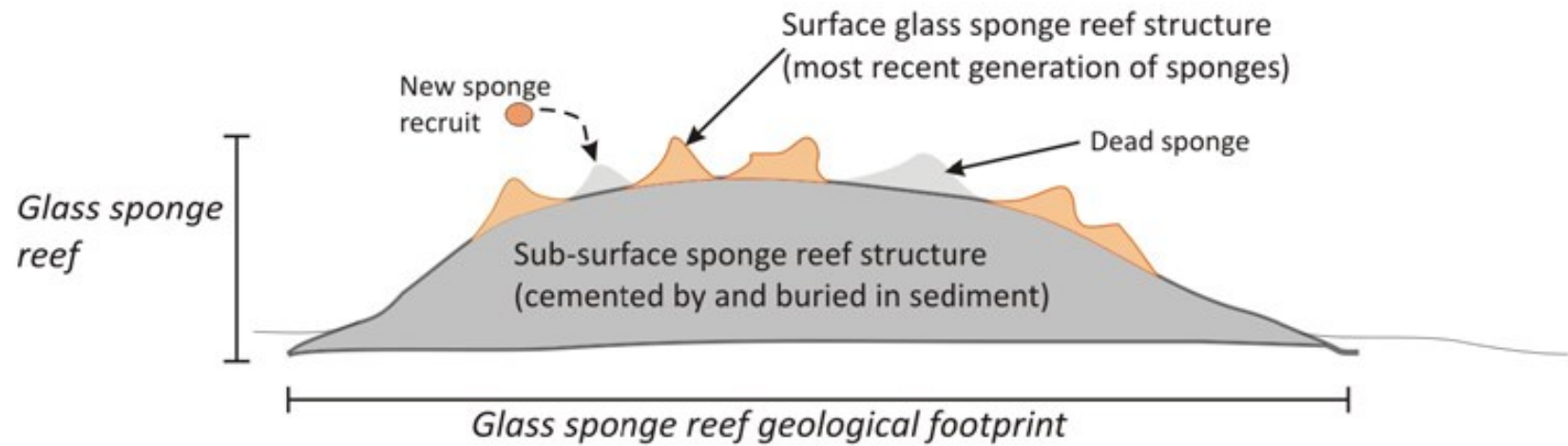
Figure 1.1. Glass Sponge Reef Schematic. Glass sponge reefs are formed when reef – building sponge aggregations die and get buried by sediment, creating a structural foundation (in grey) for new recruits (orange) to settle on. Eventually, the new recruits grow into a 1 – 2 m tall sponge community (in orange; not to scale) if conditions are favorable. Reproduced from DFO (2018, Fig 1).
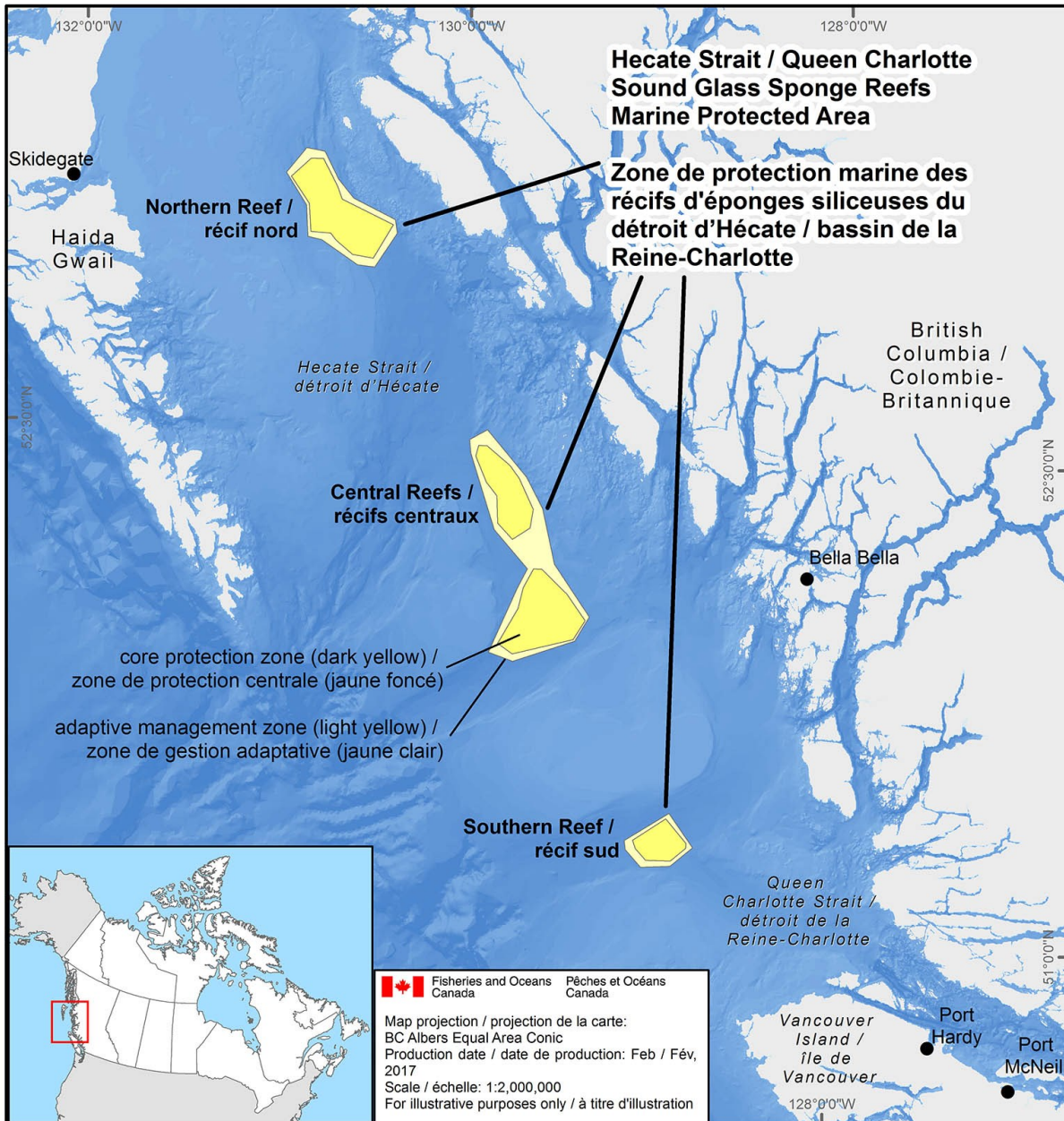
Figure 1.2. Location of the Central British Columbia Coast Reefs. The first extant glass sponge reefs were discovered in the Hecate Strait and Queen Charlotte Sound. The dark yellow polygons outline the glass sponge reefs' footprints within the current Hecate Strait and Queen Charlotte Sound glass sponge reef MPA (outlined in light yellow). Reproduced from DFO (2020a).
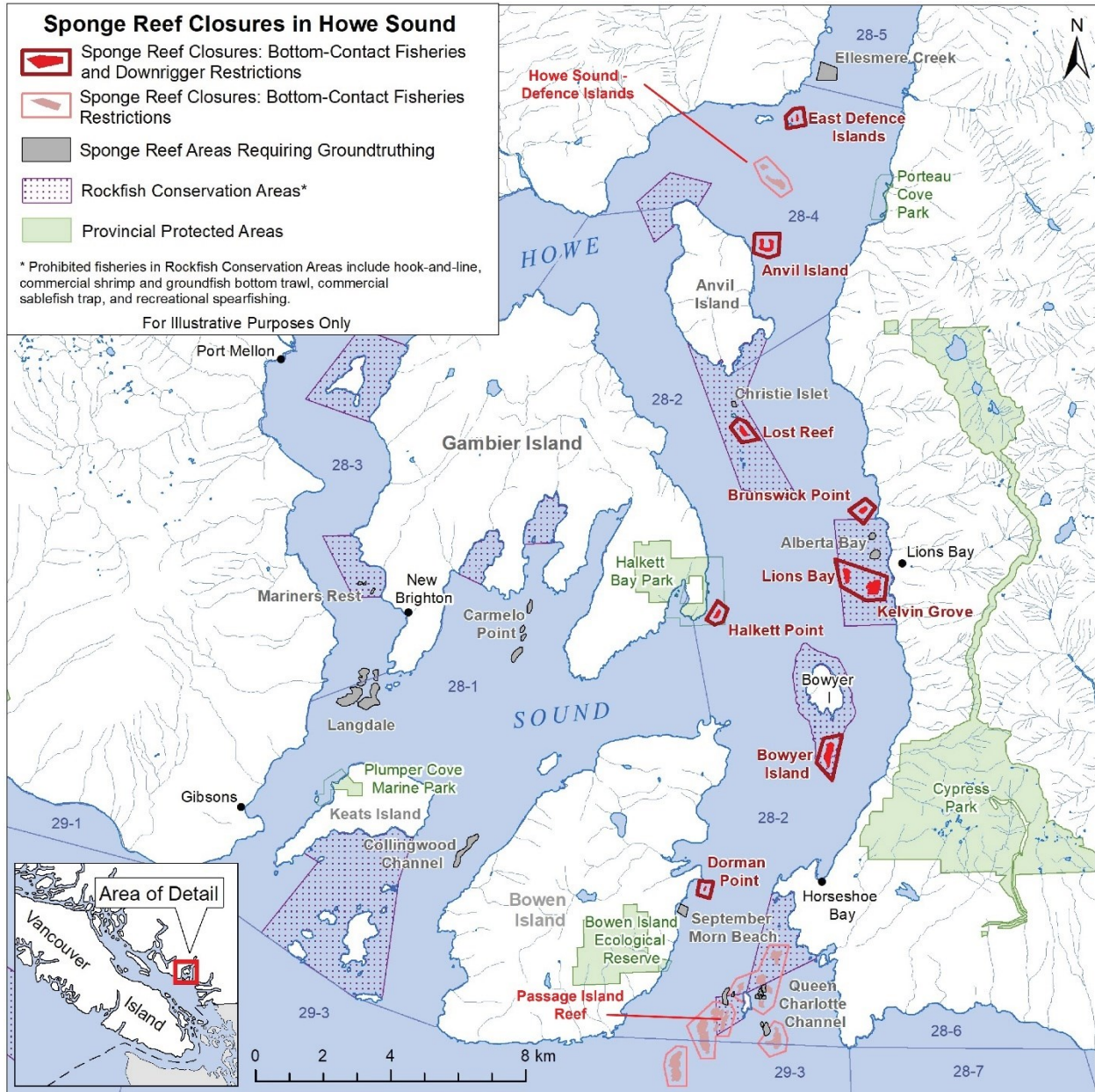
Figure 1.3. Glass Sponge Reefs in Howe Sound. The locations of all the ground truthed (red) and suspected (grey) glass sponge reefs in Howe Sound, British Columbia. Solid light and dark red polygons outline the ground truthed glass sponge reefs' footprints within the protected areas (outlined by red lines). Seven of the reefs: Dorman Point, Halkett Point, East Defence Islands Inshore and Offshore, Lost, Christie Islet, and Passage Island reefs are all within air-gas depth limits for self- contained underwater breathing apparatus (SCUBA) diving. The Passage Island reef is located within the Howe Sound – Queen Charlotte Channel Reef Complex. Adapted from DFO (2020b).

Chapter 2.   Comparing 3D Photogrammetry and Microtopographic Laser Scanning for Quantifying the Habitat Complexity of Glass Sponge Reefs

2.1. Introduction

Glass sponges (Hexactinellida) form large, biogenic reefs, found only in the Northeast Pacific, that discontinuously cover hundreds of square kilometers of seafloor on the continental shelf and in fjords of British Columbia (BC), Canada (Conway et al. 1991; Krautter et al. 2001; Conway, Barrie, and Krautter 2005; Dunham, Archer, et al. 2018). The reefs are formed by three species whose siliceous skeletons form a rigid and complex three-dimensional framework that can provide habitat for a plethora of epifauna (Cook, Conway, and Burd 2008; Chu and Leys 2010). Like coral reefs, sponge reefs have been found to support a higher biodiversity and species richness than their surrounding seascape (Dunham, Archer, et al. 2018; Dunham, Mossman, et al. 2018; Moberg and Folke 1999; Law et al. 2020; Guillas et al. 2019). Because of their role in providing habitat, especially for different life stages (Marliave et al. 2009), a large number of the reefs are now protected, some as Marine Protected Areas (Government of Canada 2017) and others with fisheries closures (DFO 2020b). However, currently there is no standardized method for monitoring glass sponge reef status over time.

The northern reefs are difficult and costly to reach because of their remoteness on the northern British Columbia coast. In contrast glass sponge reefs in the Strait of Georgia and Howe Sound are close to ports for ready access by remotely operated vehicle (ROV), and some are even within reach by SCUBA diving. Recent work has established a baseline condition for many reefs and has identified indicator species that are associated with different reef structures (Dunham, Mossman, et al. 2018; Dunham, Archer, et al. 2018; Loh, Archer, and Dunham 2019; DFO 2018). However, repeat surveys over the same sections of reef have not been carried out, and so the error of measuring habitat cover using 2D images collected from an ROV platform is unknown. Glass sponges grow slowly and previous work estimating change over time using 2D images was extremely challenging, with estimated errors of up to 10% for length measurements and up to 27% for estimates of volume (Austin et al. 2007; Leys and Lauzon 1998).

Habitat complexity is functionally important in marine ecosystems and has been shown to mediate trophic interactions, niche partitioning, inter-specific competition, recruitment and reproduction (Johnson 2007; Orland et al. 2016; Pygas, Ferrari, and Figueira 2020). A common measurement of habitat complexity over reef habitats is rugosity which is the measure of the reef's surface roughness, or small – scale variation in the amplitude of its height (Walbridge et

al. 2018). A higher rugosity value would indicate that a reef surface is more rough and consequently has more crevice shaped structures for animals to occupy (Beck 1998). Traditional techniques for measuring rugosity include the chain – and – tape method which places a chain directly onto the reef's surface along a transect (Walbridge et al. 2018). The length of the chain is then divided by the straight – line distance of that transect. However, this technique would be invasive on a glass sponge reef, since glass sponges are sensitive to mechanical stimuli (Leys, Mackie, and Meech 1999).

Instead, the straight line rugosity of a glass sponge reef can and has been measured using a remote sensing technique called microtopographic laser scanning (MiLS; Du Preez and Tunnicliffe 2012). MiLS involves collecting video footage of a reef along a transect using a camera – laser array. As long as the swim trajectory of the array is constant, the distance from the camera's lens to the reef's surface is calculated in each frame using scaling equations and Pythagorean theory and subsequently translated to a height above the bottom. Once the heights of the reef's surface along the transect are compiled, a 2D profile of the surface is generated from which a rugosity value can be calculated by dividing the profile's length by the transect length, similar to the chain – and – tape method. However, both MiLS and the chain – and – tape method capture the habitat complexity along a transect, essentially a slice of reef and this complexity may not be representative of the complexity of the whole reef's area.

In recent years, a growing number of studies have used underwater 3D structure-from-motion (SfM) photogrammetry to quantify benthic habitat complexity and estimate growth of habitat forming species (Olinger et al. 2019; Price et al. 2019; Gerdes et al. 2019; Ferrari et al. 2017; Burns et al. 2015). 3D photogrammetry has also been evaluated as a tool for monitoring MPAs and marine habitats (Bayley et al. 2019; Piazza et al. 2019; Marre et al. 2019; Fukunaga et al. 2019). While area cannot be used to quantify the amount of livable space for animals, 3D photogrammetry can capture the height variation of a reef patch from which estimates of biomass and volume can be made (House et al. 2018; Gutierrez-Heredia et al. 2016). 3D photogrammetry can also quantify and disentangle several metrics of a reef's habitat structural complexity, including the abundance, distribution, and vertical variation of habitat forming structures (Carvalho and Barros 2017; Tokeshi and Arakaki 2012; Burns et al. 2015; Fabri et al. 2019; Prado et al. 2019; Burns et al. 2016). Quantifying 3D habitat complexity on glass sponge reefs and identifying interactions with indicator species could improve estimates of reef status at high resolution and track metrics that capture more ecologically relevant information.

In this study, we evaluated the application of 3D SfM photogrammetry as a tool for monitoring changes in glass sponge reef habitat over time. We first evaluated the repeatability

and replicability (measurement error ME) of 3D SfM photogrammetry compared to measures of 2D rugosity using microtopographic laser scanning (MiLS; Du Preez and Tunnicliffe 2012) over different patches of a glass sponge reef and over time. We also evaluated the relative merits of each method in terms of 'survey effort' and ease of operation. Both techniques were assessed from a SCUBA diver platform due to the low cost of operation relative to an ROV platform and due to the potential of including citizen scientists in the long-term monitoring of glass sponge reefs, which has proven to be beneficial to the monitoring of other marine ecosystems world-wide (Freiwald et al. 2018; Ben Lamine et al. 2018; Raoult et al. 2016). Based on prior knowledge of the techniques, I hypothesized that each would have different measurement errors and survey efforts and predicted that MiLS would have consistent error over different reef patches and over time due to the precise nature of its laser and the fact that it would be easier to repeat the same swim path over the same transect multiple times. The error from 3D photogrammetry would be higher and inconsistent over different parts of a reef and over time. Additionally the effort to complete a 3D survey would be higher.

2.2. Materials and Methods

2.2.1. Study Location and Environmental Conditions

This study was carried out on the East Defence Islands glass sponge reef complex in Howe Sound, British Columbia (49°34.689' N, 123°16.343' W; Fig. 2.1. F). Howe Sound is an elongated fjord that is approximately 44 km long and 28 km wide with a maximum depth of 285 m. Water clarity varies considerably in this fjord due to freshwater discharge and high sediment loads from the Squamish River (Hickin 1989; Stronach et al. 1993), and plankton blooms which, while highly variable on a monthly basis, peak throughout the spring and summer months (Albright and McCrae 1987). Water temperature and turbidity decrease with depth following a pronounced thermocline at 10 -15 m, with 12 - 14 °C in the top 10 m to 6 – 8 °C below 20 m, and 10 – 15% transmissivity m^{-1} in the top 10 m to 50% transmissivity m^{-1} at depths below 20 m (Leys et al. 2004). The environmental conditions in Howe Sound result in relatively dark, turbid, and cold diving conditions compared to the environmental and diving conditions on tropical coral reefs (Table 2.1.).

The East Defence Islands reef complex (Fig. 2.1. E) consists of two ridge-shaped reefs that run parallel to each other approximately 100 m apart. The reefs cover 17,772 m^2 of seafloor (DFO 2018) and while most of the reef complex is in deep water, portions reach as shallow as 20 – 30 m (tide dependent). The western reef, also known as the inshore reef due to its closer

proximity to the Defence Islands (Marliave et al. 2009), has a 100 m - long stretch in the shallowest depths which can be reached using SCUBA.

2.2.2. Survey Design

We conducted 61 repeat surveys (Table 2.2.) of three square reef plots A, B, and C, each 3 m x 3 m wide, on the western (inshore) reef's apex (Fig. 2.1. D). All field work occurred in March and April of 2019. Weather and dive conditions varied among the five survey days (Table 2.1.). The best conditions for ambient light levels and water clarity occurred while surveying plots A and B (for the second survey day). Unfortunately, visibility was poorest during the surveys of plot C with high levels of suspended particles in the water column as well as high light attenuation at the surface which reduced light levels at the reef.

Dives were conducted from a 25 foot aluminum skiff owned and operated by Ocean Wise. Transit time was approximately 1 hour to and from the survey site by boat from the launch site in West Vancouver (Fig. 2.1. F). Upon arrival at the site, the boat anchored on sandy/silty bottom approximately 30 – 40 m southeast of plot B which provided a stable reference guide to and from the reef bottom, especially during heavy surface current conditions of up to 1 m s^{-1}. All survey dives were conducted in accordance with the Canadian Association for Underwater Science (CAUS) and the Ocean Wise SCUBA diving standards. As such, only air was used as the breathing gas during all dives. Additionally, divers strictly adhered to the bottom time limits outlined in the Defence and Civil Institute of Environmental Medicine (DCIEM) Canada dive tables. When working on the Western East Defence Islands reef at depths ranging from 20 m to 25 m, divers were only allowed to spend 20 minutes underwater on the first dive and 16 minutes on the consecutive dive following a 1.5 hour surface break. To minimize the decompression risks, divers were only allowed to perform two dives per day and each dive team was required to have a safety, standby diver on the boat separate to the boat captain. To maximize the total bottom time spent surveying the reef on each day, we used two dives teams on each survey day. The two teams with two divers each staggered dives such that one carried out SfM surveys while the other collected MiLS video.

Considering the logistical constraints and the large amount of human resources that were needed to conduct all the desired repeat surveys, we limited the number of sites we surveyed to three sites. However, the sites were carefully chosen based on their qualitative habitat complexity. We wanted the sites to be structurally different from each other but collectively represent the range of habitat complexities observed on Western East Defence Islands reef. This helped us test whether ME was consistent over different parts of the reef. To determine whether ME was consistent over time, we surveyed one of the plots over three

separate days. We did not survey the plot over more days nor did we survey the other two plots over multiple days due to the limited availability of human resources.

Sites were marked by inserting PVC poles into dead reef substrate, avoiding live or dead standing glass sponges. We chose a spatial scale of 3 m x 3 m for the reef plots because we were interested in measuring the structural heterogeneity at the reef patch level, not at the individual sponge scale. Since reef – building sponges can grow to a maximum of 1 m wide and 2 m tall, we wanted to ensure that we captured the reef heterogeneity which resulted from the cumulative 3D growth of several sponge individuals. We decided not to survey anything larger than a 3 m x 3 m wide reef area due to the same logistical restrictions outlined above.

A single pole was placed at each corner of a square plot and two additional poles were placed along opposite sides of the plot (Fig. 2.2.). All six poles on a plot were used as ground control points (GCPs) during 3D model reconstruction while the two middle opposing poles were used as the points of reference for single MiLS video transects (Fig. 2.2.). Depths, distances and bearings of all poles relative to each other were recorded using a tape measure, digital compass, and depth gauge. Distances and depths were recorded to the nearest 5 cm while bearings were recorded to the nearest degree.

2.2.3. Image Capture

For 3D model reconstruction and MiLS analysis, we captured high-definition video using a Sony A6500 mirrorless camera which was housed in an Aquatica aluminum camera housing attached to an Aquatica camera tray. Two 2500 lumen Light and Motion Sola flood lights were attached to the tray, 1 m apart from each other, and positioned in-line with the camera tray while projecting their light beams in parallel with the camera's optical axis. An Apinex green laser was mounted to the bottom of the camera tray using a custom-built mount which aligned the laser's beam parallel to the camera's optical axis 13 cm apart. A digital depth gauge attached to the camera housing measured the depth of the camera during image surveys. All video was recorded in full AVCHD 1080P format at 60 fps, with a focal length of 16 mm, and an aspect ratio of 16:9. All exposure parameters were left in "Auto" modes.

We surveyed each plot on a separate day while assuming that the turbidity and ambient light were uniform throughout a single day (Table 2.1.). However, we assumed that turbidity and ambient light conditions varied on each day and therefore surveyed one of the plots (plot B) over three separate days to determine the effect of variable turbidity and ambient light conditions on image and 3D model quality. Surveys were conducted only between 10 am and 2 pm to reduce the added variability in ambient light conditions based on the time of day. On each survey day,

we carried out two dives to capture video footage for MiLS analysis and two dives to capture video footage for 3D model reconstruction.

MiLS surveys were conducted in two stages following methods outlined in Du Preez and Tunnicliffe (2012): a) the in water calibration and b) the video transects (Fig 2.2.). During the calibration exercise, the camera was focused on a flat reef bottom while the diver ascended in a step - wise manner from the bottom to a depth from which the bottom was no longer visible (usually 4 – 5 meters above bottom (mab)). The calibration exercise provided measurements of the laser's image distance from the camera's optical axis in a series of images at different heights above the bottom. Only frames captured at known heights above the bottom were analyzed. Next, video footage was collected along the same transect multiple times, 1 – 2 mab along a between the two transect reference poles. The number of repeat transect surveys conducted on each plot and day varied between 5 and 12 and were limited by available bottom times and diving conditions (strong currents). The MiLS calibration exercise was carried out once on each survey day while the series of repeat video transects were carried out once over plots A and C and three times over plot B, once on each day that plot B was surveyed (Tables 2.1. and 2.3.).

For 3D model generation, video footage of the reef plots was captured from above and the sides of the reef (Fig. 2.2.). Each survey was carried out 1 – 2 mab in a boustrophedon pattern with the camera facing downwards followed by one circular pattern around the perimeter of the reef plot with the camera facing at approximately a 45° angle toward the plot (Fig. 2.2.). The survey was repeated a minimum of 4 times over plots A and C which were surveyed over 1 day each and a minimum of 4 times over plot B over three separate days. We could not conduct more repeat surveys due to logistical constraints.

2.2.4. MiLS Video Post-Processing

Video footage from the MiLS calibration exercises and the repeat video transects were processed and analyzed in free Kinovea software V0.8.15 and GNU Image Manipulation Program V2.10.12, respectively. We extracted frames from the MiLS calibration exercise and measured the distance between the laser dot and the optical axis in them to determine the refraction parameters of the surrounding water on each survey day. Likewise, frames from the repeat video transects were extracted and analyzed to determine the variation in height of the reefs along each transect. A detailed description of the methods used for the MiLS analysis in this study is available in Du Preez and Tunnicliffe (2012).

Due to changes in underwater current velocity over the reef and slight, unavoidable, variations in the swimming speed of the camera operator, repeat video transects did not all have the same duration. Therefore, using a constant frame extraction rate, e.g. 2 fps or 3 fps, among

the repeat video transects would have equated to slightly different ground distances between extracted frames from one repeat video transect to another. Consequently, repeat video transects would have had slightly different fractal dimensions (see Glossary of Terms). To ensure that the ground distance between extracted frames and the fractal dimension of repeat video transects remained as constant as possible, we altered the frame extraction rate between video transects so that the total number of frames from each repeat transect remained the same. We divided the video transect duration by the number of desired frames so that each frame-step (time interval between consecutive frames) equaled to the same approximate ground distance interval. In our case, we arbitrarily chose a ground distance interval of 10 cm. Consequently, the number of frames extracted and analyzed from each video transect remained the same among repeat transects within a plot but varied among plots. For instance, 26 frames were systematically extracted from repeat video transects within plots A and B but only 25 frames were systematically extracted from repeat video transects within plot C.

Additionally, not all of the surveyed video transects were included in the analysis of MiLS measurement error. While every effort was made by the diver to maintain a constant swim trajectory some video transects had momentary backwards motion or veered off to the side and did not end over the desired reference point (PVC pole). Table 2.3. summarizes the number of repeat surveys conducted on each day and the number of surveys that were used for analyzing measurement error.

Once the image distance between the optical axis and laser dot in each frame was measured as well as the image distance between consecutive frames was measured, 2D height profiles were generated that corresponded to the variation in the reef height along each repeat transect (Fig. 2.2.; Du Preez and Tunnicliffe (2012)). From each height profile, a rugosity ratio was calculated by dividing the profile length by the linear length. To avoid the effects of slope on the rugosity ratios, only slope-corrected height profiles were used.

2.2.5. 3D (SfM) Photogrammetry Video Post-Processing

3D models were constructed in Agisoft Metashape Professional V1.5.5 software. Metashape allows users to extract frames at specified frame-steps (2 fps, 3 fps, etc.) from video clips and manually calibrate them based on the video capture parameters (focal length, sensor size, etc.). Frames were systematically extracted at 2 fps and manually assigned a focal length of 16 mm and a pixel size of 0.00388751 x 0.00389708 mm. The pixel size was calculated using the frame's resolution (1920 x 1080 pixels) and the physical dimensions of the camera's sensor.

Next, frames were annotated by labelling the GCPs visible in each frame. Each GCP's position was calculated relative to XYZ coordinates in Euclidian space using the recorded

distance, depth and bearing measurements. The XYZ coordinates were used to ensure that frames would align in the correct positions in 3D space relative to the GCPs. The frame locations were visually checked before proceeding with 3D model reconstruction. 3D models were constructed using the procedure outlined in Burns et al. (2015). At the end of the 3D model construction process, a digital elevation map (DEM) was generated for each model and exported at 0.01 m resolution into ArcMap V10.7.1 software for further analysis (Fig 2.2.). The maximum spatial resolution of DEMs varied from model to model. Therefore, to avoid additional variation in the measurement error due to varying spatial scales, we rounded the spatial resolution of each DEM to the lowest, common resolution among all the DEMs.

In ArcMap, the DEM's planar and surface areas were measured using the "Add Surface Information" tool that is part of the 3D Analyst toolbox. The surface area was divided by the planar area to get a measure of surface complexity (SAPA ratio). In addition to analyzing the DEM's surfaces, a virtual transect was traced on each DEM surface in Metashape corresponding to the position of the MiLS repeat video transects. The height profiles and rugosity ratio of each DEM transect were generated and calculated, respectively.

2.2.6. Statistical Analyses

The MiLS and DEM transect rugosities as well as the DEM surface complexities were grouped by survey day and by plot. Each metric was averaged for plots A, B, and C as well as for the three survey days of plot B. The standard deviation was assumed to represent the measurement error (ME). When comparing the mean metrics and ME among plots, data was pooled across the three survey days of plot B, however, when comparing the mean metrics and ME across time, only data from plot B was tested and separated into the three survey days (Fig 2.3.).

Most of the rugosities and surface complexities were normally distributed based on the Shapiro - Wilks test, but they did not meet the assumption of equal variances between groups. Sphericity was assessed using the Bartlett's test of constant variance which simultaneously tested the consistency of measurement error across the three plots and across the three survey days of plot B was tested using since the measurement error was the square root of variance. When variances and consequently the measurement error varied significantly among groups, a Kruskal - Wallis test was used to determine whether the mean metric values were significantly different among the three plots and among the three survey days for plot B. If the metrics were normal and homoscedastic, a one-way single factor ANOVA was used to analyze the differences between plots and survey days of plot B.

While rugosity and surface complexity are both unitless metrics of structural heterogeneity, they represent different information about the reef's structure. Rugosity is a metric of reef roughness along a single narrow path through a reef while surface complexity encompasses the roughness of a whole area of reef. To compare the two techniques directly, first, a paired Wilcoxon signed-rank test was used to test for differences in mean rugosities when captured by MiLS as opposed to the DEMs for each plot and survey day. The rugosities should be the same as they are measuring the same surface heterogeneity over the same slice of reef. A parametric paired t – test was not used because the differences between the MiLS and DEM rugosity means were not normally distributed. Second, to test the measurement error of rugosity when captured by MiLS as opposed to DEMs, an F - test of variance was used to determine whether the variances and consequently the ME of the mean rugosities of each of the plots and survey days was different between the two techniques. Since the MiLS rugosity could not be directly compared with the DEM SAPA ratio, we first calculated the coefficients of variation (CV) as a proxy of the relative variance and therefore the relative measurement error of each metric over each plot and on each survey day (n = 5 for each metric). Then we tested the coefficients of variation (paired by plot and survey day; n = 5) between the MiLS rugosity and the surface complexity (SAPA ratio) using a paired t – test.

2.3. Results

2.3.1. Description of the Plots

Three plots (A - C) were chosen to encompass a wide range of structural habitat complexities with respect to reef sponge size, density, distribution, slope, and curvature (Fig 2.1. A - C). Depths were as follows: A, 25.9 m, B, 26.3 m, and C, 27.1 m. Plot A was a slightly arching convex reef plot with a few small live sponges, each less than 0.3 m tall, scattered among mostly flat, dead sponge rubble (Fig 2.1. A). Plots B and C contained similar sponge densities, 7-10 live and dead sponge bushes, separated by areas of flat, dead sponge rubble (Fig 2.1. B – C). Plot B's bushes were approximately 1 m tall and grew on a gentle slope with a height difference of 0.8 m across the plot (Fig 2.1. B). The shallower portion had a higher sponge density of > 1 individual m^{-2} while the deeper section was more sparsely covered. Plot C was also sloping with a height difference of 1.3 m across the plot (Fig 2.1. C). Plot C had the tallest sponge bushes most of which were merged together to form large clumps over a meter in diameter wide. While plots B and C had similar bush densities, plot B's live and dead bushes were more or less equally distributed throughout the plot while plot C's sponges exhibited noticeable segregation between

the live and dead bushes. Live sponges were primarily found on the shallower portion of the plot while the dead ones were found on the deeper portion.

2.3.2. Rugosity and SAPA Measurement Error (ME)

Rugosity ratios calculated by MiLS were normally distributed but were heteroscedastic. Mean MiLS rugosity ratios varied significantly among plots (Kruskal – Wallis' H = 20.81, p < 0.01, df = 2) and within a single plot measured on different days (Kruskal – Wallis' H = 10.08, p = 0.01, df = 2) (Fig. 2.3.). The mean rugosity ratios of plots A, B, and C were 1.18 ± 0.05 (n = 8), 1.65 ± 0.25 (n = 15), 2.82 ± 0.36 (n = 4), respectively (Fig 2.3. A). The mean rugosity ratios on each of the three days that plot B was surveyed were 1.36 ± 0.02 (n = 4), 1.62 ± 0.14 (n = 5), and 1.86 ± 0.19 (n = 6) (Fig. 2.3. B). The total ME was 0.57 across all three plots. Variance differed significantly among plots (Bartlett's χ^2 = 14.18, p < 0.01, df = 2) and within plot B (Bartlett's χ^2 = 7.95, p = 0.02, df = 2).

The rugosity ratios from the Digital Elevation Maps were not normally distributed and were heteroscedastic. Mean rugosity ratios calculated by DEM varied significantly among plots (Kruskal – Wallis' H = 11.16, p < 0.01, df = 2) as well as within plot B measured on different days (Kruskal – Wallis' H = 6.62, p = 0.04, df = 2). The DEM rugosity ratio for plot A was 1.12 ± 0.02 (n = 4), plot B, 1.57 ± 0.08 (n = 12), and plot C, 1.46 ± 0.11 (n = 5) (Fig. 2.3. C). The mean DEM rugosity ratios for repeat surveys of plot B were 1.51 ± 0.03 (n = 4), 1.55 ± 0.05 (n = 4), and 1.65 ± 0.08 (n = 4) (Fig. 2.3. D). Total ME was 0.17 across all three plots. Variance differed significantly among the plots (Bartlett's χ^2 = 6.15, p = 0.05, df = 2) but not among plot B's survey days (Bartlett's χ^2 = 1.82, p = 0.40, df = 2).

The surface area to planar area ratios (SAPA) of the Digital Elevation Maps were normally distributed except for plot A. The mean SAPA ratios of plots A, B, and C were 1.10 ± 0.01 (n = 4), 2.27 ± 0.12 (n = 12), and 2.44 ± 0.38 (n = 5), respectively, and differed significantly (Kruskal – Wallis' H = 13.17, p < 0.01, df = 2) (Fig 2.3. E). Mean SAPA ratios for the different survey days of plot B were normally distributed and homoscedastic. The mean SAPA ratios for the different survey days of plot B were 2.15 ± 0.06 (n = 4), 2.29 ± 0.09 (n = 4), and 2.38 ± 0.05 (n = 4) and varied significantly (ANOVA's F = 9.78, p = 0.01, df = 2) (Fig 2.3. F). Total ME was 0.50 across all three plots. Variances differed significantly among plots A, B, and C (Bartlett's χ^2 = 10.79, p < 0.01, df = 2) but not among the different survey days of plot B (Bartlett's χ^2 = 0.97, p = 0.62, df = 2).

2.3.3. Comparing MiLS with 3D Modelling

The mean coefficients of variation (n = 5) for rugosities calculated by MiLS and by DEM, and for surface complexity (SAPA) were 7.61 ± 4.42 % (± SD), 3.75 ± 2.28 % (± SD), and 2.68 ±

1.22 % (± SD), respectively (Fig. 2.4.). There was no significant difference in the mean absolute rugosities derived from MiLS and those derived from the DEMs according to the Wilcoxon signed-rank test (p = 0.31); however, there was a difference in the variance among the two metrics (F = 13.07, p = 0.03, df = 4). Additionally, CV varied significantly between MiLS rugosity and surface complexity of the DEM as measured by the SAPA ratio (t = -8.43, p < 0.01, df = 4).

2.3.4. *Sampling Effort*

All surveys required a total of 26 dives and a little over 10 hours to complete (Table. 2.2.). No decompression limits reduced total bottom time to 20 - 25 minutes each. Six dives were required to delineate and measure the plots; video footage for MiLS analysis and 3D model reconstruction was collected over 20 dives; MiLS surveys were conducted over 5 dives and because these occurred on separate days, they were accompanied by MiLS calibration exercise dives, one on each day.

The initial plot setup procedure was lengthy. 3D photogrammetry requires at least three ground control points (GCPs) to improve the model accuracy. We used six GCPs. The distances, depths and bearings of the ground control points (in our case the PVC poles) had to be measured. We required 150 minutes over six dives to properly delineate the three plots. If the time required to descend onto the reef, swim to the plots, and ascend safely to the surface is factored in, then the actually underwater working time spent inserting the PVC poles and measuring them was 18 minutes per dive or a total of 36 minutes per plot. For MiLS, only two reference points are required, one at each end of the transect, and the distance and bearing between the points, as well as the depth of the points do not need to be measured. We measured them anyways because they were part of the six poles delineating the whole plot and were used as GCPs to improve the 3D models' accuracies.

A necessary component of MiLS, however, was the in water camera calibration exercise which we conducted on each survey day to correct for the effect of varying turbidity and ambient light conditions on the refractive index and consequently on the image laser measurements (Du Preez and Tunnicliffe 2012). Excluding the descent time onto the reef and the ascent time from it, the average underwater working time for each calibration exercise was under 16 minutes (Table 2.2.). In – water calibration is not required for 3D photogrammetry.

Based on the length of the collected video footage, each repeat MiLS video transect 2.5 – 3 m long took an average of less than a minute to complete while each 3D model survey of a 3 m x 3 m reef plot took a little over 5 minutes to complete (Table 2.2.). We conducted anywhere from 5 to 12 repeat MiLS video transects (Table 2.3.) and two repeat 3D surveys per dive. The

additional working bottom time on each dive, which excluded the underwater transit time to and from the reef plots, was spent performing other necessary tasks. These included switching the camera – laser array and flood lights on and off, adjusting the position of the flood lights so that they faced the same forward direction parallel to the camera's optical axis, and maneuvering to the initial starting position over the reef plots after every repeat survey.

2.4. Discussion

While many studies have applied 3D SfM photogrammetry to the study of habitat complexity of tropical and subtropical marine environments, including deep sea corals and hydrothermal vents, few have quantified the measurement error (ME) of the technique using several repeat measurements. Our study is the first to carry out a comparison of techniques in situ in cold temperate waters. Here we quantified the ME of the surface area to planar area ratio (as a metric of surface complexity) and rugosity derived from SfM photogrammetry and microtopographic laser scanning (MiLS) of a glass sponge reef in the temperate cold waters of the Pacific Northeast.

While both MiLS and 3D SfM photogrammetry provided distinct measures of rugosity and surface complexity for the three reef plots, the MiLS technique had much higher measurement error between days and a larger coefficient of variation (CV) than the SfM photogrammetry. This indicated that SfM photogrammetry was reproducible over time evidenced by no significant change in the ME over the three survey days of the same plot (plot B). The reasons for these differences are largely due to the interpolation of microscale structural heterogeneity by SfM photogrammetry while MiLS can accurately detect microscale height variation of a reef. However, MiLS is more susceptible to random error introduced by the variable motion of the camera - laser system. Additionally, averaging the mesoscale structural complexity, as is the case with the surface area to planar area ratio may not be representative of the microscale structural heterogeneity. The fundamental difference between MiLS and SfM photogrammetry is the spatial scales at which structural complexity metrics are measured over.

2.4.1. MiLS and DEM Rugosity

Plot A had the lowest rugosity derived from MiLS and from the 3D DEMs. While plot C had the highest rugosity derived from MiLS, plot B had the highest rugosity based on the 3D DEMs (Fig 2.3. A and 2.3. C). However, despite the apparent difference in relative rugosities derived from MiLS and 3D DEMs between plots, there was no significant difference in the absolute rugosities between the two techniques. The rugosities for each plot were similar between the two techniques (Wilcoxon signed rank-test was insignificant, p = 0.31). On the

contrary, measurement error of rugosity derived from MiLS was significantly different than that of rugosity derived from the 3D DEMs (p = 0.03). While mean rugosities were similar between techniques for the three plots, ME of rugosity was consistent over the three surveys days on plot B only for the 3D technique.

The discrepancy between the two rugosity measurement techniques could be due to differences in the accuracy of each technique. For example, the laser can penetrate into small gaps between sponge mittens and oscula and therefore for MiLS there is greater variation in height along a transect. Additionally, the laser's projection on the reef along a repeat transect is sensitive to the camera's orientation. Despite efforts to ensure that the camera's angle was constant during the repeat surveys, random movement of the camera's yaw, pitch, and tilt, even at the slightest angle, altered the laser's direction from its intended vertical projection and artificially inflated the frame measurements (distance between optical axis and laser). Similarly, variable currents also affected the diver's ability to maintain the exact swim path and speed. Consequently, frames between repeat transects rarely aligned over the same position on the reef. These slight variations had cumulative effects on the height, horizontal length, and rugosity of a transect. Mitigating the above effects should involve designing and/or utilizing a more stable platform that can hold the camera in a steady orientation irrespective of the diver's hand movements. Some sort of underwater levelling device would go a long way towards stabilizing the camera underwater. Additionally, manually choosing frames from each repeat transect that align perfectly over the same reef location could mitigate the issue of variable diver swim trajectories but may not necessarily mitigate the effect of lateral motion, i.e. side to side deviation from the transect path. A less time-consuming solution may be to use an ROV or AUV that can maintain constant velocity in strong currents.

3D photogrammetry seems to be impacted less by the variable camera orientation and position over the glass sponge reef than MiLS does. However, 3D SfM photogrammetry has difficulty detecting small gaps between sponges (and sponge body parts) in the reef if those gaps are only captured from above the reef and not the sides; it also has trouble discerning the difference between spaces or dark gaps and the dark shade of dead sponge patches. In those cases the 3D dense point cloud interpolates the surface between the nearest neighboring structures around the small gaps and effectively drapes a mesh over them. This effect may be responsible for the lower relative rugosity calculated from the DEMs of plot C. It may also be responsible for the consistent ME of rugosity measured by the 3D technique over the three survey days on plot B.

2.4.2. DEM Rugosity and Surface Complexity

The surface complexity (SAPA ratio) between reef plots followed the same pattern as the relative MiLS rugosities but not the relative DEM rugosities. Plot A had the lowest SAPA ratio, followed by plot B, while plot C had the highest SAPA ratio. The difference between the relative complexities of the three reef plots as determined by the rugosity and SAPA ratios of 3D DEMS can be explained by the differences between microscale and mesoscale structural heterogeneity. The structural heterogeneity of a narrow slice of reef will likely be different to that of another narrow slice of reef some meters away. Likewise, the overall structural heterogeneity of a 1 m² reef area may be different to that of a 3 m x 3 m reef area that encompasses that 1 m² reef section. Therefore the observed difference in the pattern of relative complexity between the rugosity and surface complexity is a consequence of the difference between the structural heterogeneity at the slice of reef over which the virtual transects were traced and the overall structural heterogeneity of the reef area. There is a possibility that by tracing several virtual transects across different sections of the same DEM, the average rugosity of those transects would be similar to the overall DEM's surface complexity (surface area to planar area ratio; SAPA). The importance of defining the sampling scale of study was also highlighted by Bryson et al. (2017) whose larger survey areas showed little overall surface complexity differences among different sites despite the visible high spatial heterogeneity among the sites.

2.4.3. Surface Complexity (SAPA) ME

Surface complexity (surface area to planar area ratio; SAPA) ME differed significantly among reef plots A, B, and C. ME increased with increasing absolute values (SAPA ratio) which is typical for many detection techniques in the physical, chemical, and biological sciences. A similar pattern of increasing error with the increasing structural metric value derived from 3D photogrammetry was observed by Bryson et al. (2017) and Marre et al. (2019). While our study does not have enough independent samples to confirm a correlative relationship between ME and the magnitude of the SAPA ratio, we observed the pattern in our data and quantified it with the coefficient of variation (CV).

Measurement error of SAPA over the three days that plot B was surveyed on did not differ significantly, similar to the ME of rugosity derived from the DEMs over the three plot B survey days. These findings are similar to those of Bryson et al. (2017) who found that 3D surface complexity measurement error was constant over their survey days for multiple survey sites. Additionally, Raoult et al. (2017) also did not find a temporal effect of multi-day surveys of coral bommies on the bommies' volume and surface area measurements derived from 3D model reconstructions.

Surprisingly, mean SAPA ratios differed significantly among the three survey days for plot B even though there were no visible structural changes within the plot. Underwater visibility increased on each consecutive day that plot B was surveyed. We did not measure water turbidity or ambient light levels, however, both factors may have affected the accuracy of our 3D models so that they captured more structural heterogeneity at the same resolution on each consecutive survey day. Bryson et al. (2017) found similar results which showed that average surface complexity varied significantly over survey days for some of their sites. Another explanation for the increase in the surface complexity value within plot B could be that microscale structural changes within that whole reef plot had a cumulative effect on the mesoscale SAPA metric although this is highly unlikely considering the slow growth rates of reef building sponges (Leys and Lauzon 1998). Future research should investigate the relationship between in situ turbidity and 3D model quality by increasing the sample size (number of days on which a reef plot is surveyed) to compute a baseline surface complexity for a given reef area and then track changes in complexity using the relative deviation from that baseline value. This method was used by Bryson et al. (2017).

Other habitat complexity metrics derived from the analysis of the DEMs did not vary significantly among survey days for plot B. Average curvature and average slope were similar among survey days of plot B indicating that surface complexity (SAPA ratio) of a sponge reef is more likely to differ within several day time scales. Variable turbidity may have a greater effect on the 3D surface complexity than other habitat complexity metrics due to the signal-to-noise ratios during 3D model reconstruction. The excess noise in the form of suspended particulate close to the surface of the reef may not be distinguished from the physical reef and may artificially increase the reef's roughness during 3D model reconstruction. This effect needs to be addressed in further investigations, however, it is promising that other habitat complexity metrics such as curvature and slope are less influenced by ambient water properties.

2.4.4. Comparing MiLS Rugosity with DEM SAPA

When comparing the coefficients of variation between MiLS rugosity and DEM surface complexity (SAPA) to determine which technique had the lower measurement error, we found that DEM surface complexity did indeed have a significantly lower ME than MiLS rugosity (Fig 2.4.). To our knowledge, no comparison has been made between the efficacy of laser scanning and 3D photogrammetry in quantifying habitat complexity of the seafloor. However, such comparisons were made in terrestrial environments. Medjkane et al. (2018) compared terrestrial laser scanning (TLS) with a SfM photogrammetric approach to build terrain maps of a cliff-side and found that TLS had less error and was more accurate than the SfM approach.

However, their TLS technique generated DEMs of cliff-side areas, similar to the DEMs generated from our SfM photogrammetry approach. Our laser technique did not. In both cases, the accuracy of SfM 3D photogrammetry was affected by differing ambient light conditions as well as the distribution of shadows. Sponge or cliff under-hangs and tight gaps between sponge bushes or terrestrial rock features are and were less likely to be detected by the 3D rendering algorithms that generate dense point clouds and mesh layers. Instead, they appear as either straight edges or fused sections between features due to the interpolation between neighboring structures. In our case, this was most likely due to the variable shadow intensities on or within the small gap features. However, our laser scanning technique had a higher error because it quantified rugosity through a slice of reef instead of a whole reef area and any small scale variation in structural heterogeneity was not averaged across a whole reef plot as was the case in Medjkane et al. (2018).

2.5. Conclusions

3D photogrammetry has a clear advantage over MiLS as a monitoring tool. Although, both techniques have their merits. When deciding which technique (MiLS or 3D photogrammetry) to use in a monitoring framework or investigation of a glass sponge reef, it is important to determine the spatial scale under investigation and whether repeat surveys are needed (which they likely will be for monitoring long term change).

MiLS is only able to capture the structural heterogeneity of a slice of reef along a single transect and extrapolating that heterogeneity to the surrounding reef area would not necessarily be representative of the true heterogeneity of that area. However, MiLS does have the potential to capture structural heterogeneity at high spatial resolutions and is extremely accurate at the microscale. MiLS can also accurately capture the height variation along a transect irrespective of light conditions, as long as the survey is immediately preceded or followed by an in water camera calibration exercise. However, MiLS should not be used for repeat surveys due to its low replicability and repeatability over time and over different parts of a glass sponge reef. Using a stable platform that minimizes camera roll, pitch, and yaw and is able to maintain constant speed and direction may improve the repeatability of MiLS but for a citizen scientist SCUBA diver, maintaining the same camera orientation and swim trajectory is virtually impossible.

3D SfM photogrammetry is replicable and repeatable over time and captures the habitat structural heterogeneity of a whole reef area. Additionally, different swim paths around a reef area will have a smaller effect on the overall surface complexity metric, than slightly different transect swim trajectories will have on the MiLS rugosity. A factor that will likely influence the

accuracy and measurement error of 3D metrics is the number of images used to build the 3D models. We did not test this but Bryson et al. (2017) did and found that the error did change with varying image coverage but only for some of their sites. The effect of image coverage on the 3D model reconstruction of a glass sponge reef would have to be investigated further if different citizen scientists capture different quantities of images over a reef patch.

Another advantage of 3D SfM photogrammetry as a tool for the long-term monitoring of glass sponge reef habitat complexity is its ability to extract a large suite of habitat complexity metrics from a 3D DEM. Curvature and slope are only a couple more metrics that can be tracked with a high level of certainty over time and can be used in the study of reef ecology to disentangle mechanisms that attract epifauna to glass sponge reefs. Additionally, rugosity can be extracted from a 3D DEM and is likely to be similar to the rugosity from a MiLS transect over the same reef slice. Using the protocols outlined in this chapter, surface complexity (SAPA ratio) may not be a reliable indicator of the true changes in habitat complexity even though its measurement error was constant. Further investigation needs to be conducted to determine exactly how turbidity and ambient light conditions affect the SAPA ratio. Perhaps an in water calibration exercise would be necessary after all.

Lastly, an important aspect of any monitoring framework is the relative time commitment for extracting relevant information about a marine ecosystem. While it took less time to survey a MiLS transect (Table 2.2.) than it did to survey a reef area with the same width dimensions as the transect length, each set of MiLS transects conducted in one day should be accompanied by a MiLS calibration exercise. MiLS calibration, if done properly, requires at least 100 different depths from which a single frame is extracted in order to accurately correct for the laser's refraction (Du Preez and Tunnicliffe 2012) which is almost impossible to accomplish on SCUBA. The time requirement for our calibration exercises offset the low time commitment of conducting MiLS video transects and effectively evened out the total MiLS time commitment with the SfM survey time commitment. If a 3 m x 3 m reef plot is to be surveyed using 3D photogrammetry, a dive team can expect to spend approximately five minutes collecting video footage of the plot in addition to approximately seven minutes descending to the reef, swimming to the plot, and safely ascending back up to the surface (Table 2.2.). If a 3 m long transect along a reef is to be surveyed using MiLS, a dive team can expect to spend approximately half a minute collecting video footage of the transect in addition to approximately the same seven minutes descending to the reef, swimming to the plot and safely ascending back up to the surface. However, a 15 minute MiLS calibration would also be required increasing the total MiLS dive time to approximately 23 minutes. While in water calibration is not required for SfM

photogrammetry, it does require ground control points (GCPs) and their setup as well as the process of accurately measuring their relative depths, distances apart, and bearings apart does increase the time commitment of 3D photogrammetry. Again, for a hypothetical 3 m x 3 m wide reef plot, a dive team can expect to spend approximately 35 minutes delineating a plot. It would not be possible to spend this much time on the reef (due to bottom time limitations) so delineating a plot would require two separate dives each with an in water transit time of seven minutes and a working time of 17 – 18 minutes. Although, once the GCPs are installed on a reef, they can be left there throughout the duration of the monitoring program.

2.6. Acknowledgments

2.7. Financial Support

Table 2.1. Weather and Diving Conditions on each of the 5 Survey Days. Visibility was qualitatively estimated based on diver experience.

Plot and Survey Date	No. of dives	Weather	Surface conditions	Visibility (m)	Ambient light conditions on reef plot
Plot A (04/17/2019)	4	Overcast and raining	Calm	12	Ample light
Plot B (04/04/2019	4	Sunny, clear skies	Calm	7	Some light
Plot B (04/15/2019)	4	Intermittent clouds	Calm	14	Plenty of light
Plot B (04/18/2019)	4	Overcast, heavy rain	Small waves	10	Ample light
Plot C (04/05/2019)	4	Overcast	Calm	3	Dark

Table 2.2. Diving effort. Time spent delineating reef plots, conducting MiLS calibration exercises, collecting video footage of repeat MiLS transects, and surveying the reef plots for 3D model construction. The average dive time was calculated by dividing the total dive time by the total number of dives. The in water transit time was the time spent descending to the reef from the boat, swimming from the descent line to the reef plots, and safely ascending to the surface. The working time was the portion of the dive that excluded the in water transit. During the working time portion of each dive, we performed several repeat surveys and additional tasks, including camera – laser array handling and maneuvering. The average MiLS and 3D repeat survey time was calculated by averaging the length of video footage from each repeat survey of the respective techniques.

Activity	Total No. of Dives	Total Dive Time (min)	Total No. of Surveys/Plots	Average Dive Time (min)	In-water Transit Time (min/dive)	Working Time (min/dive)	Average Survey/Plot Setup Time (min/survey)
Plot Setup	6	150	3	25	7	18	36.0
MiLS Calibration	5	102	5	20.4	5	15.4	15.4
MiLS Repeat Surveys	5	108	40	21.6	7	14.6	0.4
3D Repeat Surveys	10	251	21	25.1	7	18.1	5.1

Table 2.3. Number of Surveys Conducted. Under the MiLS column, numbers in brackets represent the number of video transects that were suitable for MiLS analysis.

Plot and Survey Day	Number of Repeat Surveys	
	MiLS	3D modelling
Plot A	12 (8)	4
Plot B, Day 1	7 (4)	4
Plot B, Day 2	5	4
Plot B, Day 3	11 (6)	4
Plot C	5 (4)	5
Total	40 (27)	21
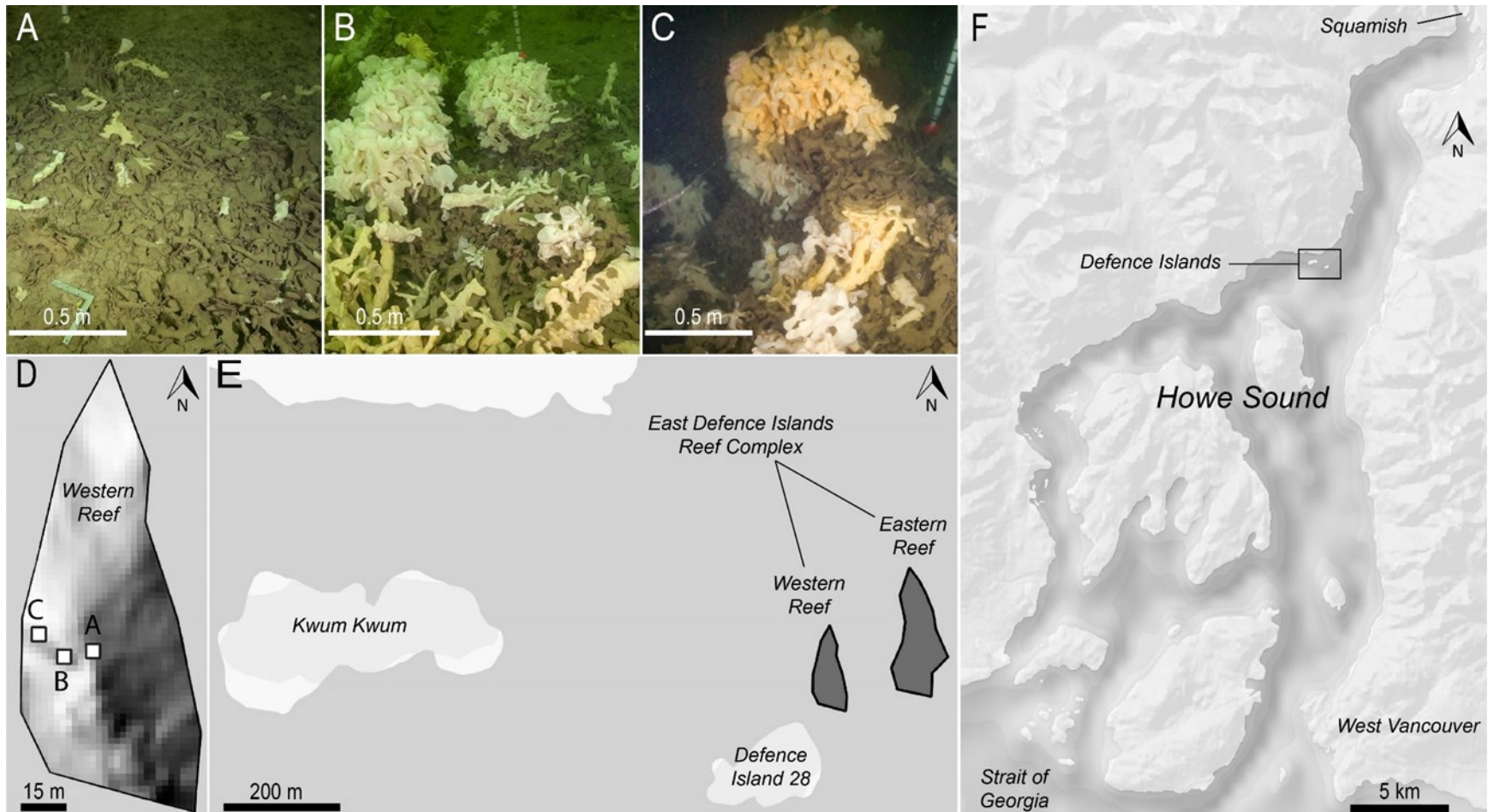
Figure 2.1. Study Area and Location of Glass Sponge Reef Survey Plots. A, B, and C are photos of the reef area within plots A, B, and C, respectively; D shows the location of reef plots A (49°34.663' N, 123°16.405' W), B (49°34.662' N, 123°16.413' W), and C (49°34.666' N, 123°16.420' W) on a raised-relief map (raster layer provided by Robert Kung; NRCan) of the western East Defence Island reef; E is a map of the Defence Islands in Howe Sound with the grey polygons (raster layer available in the supplemental materials of Dunham, Archer, et al. (2018)) outlining the East Defence Islands Reef Complex; F is a topographic chart of Howe Sound with an outline around the Defence Islands.
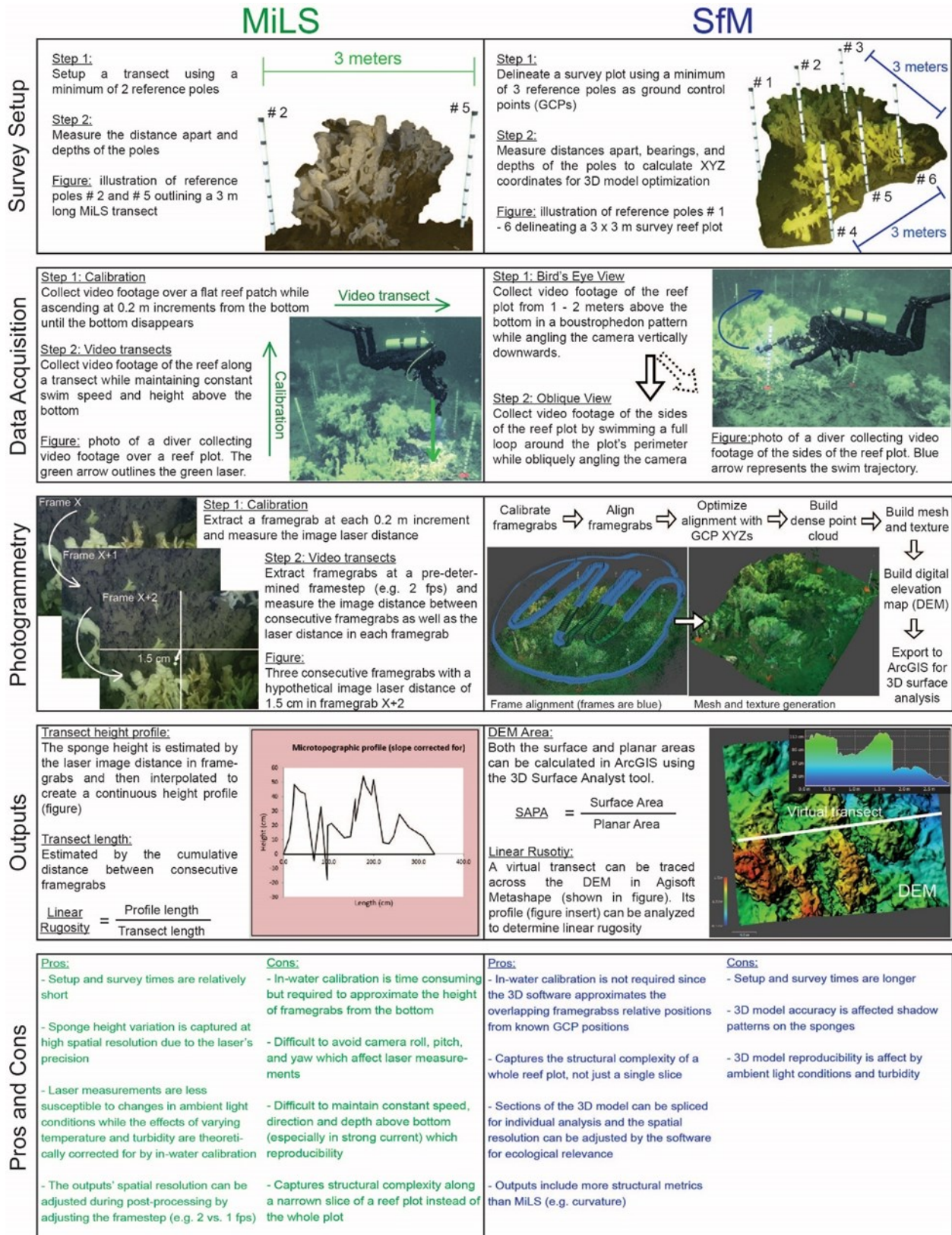
Figure 2.2. MiLS and 3D Photogrammetry Workflows. Steps and considerations for performing MiLS and 3D photogrammetry on a glass sponge reef.

Figure 2.3. MiLS Rugosity, DEM Rugosity, and DEM SAPA Ratios. Distribution of MiLS rugosity (panels A and B), DEM rugosity (panels C and D), and DEM SAPA (panels E and F) ratios in plots A, B, and C (panels A, C, and E) as well as the three days that plot B was surveyed on (panels B, D, F). All three metrics varied significantly among plots A, B, and C ($p < 0.01$; panels A, C, and E). There were also significant differences within plot B surveyed on different days for the MiLS rugosity ($p = 0.01$; panel B), DEM rugosity ($p = 0.04$; panel D), and DEM SAPA ($p < 0.01$, panel F) ratios. A similar pattern was observed for ME which varied significantly among reef plots for the MiLS rugosity ($p < 0.01$; panel A), DEM rugosity ($p = 0.05$; panel C), and DEM SAPA ($p < 0.01$; panel E) ratios. However, ME varied significantly within plot B surveyed on different days only for the MiLS rugosity ($p = 0.02$; panel B). Dots and error bars within the violin plots represent the means and standard deviations, respectively. * indicates that ME differed significantly among the three plots/days.
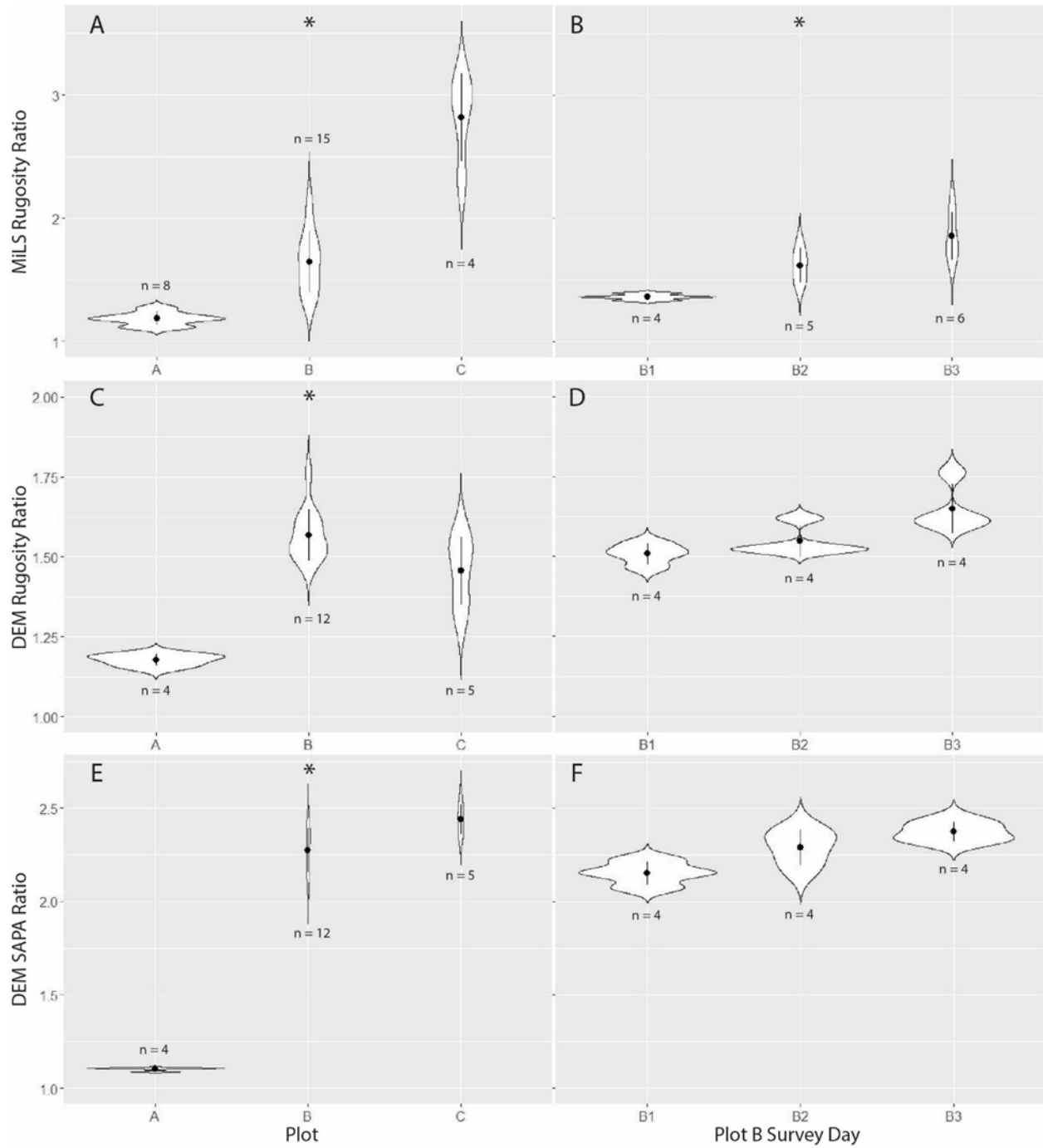
Figure 2.3. MiLS Rugosity, DEM Rugosity, and DEM SAPA Ratios.
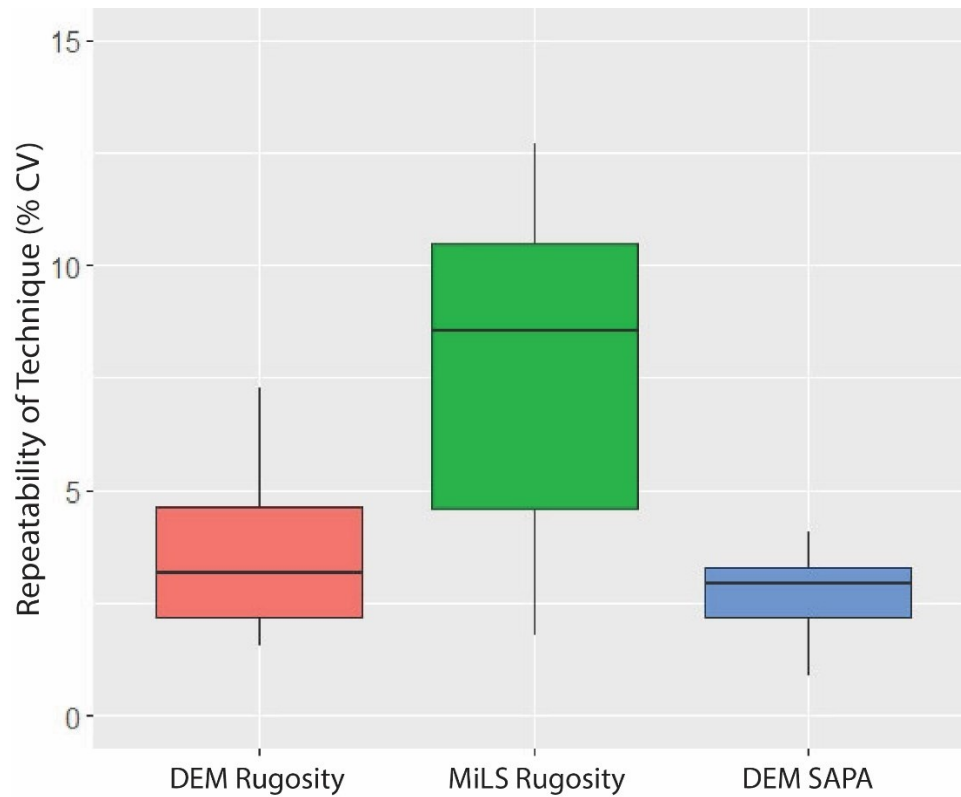
Figure 2.4. Repeatability of MiLS and 3D SfM photogrammetry techniques. %CV was calculated using the mean metric and its standard deviation from plot A, plot C, and the three days that plot B was surveyed (n = 5). The distribution of the %CV values is visualized in this graph with boxplots of the interquartile ranges around the medians. MiLS had a higher measurement error than either 3D rugosity or SAPA ratios. The coefficient of variation (CV) was significantly lower in SAPA (t = -8.43, p < 0.01, df = 4) and there was a significant difference between the variances of DEM and MiLS rugosity ratios (F = 13.07, p = 0.03, df = 4)

Chapter 3. Relating 3D Structural Complexity Metrics to Functional Traits

3.1. Introduction

Glass sponge reefs are unusual ecosystems located on the continental shelf of western Canada. Despite being formed by only three species of glass sponge, *Aphrocallistes vastus*, *Heterochone calyx*, and *Farrea occa*, the reefs have high diversity that is driven by infaunal and epifaunal communities (Guillas et al. 2019; Dunham, Archer, et al. 2018; Chu and Leys 2010; Cook, Conway, and Burd 2008). This diversity is comparable, in terms of Shannon-Wiener index values, to that of communities living on coral reefs (Planes et al. 2012; Madduppa 2012; López-Pérez and Ballesteros 2004; Pandolfi and Minchin 1996). Taxonomic richness and abundance are generally higher on the reefs than over the surrounding seascape (Dunham, Mossman, et al. 2018).

Reef building glass sponge individuals have complex and highly variable morphologies. Collectively, they form heterogeneous reefs 10s or 100s m² wide (Conway et al. 2020). Three dimensional (3D) structural complexity as well as biological variability in benthic cover type increase the spatial heterogeneity and create more habitat types for a variety of life forms on reefs, including glass sponge reefs (Chu and Leys 2010; Canterle et al. 2020; Devine et al. 2020; Hawkes et al. 2019). Many invertebrate species, including squat lobsters (*Munida quadrispina*) and sponge eualid shrimps (*Eualus spp.*) rely on the reef habitat for shelter, and a number of rockfish species (*Sebastes spp.*) use the reefs for shelter and food (Marliave et al. 2009; Archer et al. 2020). Unsurprisingly, therefore, studies show that reef structural complexity/spatial heterogeneity and epifaunal abundance and biodiversity are positively correlated (Chu and Leys 2010; Cook, Conway, and Burd 2008).

Since glass sponge reefs are biogenic habitats, they are susceptible to environmental perturbations that can cause ecological restructuring. Tank experiments have shown that individual glass sponges lose their pumping ability and show signs of necrosis under warming water conditions (Stevenson et al. 2020). Observations of die offs of reef - building sponges have been linked to El Nino – La Nina oscillations (Marliave et al. 2020) as well as hypoxia (Leys et al. 2004). Climate change - induced shifts in oceanic circulation patterns are likely to prolong seasonal upwelling along the BC continental shelf, consequently immersing many of the reefs in hypoxic, acidic waters that would cause physiological stress to the reef - building sponges (Conway et al. 2017). Lastly, incidental damage from bottom – contact fishing activities in the form of sediment resuspension clogs the sponges' filtration systems causing arrests of filtration

in some cases momentarily and in others indefinitely (Grant et al. 2019). All of these disturbances can, to different degrees, alter the 3D state of the reef.

Functionally, glass sponge reefs play an important role in bentho-pelagic coupling due to their fast pumping rates and high filtration efficiencies (Leys et al. 2011; Kahn et al. 2015). They sequester vast amounts of carbon and silicon, as well as facilitate nutrient recycling in surrounding sediments (Kahn et al. 2015; Chu et al. 2011; Kahn, Chu, and Leys 2018). However, little is known about the functional ecology of glass sponge reef communities.

Ecosystem function has been linked to the diversity and type of traits found within that ecosystem (Mouillot, Dumay, and Tomasini 2007; Mason et al. 2008; Villéger et al. 2010; Villéger et al. 2012). Consequently, trait - based approaches have been used to study the mechanisms that drive community assembly and mediate niche - partitioning among various members of the community (Mason et al. 2013; Violle et al. 2007). Trait - based approaches have also proven to be useful in disturbance ecology by interrelating functional hotspots, areas of functional loss, and ecosystem resilience to various perturbations (Mouillot et al. 2013; McIntyre et al. 1999). Trait-based approaches to describing reef communities have been sparsely used in glass sponge reef research, focusing primarily on habitat use based on associations of different species with different parts of the reef (e.g. observed on top of the reef, hiding in the reef, or hovering above the reef; Cook, Conway, and Burd 2008). Beyond habitat-use traits, glass sponge reef fish and invertebrate species also possess a wide range of dietary, behavioral, and morphological traits, all of which have not been tested yet. Aside from bridging the link between community ecology and ecosystem functioning, a functional trait-based approach could uncover patterns of species coexistence or competitive exclusion following the concepts of niche filtering and limiting similarity, respectively (Zobel 1997; Hardin 1960; Macarthur and Levins 1967; Mason et al. 2007; Mouillot, Dumay, and Tomasini 2007). Functional analyses could uncover highly diverse yet functionality redundant community assemblages that would indicate a relatively narrow set of environmental gradients driving community composition (niche filtering). On the contrary, a small set of species could possess a wide range of functional traits that would indicate a functionally diverse community. In the latter case, a functional traits-based approach could uncover greater community diversity. Lastly, the unknown effect of the presence of cryptic or undiscovered species (Law et al. 2020; Guillas et al. 2019) on the functional ecology of glass sponge reefs needs to be tested since it could reveal further patterns of niche partitioning and geographic structuring of communities (Pertierra et al. 2020; Villar et al. 2020; Gutiérrez López, Isla García de Leaniz, and Trigo Aza 2020).

In this study we used a functional trait - based approach to describe the condition of three glass sponge reefs in Howe Sound, British Columbia and to investigate the importance of 3D structural heterogeneity in relation to the functional assembly of the epifaunal communities. We focused on dietary traits to elucidate trophic interactions and how different trophic niches can be mediated by habitat types on a glass sponge reef. First, we analyzed the 3D structural complexity of reefs using a 3D photogrammetric technique and correlated structural complexity with Rao's Q quadratic entropy index of functional diversity (Rao 1982). We then used a null model approach, along with non-metric multidimensional scaling (NMDS) to further characterize the mean and variability of the functional composition of reefs as well as to identify any reef habitat complexity gradients that affected community assembly among reefs. We hypothesized that functional diversity, measured by Rao's Q, would increase with increasing 3D structural complexity of the reef assuming that greater 3D complexity would create more livable space for a wider variety of functional traits. Furthermore, we predicted that the variability of community composition along a structural complexity gradient would be driven by traits associated with dietary preference towards benthic crustaceans (i.e. driven by fish species that feed on crustaceans that live on the glass sponges). Lastly, by investigating the effect of a gradient of 3D structural complexity on the functional composition of glass sponge reefs, we would be better equipped to predict the functional restructuring of glass sponge reefs in response to environmental disturbances.

3.2. Materials and Methods

3.2.1. Study Location and Environmental Conditions

This study was carried out on two reef complexes: the East Defence Islands reef complex in Howe Sound, and the Howe Sound – Queen Charlotte Channel reef complex, which lies at the mouth of the sound that joins the Strait of Georgia (SoG), British Columbia (BC; Fig. 3.1. A). The SoG and Howe Sound have similar oceanographic conditions, influenced primarily by freshwater input from surrounding rivers and streams (Thomson 1981). The conditions in Howe Sound have been described previously (Sergeenko, Schultz, and Leys in prep. Chapter 2). Howe Sound receives freshwater and suspended sediments primarily from the Squamish River, while the SoG gets most of its sediments and freshwater from the Fraser River (Thomson 1981; Waldichuk 1957). As in Howe Sound, stratification is also prominent in the SoG, with a brackish surface layer approximately 50 m deep. However, whereas circulation in Howe Sound is primarily wind - driven, in the SoG both wind and tidal currents play an equal role in driving water circulation (Syvitski and Macdonald 1982; Waldichuk 1957; Thomson 1981).

The Howe Sound – Queen Charlotte Channel glass sponge reef complex has 13 separate reefs of varying shapes and sizes (Fig. 3.1. C). Here we surveyed the Passage Island (PI) reef (Fig. 3.1. E; reef 2K in Dunham, Mossman, et al. (2018)). The PI reef is elongate, lying on a ridge, and is approximately 0.5 km long and 100 m at its widest (Fig. 3.1. E). At its shallowest part the reef is 25 – 30 m deep and is accessible by SCUBA diving during slack tides when tidal currents are least strong.

3.2.2. Survey Design

We surveyed 15 sites, five at each of the East Defence Islands inshore (DI) and offshore (DO) reefs as well as five at the PI reef (Fig. 3.1. D - E). The sites were selected to represent the range of structural complexity observed across the respective reefs (Fig. 3.2.). Each site was marked at the corners of a 2 m x 2 m plot with 4 striped PVC poles that were inserted into dead, flat rubble. The PVC poles served as ground control points (GCPs) in the 3D model reconstruction process as well as reference guides for SCUBA divers capturing video of the sponges at each site. The depths, distances of all poles (to the nearest 5 cm), and their bearings (to the nearest degree) relative to each other were recorded using a tape measure and a dive computer with built-in digital compass and depth gauge. This data was used for georeferencing in the 3D model reconstruction process.

Video imagery was captured by SCUBA divers using a Sony A6500 mirrorless camera, housed in an Aquatica aluminum camera housing that was attached to an Aquatica camera tray. Two 3500 lumen Big Blue flood lights were attached to the tray, approximately 1.5 m apart from each other, and positioned in-line with the camera's optical axis while projecting light parallel to the axis. Video was captured in full AVCHD 1080P format at 60 fps, with a focal length of 16 mm, and an aspect ratio of 16:9. All exposure parameters were left in "Auto" modes. The diver first swam approximately 1 m over the reef area in a boustrophedon pattern while facing the camera downwards to capture a bird's eye view of the site. Then the diver swam around the site twice while facing the camera into the reef area to capture video of the sides of the sponges that made up the reef site. During the first circular swim path, the diver swam approximately 1.5 m above the reef, angling the camera at 45 - 50°. The second circular swim path was closer to the reef, at approximately 0.5 m above the reef and with a camera angle of 25 - 30°. To capture more of the structural complexity that is only visible from the side of the reef and not from a bird's eye view (Sergeenko, Schultz, and Leys. in prep. Chapter 2), we did an extra circular swim path at a different height above the reef and with a different camera angle.

Due to logistical challenges, including strong tidal currents, weather conditions, limited bottom time divers could spend working at the reef depths, sites were surveyed on different days

between August 14th and August 30th of 2018. Video and biodiversity surveys of each plot took 5 minutes each; however biodiversity surveys were done first for fish and then for all other animals. To avoid counting the same fish twice over different sites on separate dives, we first conducted a fish survey over all five reef plots on the same reef in a single dive and included all the fish within the boundaries of each site and up to 5 m above each site. Then, we revisited each plot on separate dives to count all other animals. All animals within the boundaries of PVC poles were counted. All animals were identified visually to the lowest taxonomic resolution possible.

3.2.3. 3D Photogrammetry

3D models of sites were constructed in Agisoft Metashape Professional V1.5.5 software following as described previously (Sergeenko, Schultz, and Leys in prep. Chapter 2) and in Burns et al. (2015). Frames were extracted from video imagery at a rate of 2 fps. Due to the mineral composition of ambient water and the high light attenuation with depth over the reefs, the objects in the raw frames were tinted green. To improve the clarity of frames prior to 3D model reconstruction, they were processed in Adobe Photoshop Lightroom V4.0. We adjusted their white balance so that objects appeared normal in color and we reduced the haze and increased the image contrast. We tested the frame alignment in Metashape with raw frames and with processed frames and found the more of the processed frames aligned accurately in 3D space than raw frames for the same site. Once the frames were processed in Lightroom, we manually calibrated them in Metashape by assigning a focal length of 16 mm and a pixel size of 0.00388751 x 0.00389708 mm. The tops and bottoms of the PVC stakes where visible in each frame were annotated as ground control points (GCPs) and georeferenced using depth, distance, and bearing measurements. Following 3D model reconstruction, a digital elevation map (DEM) of each site was generated and analyzed in ArcMap V10.7.1 software (Fig 3.3.). In ArcMap, the DEMs' planar and surface areas were measured using the "Add Surface Information" tool which is part of the 3D Analyst toolbox. The surface area was divided by the planar area to get a measure of surface complexity (SAPA ratio). The relief of each site was also calculated using the "Add Surface Information" tool. Additionally, tools from the Benthic Terrain Modeller toolbox in ArcMap were used to measure the slope and curvature of each site.

3.2.4. Functional Traits

Traits chosen included dietary preference and habitat use traits (e.g., where the animals were commonly found on a glass sponge reef; Table 3.1. and Table S.1.1). Neither life-stage nor size were possible to determine by visual survey, and therefore these were not included in the analysis. Traits were assigned to animals under the assumption that all observed animals were in their adult life stage. Unfortunately, we could not find published literature that assigned

functional traits to any of our observed species, or any of common marine fish and invertebrate species found in the Northeast Pacific. Instead, functional traits were chosen based on traits used in the coral reef literature (Table 3.1.; Plass-Johnson et al. 2016; Rojas-Montiel et al. 2020; Floyd et al. 2020; Caceres et al. 2020). Traits were then assigned to species based on species descriptions from sources such as, www.fishbase.org and its cited sources, as well as Lamb and Hanby (2005; Table S.1.1.).

A species – by - species functional distance matrix was generated using Gower's distance to determine the similarities/dissimilarities among species (Pavoine et al. 2009), similar to the approach outlined in Plass-Johnson et al. (2016). When multiple functional traits are assigned to a single species, that species becomes a functional entity. Functional entities may vary depending on the composition, number, relative ecological importance of the functional traits they possess. Not all functional traits may be equally important to the overall ecosystem function (Chapman, Tunnicliffe, and Bates 2018). Differences in the relative importance of functional traits are distinguished by the weights assigned to traits during the calculation of Gower's distances among functional entities (Pavoine et al. 2009). While no direct relationships between functional traits of animals inhabiting glass sponge reefs (or animals from the Pacific Northeast) and their ecological importance are known, traits were assigned a weight of 2 or 3, based on their interpreted ecological importance on the glass sponge reef at the reef patch scale (Table 3.1.). A similar approach was used in Plass-Johnson et al. (2016). For instance, diet based traits were weighted more strongly due to their important role in the regulation of food web structure and network topology (Archer et al. 2020; Chu and Leys 2012), nutrient cycling (Kahn, Chu, and Leys 2018), and their direct link to primary production (Yahel, Eerkes-Medrano, and Leys 2006; Kahn et al. 2015). Habitat use traits were weighted less strongly due to their inherent variation depending on social structure (schooling rockfish vs single rockfish), life stage (Marliave et al. 2009), season (Marliave and Borden 2020) as well as time of day and depth (Jamieson and Pikitch 1988; Chew et al. 1973). Additionally, habitat use traits within a reef patch may be transient depending on the home ranges of different species within a reef.

Using the species - by – functional trait distance matrix as well as the abundance data for each taxonomic group, we calculated Rao's quadratic entropy (Rao 1982) following Laliberté and Legendre (2010). Rao's quadratic entropy (RaoQ) is an abundance - weighed measure of functional diversity within a community based on differences in pairwise functional distances between functional entities (Botta-Dukát 2005). It is not only affected by the abundance of each functional trait but also the dissimilarity between functional traits (Gower's distance; Mouchet et al. 2010). The primary reason for choosing Rao's Q as opposed to other functional diversity

metrics, such as functional richness, is that Rao's Q is widely used in a lot of the functional traits literature. Additionally, a study by Mouchet et al. in 2010, which compared the performance of several functional diversity metrics, found differences and redundancies among the metrics. They concluded that Rao's Q was more sensitive to detecting niche filtering patterns where coexisting species are more similar to one another due to environmental conditions that act as a filter to allow for a narrow spectrum of traits to persist. This was relevant in our case since we wanted to determine the effects of habitat complexity on the functional community. However, communities with a narrow spectrum of traits may be unstable and less resilient to disturbances (Mouchet et al. 2010) which would also be useful to know when monitoring the sponge reefs.

3.2.5. Modelling the Variability of Functional Diversity

To determine whether the observed RaoQ values arose by chance from random assembly of the communities at each site, or whether they arose due to non - random, site - specific factors, such as environmental variables, we compared our observed RaoQ values to those generated by null models. A null model generates a simulated functional community by randomly sampling the community (species and abundances) observed at each site while maintaining the observed functional traits composition (traits matrix). As such, the functional composition in each model remains the same while the structure (based on abundances and species present) changes. Consequently, any influence of non - random factors that may have structured our observed functional communities is expected to be effectively removed from each null model. Subsequently, we assessed any differences between the observed RaoQ values and the hypothetical values for each site using the standardized effect size (SES) of observed RaoQ following Gotelli and McCabe (2002). The SES is calculated much like the Z-score and allows the comparison of multiple observed RaoQ values on the same scale by converting the values to an effective number of standard deviations:

$$SES_R = (R_{obs} - R_{sim})/SD_{sim} ,$$

where R_{obs} is the observed RoaQ, R_{sim} is the simulated RaoQ, and SD_{sim} is the standard deviation of the simulated mean RaoQ generated by the null model for each site. As such, SES_R is the standardized effect size for RaoQ. The null models were permutated 1000 times using the "independent swap" algorithm of Gotelli (2000). This method maintains the species richness in each permutation while randomizing each species' occurrence at each site. The null model generation was performed in R (R Core Team, 2020) using the 'picante' package (Kembel et al.

2010) following Plass-Johnson et al. (2016). RaoQ and Gower's distance were also calculated in R using the package FD (Laliberté, Legendre, and Shipley 2014).

3.2.6. *Assessing Relationships Between Habitat Structural Complexity and Functional Diversity*

To determine whether habitat complexity had an effect on the functional diversity (RaoQ) of our sites, we regressed RaoQ against several habitat complexity metrics that were derived from the analysis of digital elevation maps (DEMs) of our sites in ArcMap. Surface complexity, measured by the SAPA ratio, as well as slope, curvature, and relief were all used as habitat complexity metrics. Residuals were assessed for normality using the Shapiro-Wilks test and collinearity was assessed using the variance inflation factors (VIF). Metrics with a VIF of greater than 5 were considered collinear. In addition, we fitted linear mixed - effect models (LMM) to our data using the lme4 package in R (Bates et al. 2015) to account for any structured variation in the data based on similarities of sites within reefs and to avoid pseudo-replication. Model fits were assessed using the corrected Akaike criterion (Sakamoto, Ishiguro, and Kitagawa 1986). Based on the corrected Akaike criterion (AICc) values, models within 2 AICc units of each other were considered indistinguishable.

3.2.7. *Assessing Community Composition Among Sites*

To determine any similarities or differences in the community composition among sites and reefs, as well as to determine which taxonomic groups and functional traits were driving those similarities or differences, we performed analysis of similarity (ANOSIM) tests and displayed our results using non-metric multidimensional scaling biplots (NMDS). NMDS was chosen over other ordination techniques because it is non – metric and makes no assumptions about the data which was useful for us since our counts data were not normally distributed. Additionally, NMDS can accurately position samples that are in multidimensional space along two dimensions by correcting the 2D distances between samples for any additional distances in the third or fourth dimension. In other words, NMDS can accurately visualize the clustering of multidimensional data in two dimensions. Additionally, the NMDS axes are unitless and simply indicate the similarity or dissimilarity of data points. This allows for additional data vectors such as, environmental gradients to be overlaid onto the biplots to examine whether those gradients have the potential to explain the clustering patterns. In our case, we overlaid the gradients of our 3D complexity metrics.

Both ANOSIM tests and NMDS plots were first conducted on the species by abundance data and then on the functional traits by abundance data. For each analysis, we used the Bray-Curtis method to calculate a distance matrix among groups (De Cáceres, Legendre, and He 2013). Additionally, we performed a stress test to determine the optimal number of axes that explain the patterns in our data. Stress test values of less than 0.2 were considered adequate for explaining the variation in the data. Lastly, we overlaid vectors for the 3D complexity metrics (surface complexity (SAPA ratio), slope, curvature, and relief metrics) onto the NMDS plots when they had a significant relationship with the observed species and trait compositions among sites. The NMDS and ANOSIM analyses was performed in R (R Core Team 2020) using the packages vegan (Oksanen et al. 2019) and ape (Paradis and Schliep 2019).

3.3. Results

3.3.1. Taxonomic Groups

A total of 3198 individual organisms were counted and arranged into 41 taxonomic groups. Animals that could not be identified to the species level were grouped into the next highest taxonomic group. Out of the 41 groups, there were three genera, two families, one infraorder, 2 classes, and one phylum (Supplemental Table S.1.2.). The other 32 groups were species. Non-reef building sponges were grouped together as Porifera, except for four pipe cleaner sponges (*Lycopodina occidentalis*) and one demosponge (Demospongiae). Reef building sponges were not included in the analyses as they were considered to be the physical structures that provided habitat for the other organisms. Mean taxonomic richness was similar between the DI (10 ± 3 groups), DO (9.2 ± 1.48 groups), and PI (9.4 ± 1.52 groups) reefs.

3.3.2. Assessing Functional Variability

Null models generated 1000 new simulated communities for each of the 15 reef sites. The distribution of simulated functional diversity (RaoQ) as well as the observed RaoQ values for each site are shown in Figure 3.4. Simulated RaoQ appeared highly variable (wide range) at all survey sites with no visible difference between sites or reefs (Fig. 3.4. A). Observed RaoQ values fell within the 95% quantile and 2 SES of the simulated RaoQ values for all the reef sites (Fig. 3.4. B) except site 14 on the Passage Island reef indicating that at site 14, the structuring of the functional community was nonrandom. In other words, the significantly higher than expected observed RaoQ value at site 14 was a result of one or more underlying non-random factor(s) driving the functional diversity.

3.3.3. Surface Complexity and Functional Diversity

Rao's Q showed a decreasing trend with increasing habitat complexity; however, the relationship was significant only in the case of curvature (F = 6.09, p = 0.03, R^2 = 0.32) with a low coefficient of determination (R^2 = 0.32) indicating high variability (Fig 3.5.). When assessing which combination of complexity metrics had the best fit, combinations with curvature and one other metric consistently yielded the lowest AICc values which were similar to those of the curvature linear model alone and had significantly better fits than the combinations of other metrics (Table 3.2.). The curvature linear model alone had an AICc value of -70.88.

When only the invertebrate traits were assessed, Rao's Q also showed a decreasing trend with increasing habitat complexity and had significant relationships with all but the curvature metric (Fig 3.6.). Similarly, a large number of combinations of complexity metrics had significant relationships with RaoQ but the best fitting models included slope and one other metric (Table 3.2.). Slope alone had the best fit with an AICc value of -71.90.

When assessing the fish traits alone, Rao's Q could only be calculated for 9 of the survey sites due to low fish abundances over the other sites. Rao's Q did not have any significant relationships with any of the individual complexity metrics (Fig 3.7.) or any combination of metrics (Table 3.2.). Generally, the relationships were highly variable with large 95% confidence bands and very low coefficients of determination (Fig 3.7.).

Despite the normal distribution of residuals for all linear models, we attempted to account for any inherent structure in the variability of our Rao's Q values due to reef specific similarities between sites. However, the mixed effect linear models (LMM) had lower AICc values than their linear counterparts.

3.3.4. Assessing community composition

There were no differences in the assemblages of taxonomic groups between reefs (Fig 3.8.). Similarly, the three reefs had similar functional assemblages (Fig 3.9. and Fig 3.11.) except in the case of fish taxonomic groups and traits (Fig 3.12. and Fig 3.13.). The fish taxonomic and functional communities were significantly different on the Passage Island Reef from those on the two Defence Islands reefs (Fig 3.12. and Fig 3.13). This aligns with our in – water observations of higher fish species richness and fish abundances on the Passage Island (PI) reef.

The taxonomic communities were very similar at all sites of the PI reef, illustrated by the tight clustering of PI sites relative to those from the Defence Islands reefs, except for site 13 which appeared to be an outlier (Fig. 3.8. B). The similarity in taxonomic communities between the other four PI sites appeared to be driven by an abundance of vertebrate species, primarily rockfishes (*Sebastes spp*.) and shiner perch (*Cymatogaster aggregata*). An abundance of

invertebrate species, including the vermilion star (*Mediaster aequalis*) and the squat lobster (*Munida quadrispina*), also drove the pattern of similarity between communities on the PI reef. In contrast, site specific taxonomic community composition varied greatly on the Defence Islands reefs. Differences in taxonomic community composition among DI sites were driven by different abundances of crustaceans vs. soft bodied invertebrates. Similarities among sites 1, 4, and 5 can be attributed to high abundances of sponge eualids (*Eualus spp.*), decorator crabs (*Chorilia longipes*), as well as isopods, whereas similarities among sites 2 and 3 can be attributed to high abundances of hydroids, worms (*Terebellida spp.* and *Myxicola infundibulum*), and tunicates (*Styela gibbsii*) (Fig 3.8. and Fig 3.10.). Communities within the DO reef were very different between sites (sites were spread out the most on the NMDS plot; Fig 3.8. B) consisting of vertebrates, crustaceans, and soft-bodied invertebrates. The lack of reef specific community clustering indicates that drivers of community composition are on the reef - patch scale, not on the reef scale.

Functional community composition was also driven by factors at the reef – patch scale, as evident from the large differences in functional composition within the three reefs (Fig. 3.9). Unlike taxonomic community composition, more of the variation in functional composition was explained by one non-metric multidimensional scale, indicating that either a narrow set of environmental gradients were structuring the observed functional communities across all three reefs or that the functional communities were highly redundant among many of the sites. Three visible clusters were apparent. Sites 2, 3, 9, and 13 were dominated by zooplanktivores, crustaceavores, and piscivores, and schooling behavior was predominantly observed at these sites. The second cluster included sites 1, 4, 5, and 7, which were dominated by crevice-dwelling benthivores, detritivores, and planktivores. The third cluster made up of sites 6, 8, 10, 11, 12, 14, and 15, were evenly composed of active schooling predators and more passive, benthic-dwelling detritivores and benthivores.

The shift in functional composition from schooling predators to benthic detritivores appeared to be strongly correlated with surface complexity (SAPA ratio: Fig 3.9.), indicating that surface complexity has the potential to drive abundances of animals that live directly on the glass sponges and feed on decaying matter that accumulates on or around the sponges. While slope also exerted significant pressure on the functional composition, it appeared to affect the habitat use traits more than the dietary traits. For instance, differences between schooling and crevice dwelling communities were better explained by a slope gradient while differences between zooplanktivores and detritivores were better explained by surface complexity.

SAPA and slope had significant impacts on the taxonomic and functional community structure of reefs (Fig 3.8. – 3.13.). Relief also had a significant relationship with community composition for all but the invertebrate communities (Fig 3.10). On the other hand, curvature did not appear to be a potential driver of community structure for any of the taxonomic or functional assemblages despite its significant negative relationship with RaoQ (Fig 3.5.). Out of the three reef structural complexity metrics measured in our 3D models, surface complexity (SAPA ratio) had the most significant relationship with community composition, indicating that it is potentially the strongest driver of community structure. Surface complexity appeared to drive differences in communities on the DI reef, with sites 1, 4, and 5 having higher SAPA ratios than sites 2 and 3 (Fig 3.8. B). Sites 2, 3, 9, and 13 were relatively flat reef patches, primarily covered by dead sponge rubble. While slope had a similar effect to surface complexity, it had a stronger influence on the vertebrate community structure, driving abundances of rockfishes (Fig 3.8. B and Fig 3.12.). Slope also seemed to drive abundances of squat lobsters, more so than surface complexity (Fig 3.8. B and Fig 3.10).

3.4. Discussion

One of the drawbacks of using classical biodiversity measurements (e.g., Shannon-Wiener Index) is that they assume that all species are equal and all individuals are the same (Magurran 2004). However, individuals of the same species can vary in size and morphology as well as different species can provide different ecosystem goods and services (Diaz et al. 2008). Therefore, species are not all equal in their effects on ecosystem function. This study is the first to characterize the functional communities on glass sponge reefs in British Columbia and is the first to relate functional community structure to 3D habitat complexity. While the results are data-limited (i.e. data came from three reefs with a total of 15 sites) and our conclusions about which functional traits contribute most to differences in functional diversity across a reef's structural complexity gradient are restricted to glass sponge reefs in Howe Sound, this study has provided a baseline of reef structural and functional condition for the Passage Island reef as well as the East Defence Islands complex. Additionally, this study has established a workflow for assessing relationships between the 3D habitat and its inhabiting megafaunal community which can be applied to other reefs in the Strait of Georgia and the Hecate Strait.

3.4.1. Functional Diversity (Rao's Q)

Contrary to our hypothesis, functional diversity (Rao's Q index) decreased with increasing 3D metrics of habitat complexity. This relationship was only significant with curvature (Fig 3.5.) and marginally insignificant with surface complexity (SAPA) and slope. It is

important to note that all four relationships (Rao's Q vs curvature, SAPA, relief, and slope; Fig 3.5.) were highly variability, as evident from the relatively low coefficients of determination (R^2), suggesting that either the data were inherently variable, that this study was data limited, or both. Interestingly, when the functional diversity of invertebrates traits was analyzed (Fig. 3.6.), Rao's Q decreased significantly with increasing surface complexity (SAPA), slope, and relief, but not curvature. These three significant relationships also had higher coefficients of variation (Fig 3.6.) than their counterpart relationships with the full functional diversity (all traits included; Fig 3.5.). The opposite was true for the relationships with the functional diversity of fish traits which were all insignificant and even more variable (Fig 3.7.) than the relationships with the full diversity (Fig 3.6). These results suggest that the functional diversity of the three reefs in Howe Sound was primarily driven by the invertebrate functional traits. This is unsurprising considering the disproportionately higher abundances and species richness of invertebrates observed on our sites relative to fish abundances and richness. Additionally, many of the sites had so few fish that Roa's Q for fish functional diversity could not be calculated. These findings also highlight the importance of clearly defining the part of an ecological community for which functional diversity is assessed. Different groups of animals within a community will inherently have very dissimilar traits so lumping all the traits into the same analysis may obscure underlying relationships. In this study, we observed an interaction effect where the community - wide functional diversity had a strong relationship with curvature, however, neither the invertebrate community's nor the fish community's functional diversities alone showed the same trend. Subsequent analyses (Fig 3.8. – 3.13.) showed no indication that curvature had any effect on the functional community compositions. Curvature alone may be a poor indicator of how the functional community is structured or whether it is diverse or not but curvature did appear to be a good covariate of habitat complexity (Table 3.2.).

While few aquatic and marine studies have investigated the effects of environmental gradients, such as, habitat complexity, on the functional diversity of communities, one study's results show some resemblance to the results of our study. Plass-Johnson et al. (2016) surveyed coral reef fish along transects in the Spermonde Archipelago and found that many of the individual life-history traits were negatively correlated to rugosity and live coral cover. As was the case in our study, their results had weak relationships that were highly variable despite having a sample size of 25 reefs with 60 transects. However, Plass-Johnson et al. (2016) did not investigate the relationships of rugosity and live coral cover with absolute functional diversity. Instead, they investigated the effects of environmental gradients on the standardized effect size

(SES) of functional diversity (see Methods section 3.2.5.) but found not apparent trends (Plass-Johnson et al. 2016).

On the contrary, a number of studies in terrestrial habitats have reported increases in functional diversity with increasing habitat heterogeneity. For example, Nooten et al. (2019) studied the functional traits of ants in urban green spaces and parks and found strong positive relationships between ant traits and vegetation characteristics, such as, tree biomass and density, shrub density, and herb cover. Riemann et al. (2017) studied frog functional traits in dense forests, fragmented forests, and cultivated farm land and found higher functional richness in the more structurally complex and heterogeneous dense forests. Yet, studies in aquatic environments appear to have weak trends or inconclusive relationships between habitat complexity and functional diversity. Verdonschot, Didderen, and Verdonschot (2012) planted inanimate replicas of macrophytes into water bogged ditched and canals to observe the settling macroinvertebrate community. While certain macroinvertebrate traits were strongly correlated to specific macrophyte morphologies, overall, macroinvertebrate functional diversity did not increase with macrophyte structural complexity.

A potential explanation for the disparity in results and conclusions between terrestrial and aquatic studies, may be the differences in how Rao's Q is calculated from study to study. Rao's Q relies on a dissimilarity matrix where certain traits are assigned weights that dictate their relative importance and hence their similarity to other traits. The assignment of weights to traits is arbitrary and at the observer's discretion. This means that the same traits can be assigned different weights in different environments based on expert opinion. Secondly, the inclusion of traits in the overall calculation of Rao's Q is also arbitrary and will inevitably depend on the research question (discussed earlier in this section). As is shown in this study, the outcome of the analysis was dependent on which traits were included. For example, Rao's Q had a negative correlation with curvature when only the invertebrate traits were included in the analysis, however, when fish traits were used, Rao's Q had a weak but positive correlation.

The null models predicted a significantly lower RaoQ value than observed on site 14. Site 14 on the PI reef, was one of the more structurally complex sites and had higher species abundances than the other PI sites but with similar species richness. The relatively low diversity in traits on site 14 is most likely the reason for the low simulated Rao's Q index. This poses the question of whether increasing habitat complexity simply increases species/trait abundances or whether it also increases functional diversity. Evidence from this study suggests the former case. With a disproportionate increase in abundances of a few species/traits, Rao's Q decreases

despite the presence of more animals on a reef patch that has more surface area to accommodate those animals.

3.4.2. Community Compositions

There was little structuring of taxonomic and functional communities at the reef level. All three reefs had similar communities (Fig 3.8. – 3.11.) indicating that differences in communities were site specific within a reef and that factors at the reef – patch spatial scale were influencing the combinations and abundances of taxonomic groups and functional traits. However, during the analysis of fish traits alone, community structuring at the whole reef spatial scale was revealed (Fig 3.13.). Fish functional composition was significantly different at the PI reef from those at the DI and DO reefs. This difference was driven by an abundance of highly mobile fish that exhibited schooling behavior on the PI reef and could opportunistically feed on both benthic as well as pelagic prey. Communities on the DI and DO reefs appeared to be driven by abundances of fish that were constrained to the seafloor and fed solely on benthic crustaceans. The two East Defence Islands reefs (DI and DO) are located approximately 100 m apart, however, the Passage Island (PI) reef is located some 20 – 25 km away from the other two reefs (Fig 3.1. A). It would be relatively easy for even the benthic fish species to mix between the two East Defence Islands reefs but less so with the PI reef species. Additionally, the geographic proximity of the PI reef to the Strait of Georgia (SoG) may result in the mixing of fish populations from Howe Sound and the SoG, consequently increasing the fish species richness and abundances at the PI reef. The differences in fish community compositions among reefs were not reflected in the taxonomic analysis (Fig 3.8.) because site 13 influenced the overall reef community structure. Site 13 was a flat reef patch containing dead sponge rubble buried under fine sediment. Site 13 had a disproportionately lower abundance of fish relative to invertebrates compared to the other PI sites. These fish were a group of wandering shiner perch (*Cymatogaster aggregate*) that swam above 5 m from the reef bottom and but occasionally dipped down to within 5 m above the reef. Additionally, the invertebrate species of site 13 were dominated by *Myxicola spp.* worms. Without site 13, the other four PI sites formed a relatively tight cluster without any overlap with the other 10 East Defence Islands sites. Consequently, the communities at the four PI sites (excluding site 13) were driven by abundances of rockfishes (*Sebastes spp.*) and shiner perch (*Cymatogaster aggregate*) which corresponded to the schooling, bentho – pelagic, opportunistic fish feeding traits (Fig 3.13.). On the other hand, the two East Defence Islands reefs had higher relative abundances of benthic fish species, such as, the lingcod (*Ophiodon elongatus*) and the kelp greenling (*Hexagrammos decagrammus*) that feed on benthic crustaceans.

Despite having the strongest relationship with the whole community - level functional diversity, curvature did not correlate with differences in taxonomic or functional community compositions among sites which indicates that curvature does not have the potential to structure glass sponge reef communities (Fig 3.8. – 3.13.). Instead, surface complexity (SAPA), relief, and slope all influenced differences in the functional and taxonomic communities with SAPA having the strongest effect on invertebrate species that use the sponge as refuge (Fig 3.8. and Fig 3.11.). All three metrics also significantly impacted the differences in functional assemblages of fish (Fig. 3.11.). However, the fish traits were all narrowly aligned along a single NMDS axis while the 3D complexity metric vectors aligned along the second NMDS axis. It is likely that the fish functional assemblages were composed of redundant functional traits that did not show a wide distribution along the 3D metric gradients and consequently indicated a weak relationship between the structuring of our chosen fish traits and the analyzed 3D metrics. Once again, this could be related to the inherent variability of the fish traits data (Plass-Johnson et al. 2016) or it could be attributed to the lower weights assigned to fish habitat use traits. Since most fish are highly mobile and are not confined to a small reef patch, tracking their habitat use preferences would not yield ecologically meaningful information. Perhaps, drivers of fish functional assemblages are related to prey availability, specifically, the invertebrate community assemblages. It is clear that higher surface area increases the abundances of crustacean invertebrate species, such as, sponge eualids (*Eualus spp.*), spot prawns (*Pandalus platyceros*), and gammarid amphipods which in turn possess traits, such as, benthic detritivore, benthivore, and planktivore. These higher abundances of a few select crustaceans are likely lowering the biodiversity and functional diversity with a reef patch. However, the productivity of such reef patches is high and is likely what attracts predators, such as rockfishes to these reef patches.

Whether the crustacean invertebrates use the sponges as refuge or not is a question that needs to be examined directly. An alternative explanation to the higher abundances of these animals on reef patches with higher surface area is that there may be a greater availability of detritus on the reef patches for the crustaceans to feed on. This detritus could be deposited on the sponges which baffle the ambient currents and create a physical trap with high surface area to catch passing by detritus. Glass sponges have been documented to accumulate a lot of particulate matter on their outer walls (Leys and Lauzon 1998; Barthel and Wolfrath 1989) and have adapted sloughing mechanisms to shed the particulate matter. These mechanisms have never been reported on reef-building sponges but perhaps these sponges have a symbiotic relationship with their small inhabiting detritivore crustaceans.

3.5. Conclusions

Functional diversity, measured by Rao's Q index, of invertebrate species decreases as the SAPA ratio, slope, and relief of a glass sponge reef patch increase. The functional diversity of fish traits has no relationship with 3D structural complexity. Community wide functional diversity has a significant negative relationship with curvature but this relationship is likely obscuring interaction effects with other 3D complexity metrics and among different functional entities of a glass sponge reefs community. Benthic detritivores, such as sponge eualids (*Eualus spp.*), and spot prawns (*Pandalus platyceros*) have a positive relationship with 3D habitat complexity metrics SAPA, relief, and slope. Benthopelagic crustaceavores, such as rockfishes (*Sebastes spp.*) also have a positive relationship with the three complexity metrics but are more strongly associated with slope. While functional diversity has a weak relationship with 3D habitat complexity metrics, individual traits are likely being driven by these metrics so it is more useful to examine reef community functional compositions instead of relying on the functional diversity index alone for insight on the functional status of the reef's community.

3.6. Acknowledgments

3.7. Financial Support

Table 3.1. Functional Traits Assignment and Justification. Summary of the main functional traits used in our analysis of functional diversity and community composition. Assigned weights were used in the calculation of Gower's distance.

Trait group	Justification and Functional Significance	Traits and Definitions	Assigned Weight
Dietary preference	Assigned based on the most important dietary constituents. Dietary traits plays an important role in regulating food web structure and network topology (Archer et al. 2020; Chu and Leys 2012), nutrient cycling (Kahn, Chu, and Leys 2018), and their direct link to primary production (Yahel, Eerkes-Medrano, and Leys 2006; Kahn et al. 2015). This is why they were weighed	**Filter feeder** - filters organic matter or minute organisms from the water	3
		Detritivore - feeds on dead and decaying matter on the seafloor	3
		Planktivore - feeds on phytoplankton and zooplankton	3
		Zooplanktivore - feeds on zooplankton	3
		Piscivore - feeds on fish	3
		Benthivore - feeds on exclusively benthic prey	3
		Spongivore - feeds on sponges	3
		Crustaceavore - feeds on crustaceans	3
Habitat use	Assigned based on the most common habitat types that the species are found living in/on. These can be highly variable for a single species depending on social structure (schooling rockfish vs single rockfish), life stage (Marliave et al. 2009), season (Marliave and Borden 2020) as well as time of day and depth (Jamieson and Pikitch 1988; Chew et al. 1973).	**Schooling** - behavioural grouping together of highly mobile, pelagic fish	2
		Benthic - live exclusively on the seafloor/benthos	2
		Bentho-pelagic - live on or near the bottom but occasionally float in the water column	2
		Crevice dwelling - live in holes, cracks, and crevices	2

Table 3.2. Multiple Regression Analysis Statistics. Summary of multiple regression analysis of RaoQ against habitat complexity metrics. Bolded p - values are significant (≤0.05) while bolded AICc values represent the models with the best fit only when the model represents a significant relationship. For models with a single predictor, the R^2 of the model is displayed, not the adjusted R^2.

Model	All Traits				Invertebrates				Fish			
	F	p	(Adjusted) R^2	AICc	F	p	(Adjusted) R^2	AICc	F	p	(Adjusted) R^2	AICc
SAPA	4.05	0.07	0.24	-69.19	9.42	**< 0.01**	0.42	-67.68	0.23	0.65	0.03	-50.98
Curvature	6.09	**0.03**	0.32	**-70.88**	0.84	0.38	0.06	-60.45	< 0.01	0.93	< 0.01	-50.70
Slope	4.29	0.06	0.25	-69.40	16.71	**< 0.01**	0.56	**-71.90**	0.02	0.90	< 0.01	-50.71
Relief	2.13	0.17	0.14	-67.40	4.60	**0.05**	0.26	-64.05	0.90	0.37	0.11	-51.78
SAPA + Slope	2.14	0.16	0.14	-65.87	7.72	**0.01**	0.49	-68.09	0.40	0.69	-0.18	-44.62
SAPA + Relief	1.88	0.20	0.11	-65.38	4.35	**0.04**	0.32	-63.87	1.30	0.34	0.07	-46.73
SAPA + Curvature	5.05	**0.03**	0.37	**-70.47**	4.55	**0.03**	0.34	-64.16	0.12	0.89	-0.28	-43.83
Slope + Relief	2.01	0.18	0.13	-65.64	8.74	**0.00**	0.53	-69.16	3.62	0.09	0.40	-50.61
Slope + Curvature	6.05	**0.02**	0.42	**-71.76**	8.45	**0.01**	0.52	-68.87	0.01	0.99	-0.33	-43.53
Relief + Curvature	5.42	**0.02**	0.39	**-70.96**	2.97	0.09	0.22	-61.72	0.40	0.69	-0.18	-44.61
SAPA + Slope + Relief	1.38	0.30	0.07	-61.42	5.49	**0.01**	0.49	-64.74	2.31	0.19	0.33	-39.31
SAPA + Slope + Curvature	3.70	**0.05**	0.37	-67.10	5.17	**0.02**	0.47	-64.21	0.24	0.87	-0.40	-32.70
SAPA + Relief + Curvature	3.40	0.06	0.34	-66.47	2.79	0.09	0.28	-59.51	0.86	0.52	-0.06	-35.24
Slope + Relief + Curvature	3.77	**0.04**	0.37	-67.25	5.62	**0.01**	0.50	-64.95	2.27	0.20	0.32	-39.23
SAPA + Slope + Relief + Curvature	2.58	0.10	0.31	-61.43	3.87	**0.04**	0.45	-59.21	1.94	0.27	0.32	-17.21
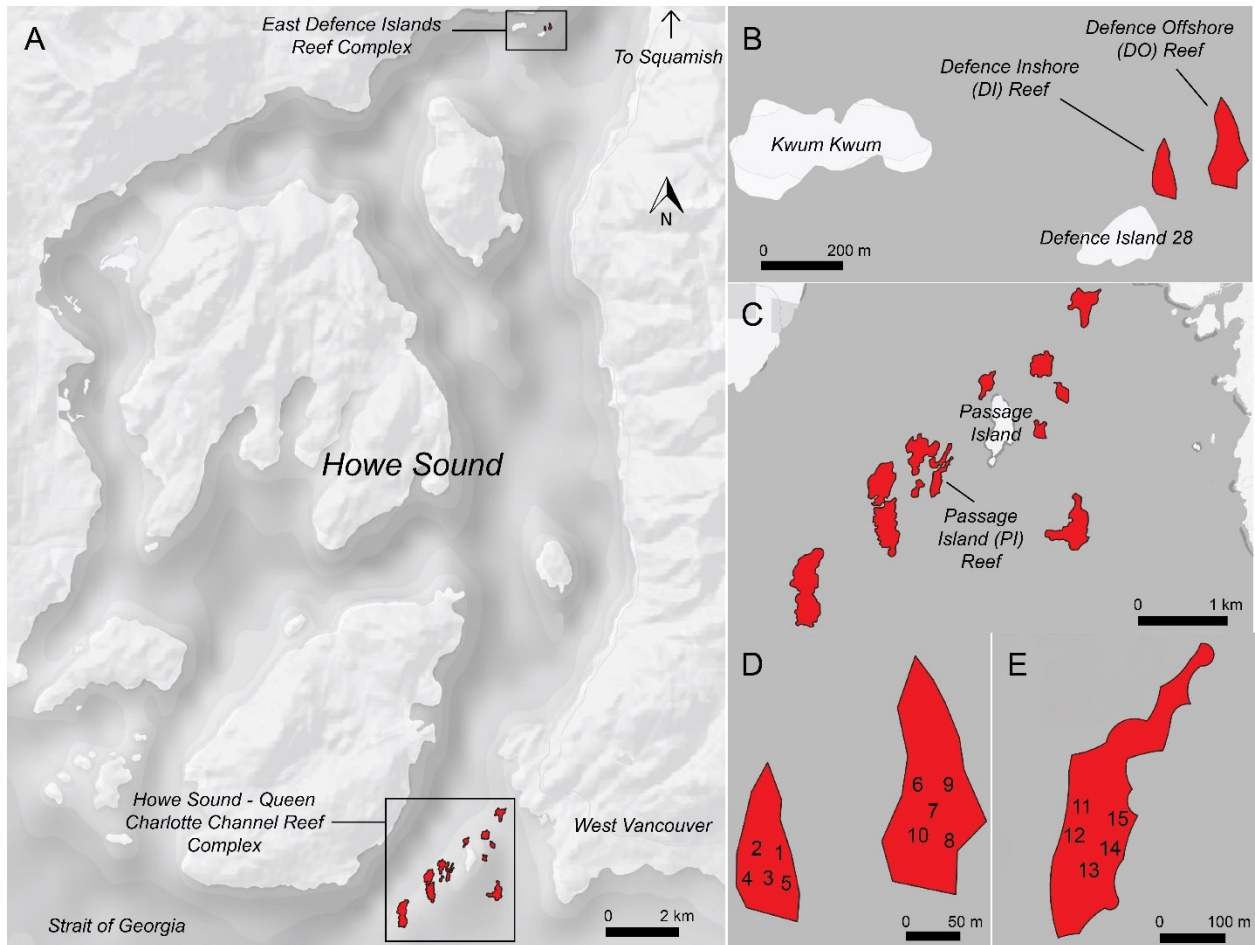
Figure 3.1. Study Location. A: Chart of Howe Sound with the East Defence Islands and Howe Sound – Queen Charlotte Channel Reef Complexes highlighted in red. B: Map of the East Defence Islands Reef Complex. C: Map of the Howe Sound – Queen Charlotte Channel Reef Complex. D: Relative positions of reef plots on the two East Defence Islands reefs. E: Relative positions of reef plots on Passage Island reef. Reef polygons were generated using shapefiles in the supplementary data of Dunham, Archer, et al. (2018).
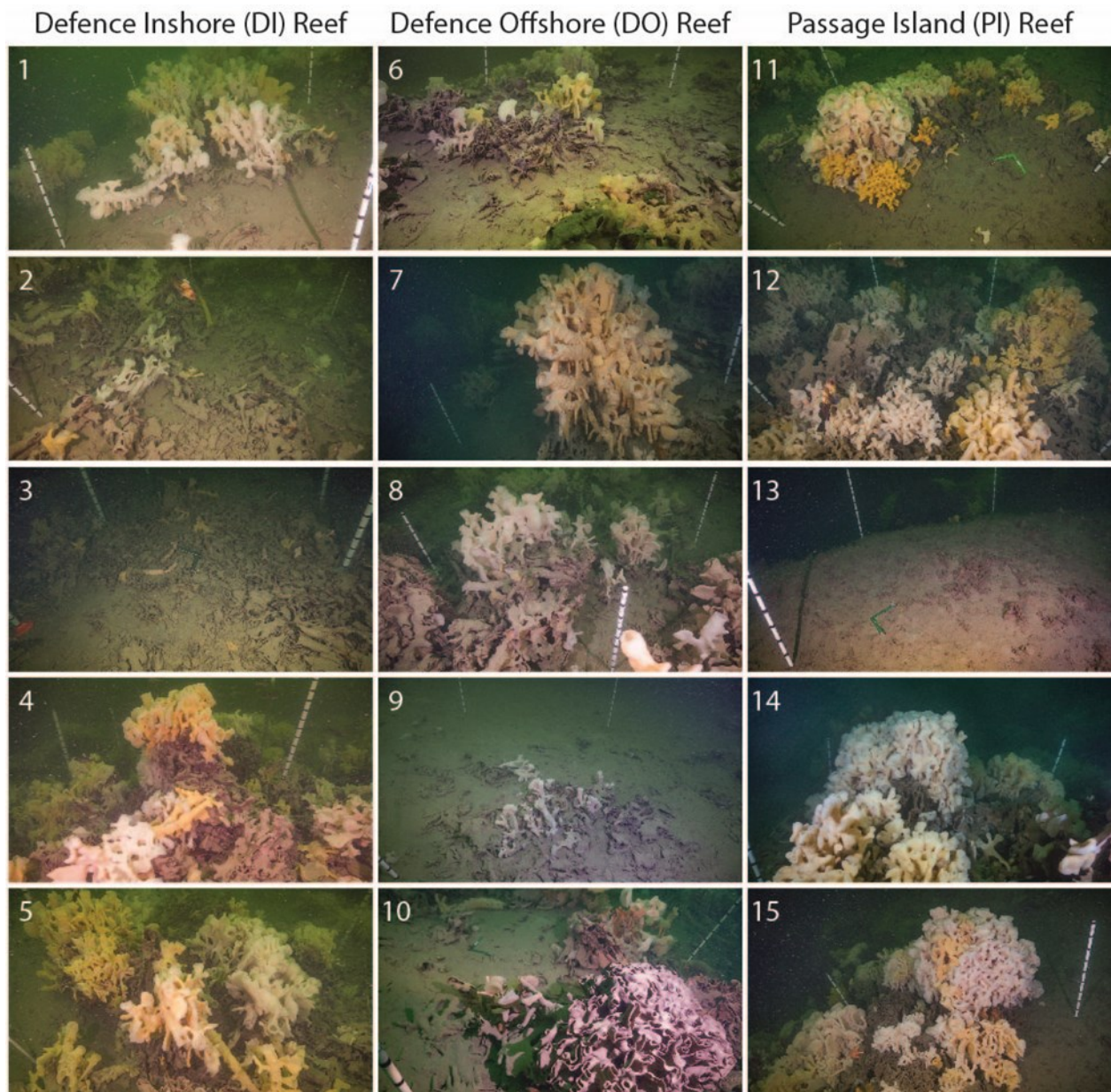
Figure 3.2. Survey Sites. Photographs of reef plots 1 to 5 on the Inshore Defence reef, 6 to 10 on the Offshore Defence reef, and 11 to 15 on the Passage Island reef.
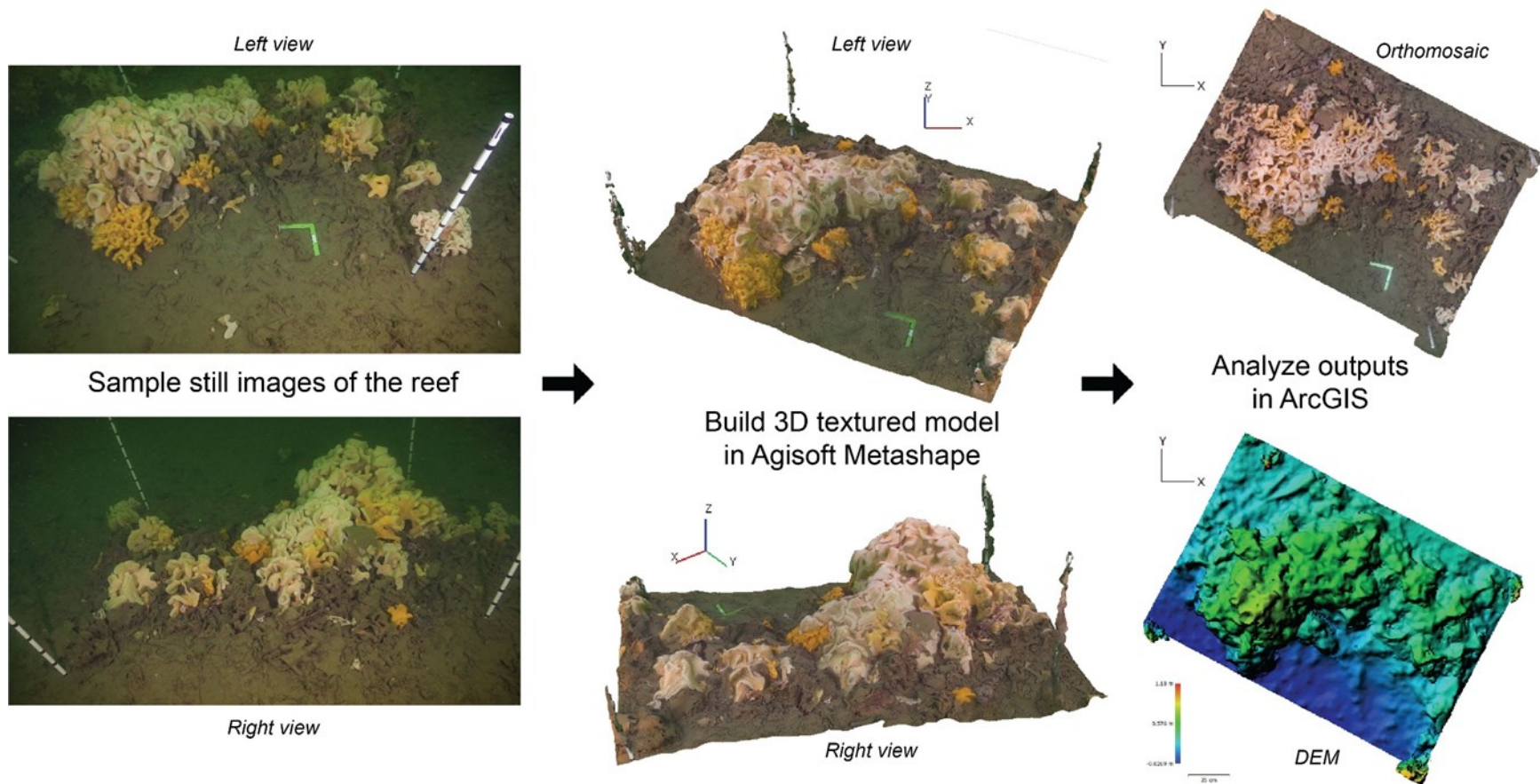
Figure 3.3. 3D SfM Modelling Protocol. Protocol for constructing 3D models of reef sites/plots to extract 3D complexity data from them. Still images were extracted from video footage of reef plots and uploaded into Agisoft Metashape. Images were aligned based on manually annotated marked PVC stakes (ground control points; GCPs) within each image. Next, a dense point cloud was generated by Metashape from each a 3D textured model was constructed. Digital elevation maps were extracted from each model and analyzed in ArcMap for structural complexity data.
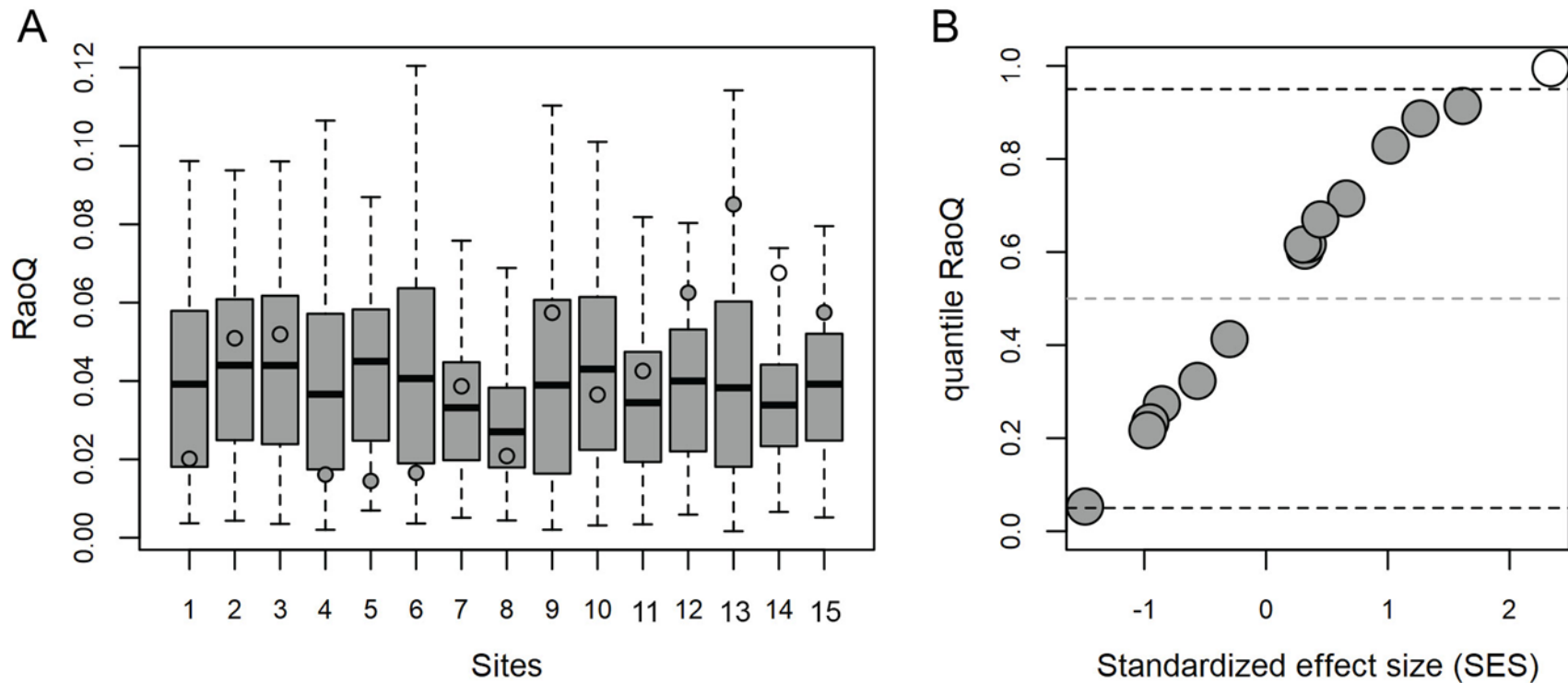
Figure 3.4. Null Model Simulations. Distributions of simulated RaoQ values from 1000 simulated communities for each of the 15 surveys sites. A: Box plot whiskers represent the ranges of simulated RaoQ values, solid lines represent the median, and the circles within each box represent the observed RaoQ based on our sampled communities. If the circle is white, then the observed RaoQ is outside of the 95% quantile of the expected simulated data. B: plot of RaoQ quantile against the standardized effect size confirms which points are outliers. The observed functional diversity of site 14 is outside of the 95% quantile for expected RaoQ values and is outside of the 2 x SES suggesting that the diversity is driven by a non-random variable.

Figure 3.5. Regression Analysis For All Traits. Linear regression models of RaoQ against habitat complexity metrics Curvature, Relief, SAPA, and Slope when RaoQ was calculated using all the traits. Red bands around the black lines of best fit represent the 95% confidence intervals and p-values colored in red indicate a significant relationship.
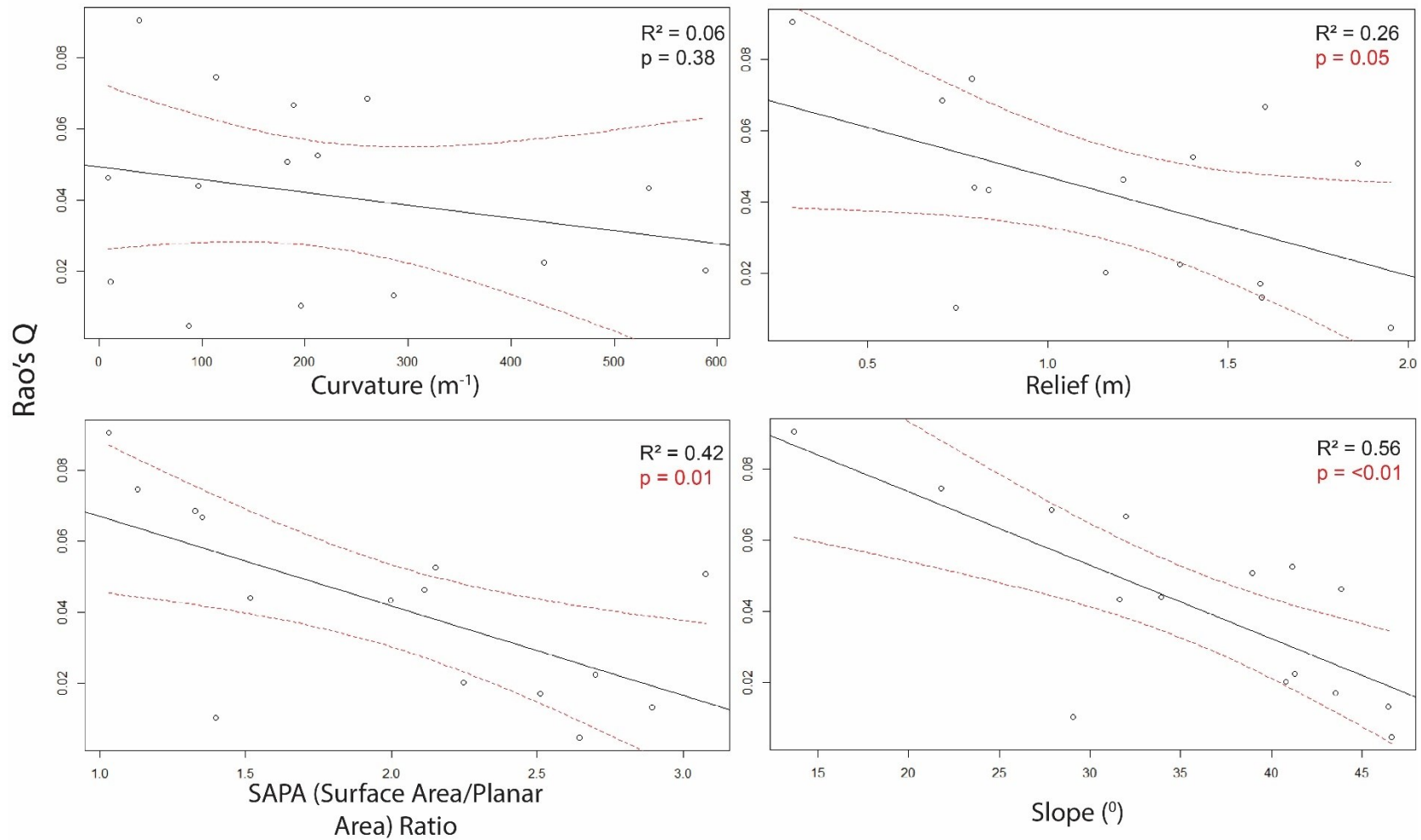
Figure 3.6. Regression Analysis For Invertebrate Traits. Linear regression models of RaoQ against habitat complexity metrics Curvature, Relief, SAPA, and Slope when RaoQ was calculated using traits of invertebrates only. Red bands around the black lines of best fit represent the 95% confidence intervals and p-values colored in red indicate a significant relationship.
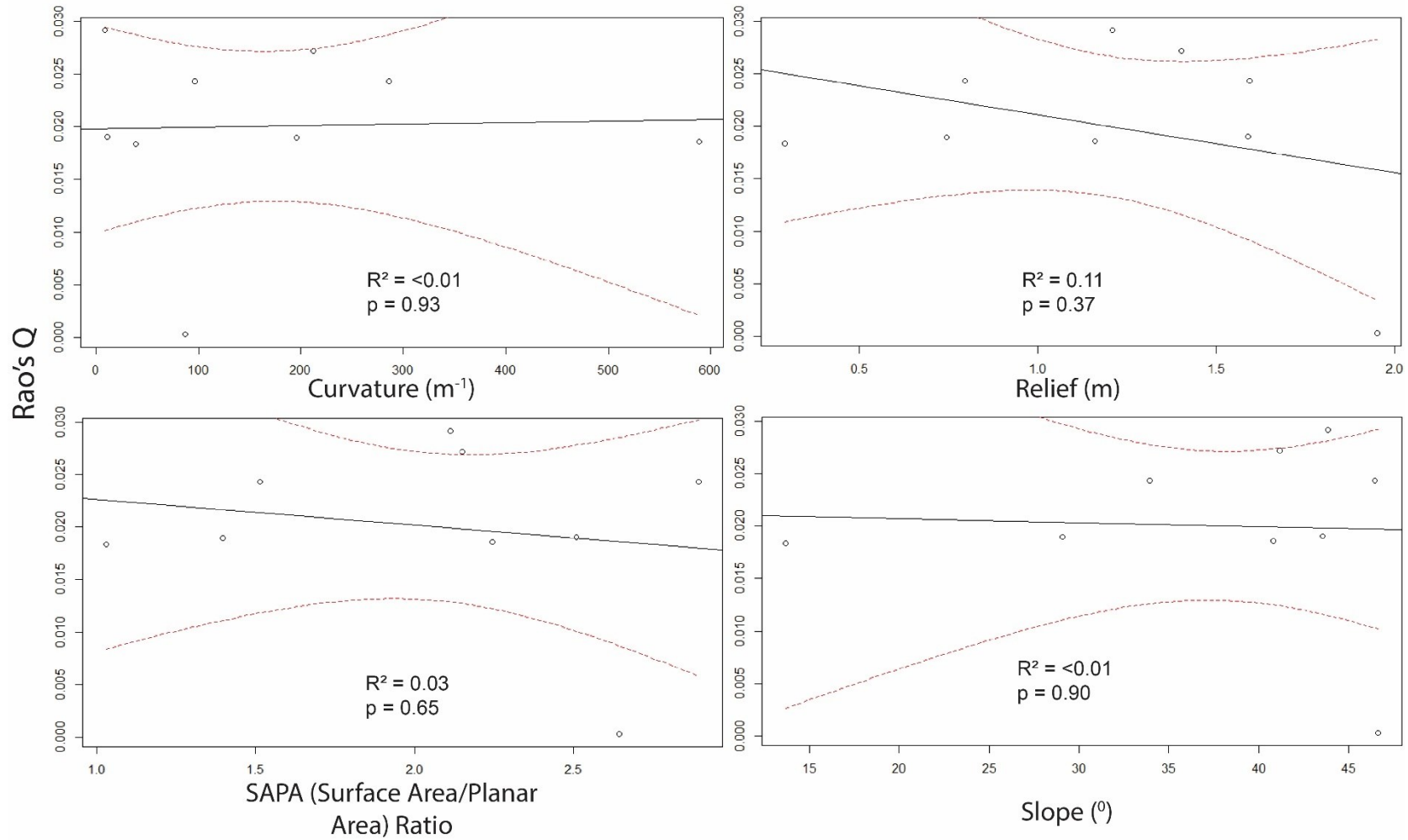
Figure 3.7. Regression Analysis For Fish Traits. Linear regression models of RaoQ against habitat complexity metrics Curvature, Relief, SAPA, and Slope when RaoQ was calcula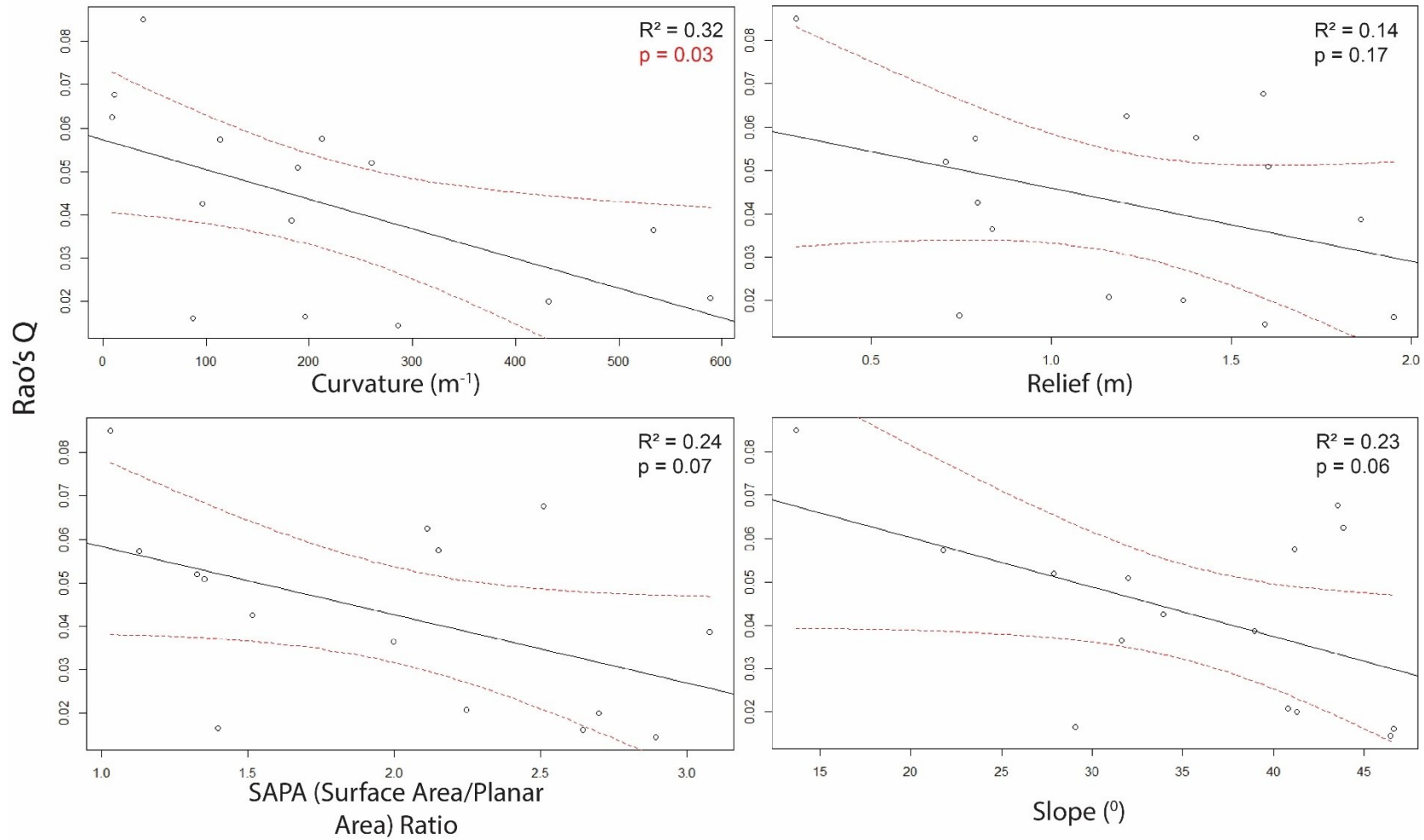ted using traits of fish only. Red bands around the black lines of best fit represent the 95% confidence intervals and p-values colored in red indicate a significant relationship.

Figure 3.8. Taxonomic Community Analysis. NMDS plots of community analysis by site for taxonomic groups. (A) shows the survey sites and taxonomic groups or functional traits in multidimensional space. The stress test result for the two NMDS dimensions is shown in the bottom right corner of plots (A). (B). shows the survey sites highlighted by reef with sites 1 - 5 on the DI reef highlighted in red, sites $6 - 10$ on the DO reef highlighted in blue, and sites $11 - 15$ on the PI reef highlighted in green. ANOSIM results for comparing the similarity in community and compositions of sites between reefs are shown in the bottom right corner. Habitat complexity metrics that are significantly correlated with community composition and potentially drive the differences/similarities in communities are overlaid as vectors in (B). R^2 and p values for the significant metrics are shown in the bottom right corner of (B). SAPA ratio, relief, and slope all had significant relationships with taxonomic community composition.
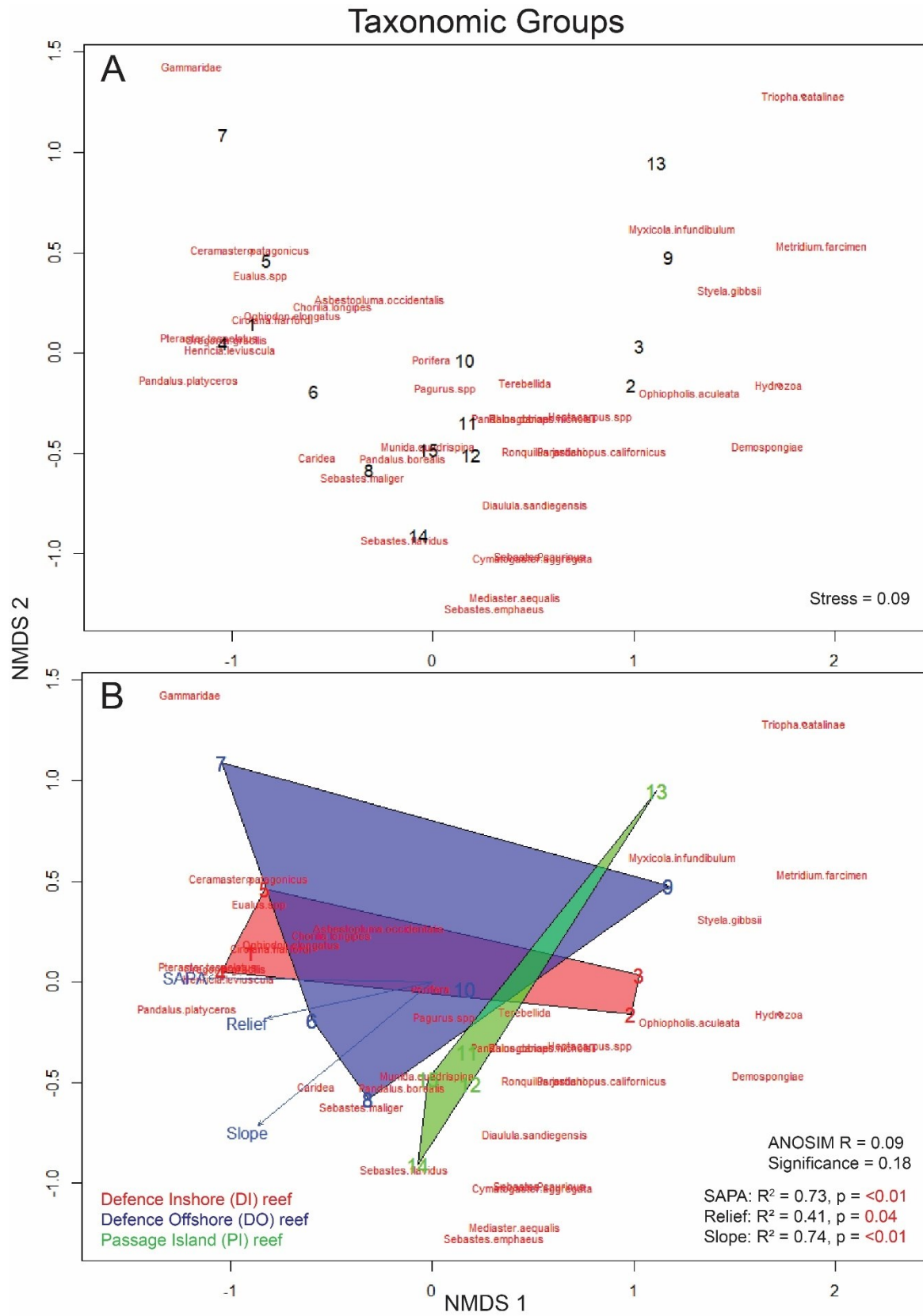
Figure 3.8. Taxonomic Community Analysis.

Figure 3.9. Functional Community Analysis. A. NMDS plots of functional traits and survey sites with the stress level for two NMDS axes. B. NMDS plot highlighting the sites within each reef and showing complexity metrics that are significantly correlated with community composition. The ANOSIM compared the communities between the three reefs.
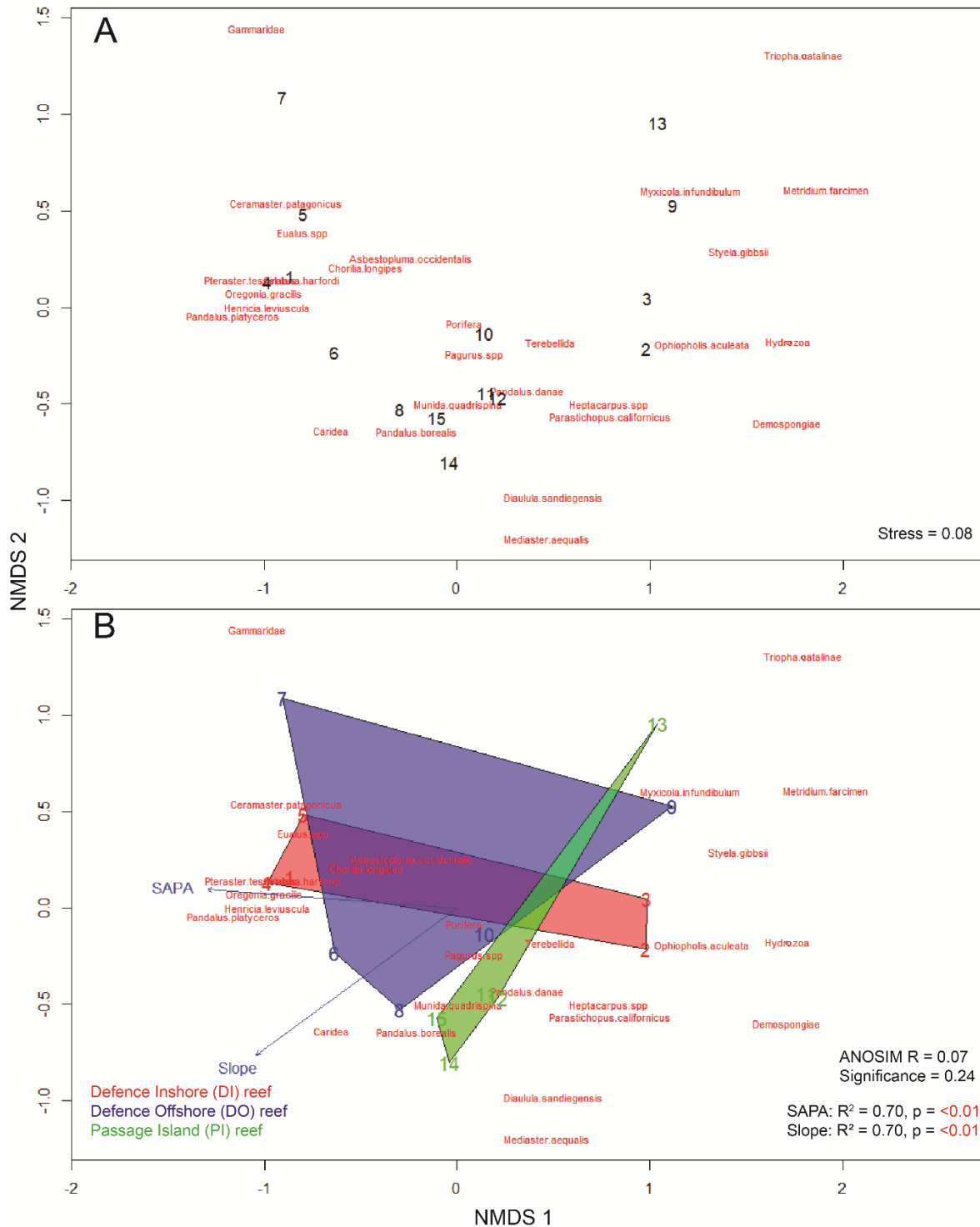
Figure 3.10. Invertebrate Community Analysis. A. NMDS plots of invertebrate species and survey sites with the stress level for two NMDS axes. B. NMDS plot highlighting the sites within each reef and showing complexity metrics that are significantly correlated with community composition. The ANOSIM compared the communities between the three reefs.
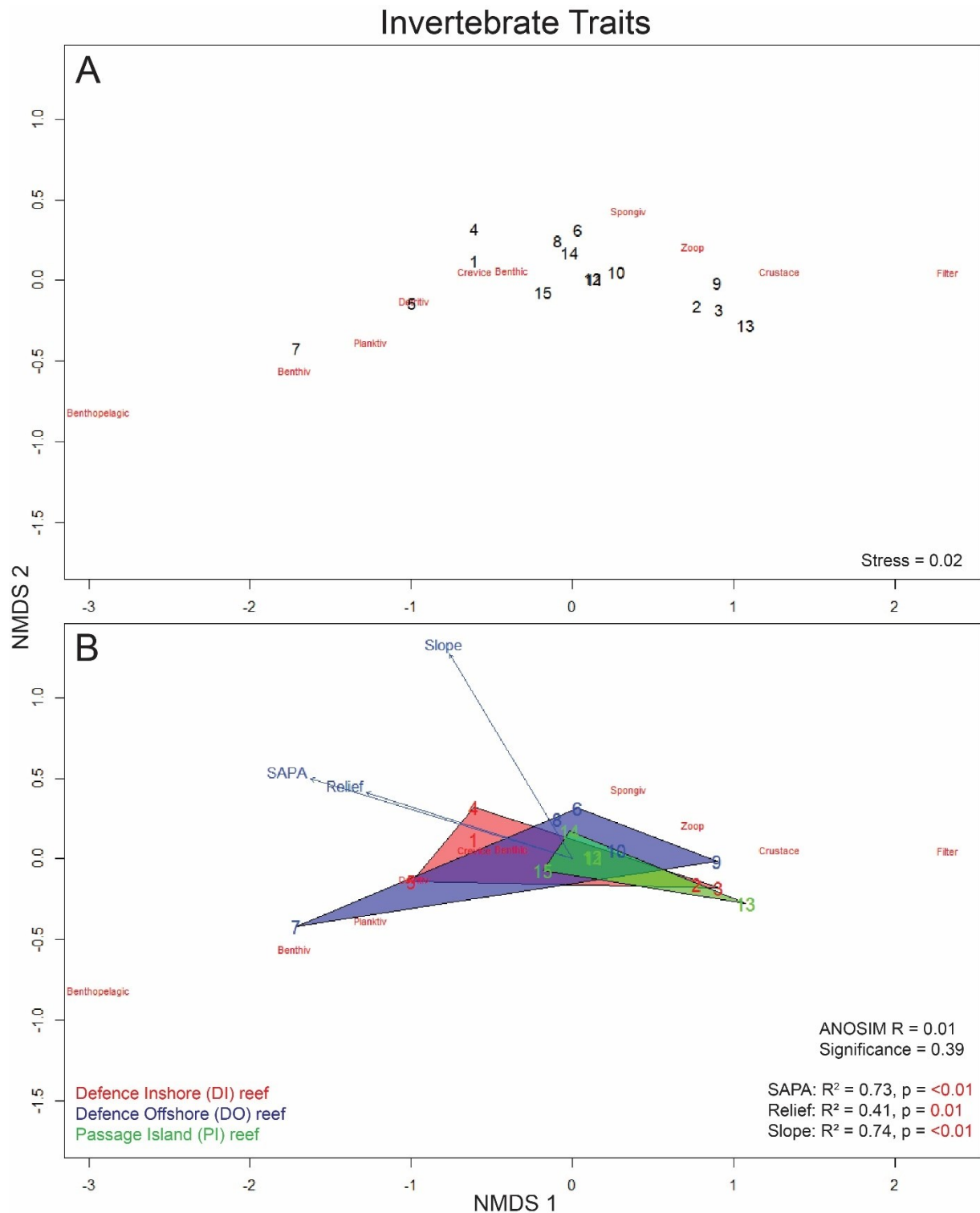
Figure 3.11. Invertebrate Traits Analysis. A. NMDS plots of invertebrate functional traits and survey sites with the stress level for two NMDS axes. B. NMDS plot highlighting the sites within each reef and showing complexity metrics that are significantly correlated with invertebrate traits composition. The ANOSIM compared the composition between the reefs.
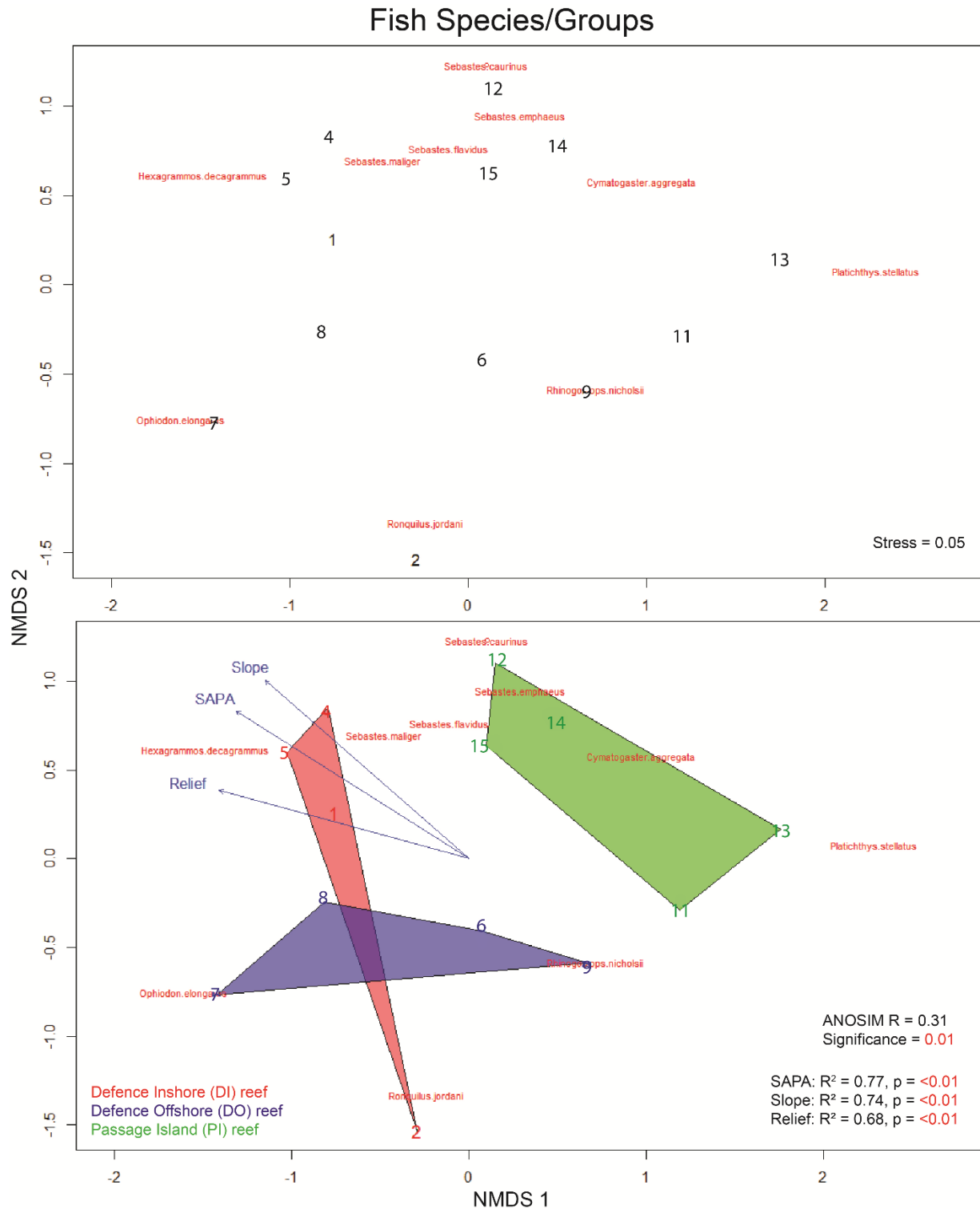
Figure 3.12. Fish Community Analysis. A. NMDS plots of fish species and survey sites with the stress level for two NMDS axes. B. NMDS plot highlighting the sites within each reef and showing complexity metrics that are significantly correlated with fish species composition. The ANOSIM compared the composition between the reefs.
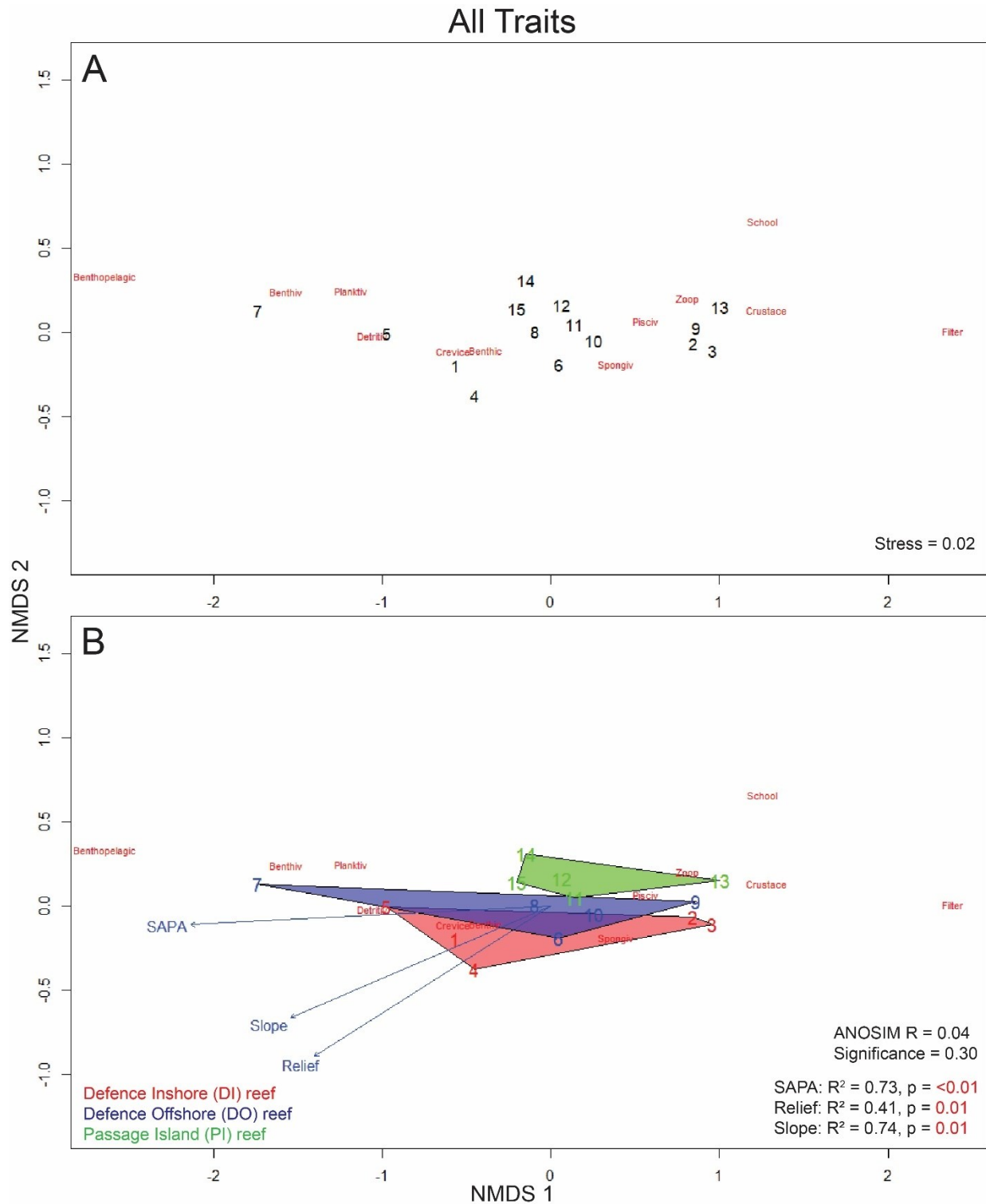
Figure 3.13. Fish Traits Analysis. A. NMDS plots of fish functional traits and survey sites with the stress level for two NMDS axes. B. NMDS plot highlighting the sites within each reef and showing complexity metrics that are significantly correlated with fish traits composition. The ANOSIM compared the composition between the reefs.
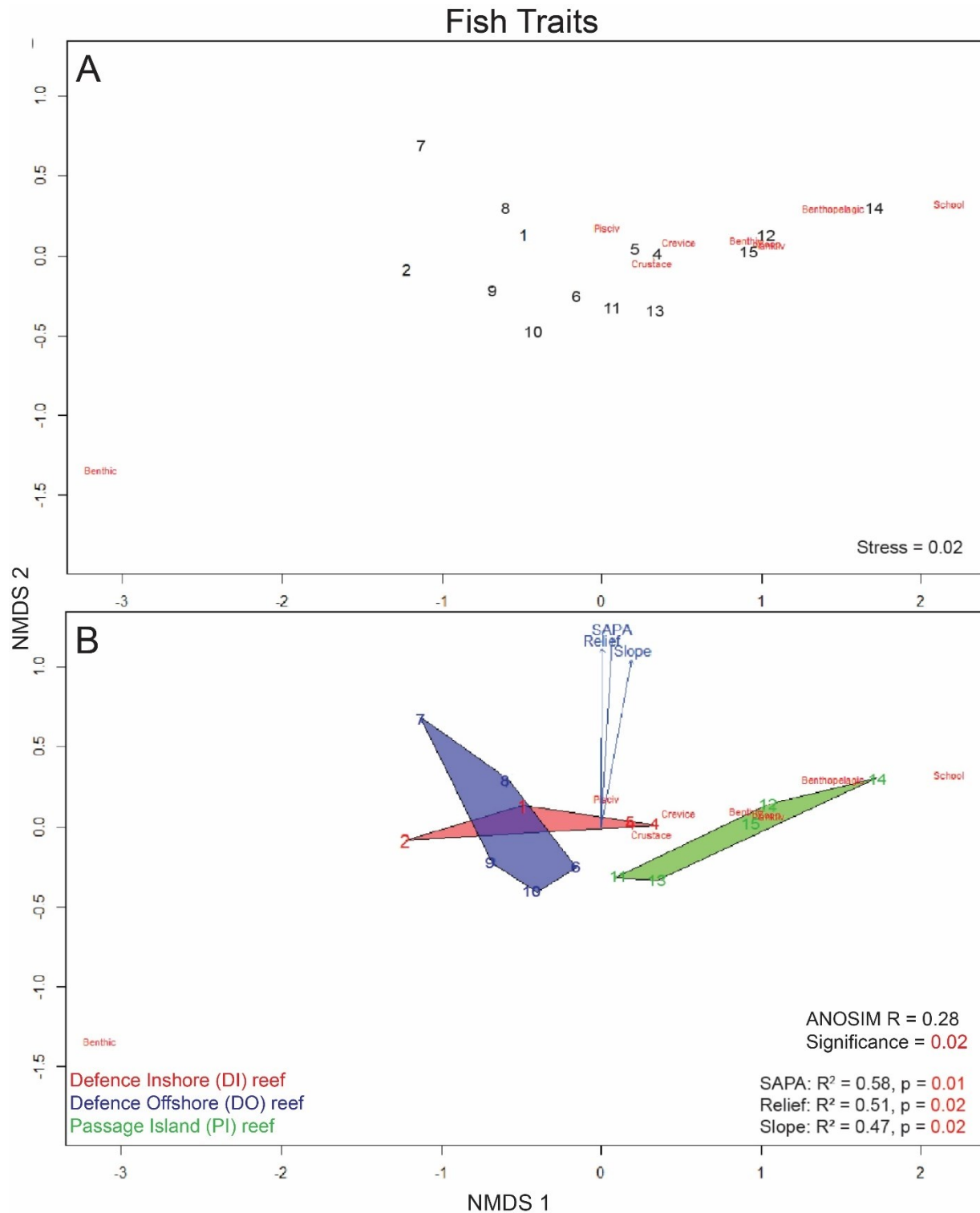
Chapter 4.   A General Discussion

4.1. Structural Complexity and Functional Complexity in Sponge Reefs

The objectives of this thesis were to 1) evaluate the efficacy of applying 3D SfM photogrammetry to the study of glass sponge reef habitat complexity, and 2) determine the relationship between 3D habitat complexity metrics and the functional reef community composition. The ultimate goal was to propose a set of protocols and practices for monitoring glass sponge reef status within the current MPAs and reef closure areas. An ideal set of protocols would involve directly measuring the physical 3D structure of glass sponge reef patches to track changes in their physical condition over time as well as tracking the abundances of functional traits on reef patches that would serve as indicators of the status of ecosystem goods and services provided by the functional communities of the reefs. Lastly, it was important to determine whether a monitoring framework could involve SCUBA divers as citizen scientists. SCUBA diving citizen scientists could not only increase the temporal resolution of the data collected from the reefs by divers but also promote glass sponge reef awareness and environmental stewardship within the general public. To address the objectives of this thesis, a team of scientific divers from Ocean Wise and I conducted surveys of three glass sponge reefs, all accessible on air – gas SCUBA, in Howe Sound, British Columbia (BC).

To address the first objective, a comparative study was conducted into the measurement error and repeatability of two underwater remote sensing techniques that could measure the vertical height variation in sponge reef patches: 3D SfM photogrammetry and microtopographic laser scanning (MiLS). 3D photogrammetry was hypothesized to have higher measurement error since it captured the structural heterogeneity over a larger area. Surprisingly, the results showed that MiLS had the larger measurement error of the two techniques. Measurement error increased with the absolute value of the metric that was measured as is common with most detection techniques in the physical, chemical and biological sciences. Reef patches with higher structural complexity, measured by the SAPA and rugosity ratios, had higher measurement error. This trend was similar to that in another study of 3D photogrammetric measurement error but on coral reefs (Bryson et al. 2017). When measuring the linear rugosity of a reef patch using MiLS, the rugosity can be reported with an error of 7.61%. When measuring the linear rugosity of a reef patch via a digital elevation map (DEM) derived from a 3D reconstruction of that reef patch, the rugosity can be reported with an error of 3.76%. When measuring the surface complexity (SAPA ratio) of a reef patch from a 3D reconstruction of that reef patch, the SAPA ratio can be reported with an error of 2.68% (Fig 2.4).

Both techniques were able to detect differences in habitat complexities between different reef patches. However, both techniques had poor repeatability over time (several day time scale). MiLS rugosity had inconsistent measurement error for a reef plot surveyed on three separate days. Additionally, MiLS measured a significantly different rugosity value for the same reef plot on each of the three survey days even though there were no noticeable changes in the sponge structure. The rugosity and SAPA ratios measured from the 3D models of the same reef patch had consistent measurement error over three survey days but measured significantly different values for the two metrics just as MiLS did for rugosity. For MiLS, the high error was likely due to slight inconsistencies in the swim path between repeat video transects making it difficult for SCUBA divers to conduct repeat measurements of the same reef section over time. For 3D SfM photogrammetry, varying ambient light and turbidity conditions of the water likely influenced the signal – to – noise ratio in the collected imagery which consequently affected 3D model accuracy. However, this was a problem only in the case of the SAPA ratio which measured the surface heterogeneity for a given area. Other 3D complexity metrics curvature and slope were the same in 3D models of the one reef plot surveyed on three separate days. Particulate matter close to the reef's surface may have been incorporated into the reef's reconstructed surface by 3D algorithms in Metashape. These slight variations in the reconstructed surface of the same reef plot had a cumulative effect across the whole area of the plot and consequently skewed the SAPA ratio from day to day. Therefore, the SAPA ratio derived from a reef's 3D model may not be a reliable metric of habitat complexity and should be analyzed as a covariate along with other 3D complexity metrics, such as, curvature or slope.

To address the second objective of this thesis, 15 reef patches/sites on three separate reefs were surveyed. Video footage of the patches was collected for 3D model reconstruction from which structural complexity metrics SAPA, relief, curvature, and slope were derived. Additionally, animals > 2 cm were counted and classified in each site. These animals were assigned functional traits and the whole functional community of each site was characterized. We hypothesized that functional diversity, measured by the Rao's quadratic entropy (Q) index (Rao 1982) would have strong positive relationships with each of the four 3D complexity metrics. On the contrary, the results showed negative relationships between Rao's Q and the four complexity metrics. This analysis highlighted the importance of dividing the functional community of a glass sponge reef into clearly defined subgroups instead of lumping all functional traits into one analysis. The fish functional diversity was less affected the 3D complexity gradients but the invertebrate functional diversity had strong negative relationships. Nonetheless, our data was highly variable and the negative relationships had weak explanatory

power. Similar findings were reported in other studies (Verdonschot, Didderen, and Verdonschot 2012; Plass-Johnson et al. 2016).

A deeper look at the taxonomic and functional compositions of glass sponge reef communities revealed that communities were structured within a reef by factors at the reef – patch spatial scale. Communities were similar among the three reefs except in the case of fish communities which were different on the Passage Island (PI) reef. Analysis of the 3D complexity drivers of community composition revealed that surface complexity (SAPA) appeared to drive abundances of small benthic crustaceans whereas slope was a strong potential driver of mobile fish abundances. However, our analysis did suggest that a large portion of the functional traits observed on the reef communities were redundant. Whether this pattern is truly representative of the glass sponge reef functional communities in Howe Sound or simply a side – effect of the assignment of functional traits to the observed taxonomic group is unclear and needs to be investigated further.

4.2. Recommendations for Further Investigation

When determining which technique was best at monitoring changes in glass sponge reef structure over time, 3D SfM photogrammetry would be the better choice. Both techniques had similar sampling efforts since each set of MiLS surveys needs to be accompanied with an in – water calibration. There is no need for in – water calibration for 3D photogrammetry, however, ground control points (GCPs) need to be installed on the reef surface and georeferenced which increases the survey effort. Both techniques measured different complexity metric values over the same reef patch on consecutive sampling days despite no noticeable changes in the structure within the patch. MiLS should be tested for measurement error from a more stable platform, such as, an ROV and 3D photogrammetry protocols need to be improved to account for the effects of varying turbidity and ambient light conditions on the measurement outcomes. Additionally, the measurement error of both techniques needs to be further disseminated to determine the relative proportions of error attributable to random/chance error, systematic/bias error, and instrument error. A further analysis of error of 3D photogrammetry using different camera and lighting equipment is needed in order to apply the technique from various platforms, including an ROV platform. This is especially important if 3D photogrammetry is to be used as a monitoring tool on the deeper glass sponge reefs in depths beyond the air-gas SCUBA diving depth limits.

Regarding the functional ecology of glass sponge reefs, it would be important to determine whether the glass sponge reef functional communities are composed of redundant

traits and how a different assignment of traits would influence the analyses in Chapter 3 of this thesis. Additionally, it would be beneficial to test the relationships between individual traits and 3D complexity metrics as a comparative analysis with the relationships found on coral reefs (Plass-Johnson et al. 2016). Finally, a next step in applying a functional traits – based approach to monitoring glass sponge reefs would be to analyze functional restructuring of communities in response to disturbances and stressors. Determining the relative importance of certain traits to the resilience of glass sponge reefs could help us implement targeted protection measures for certain reefs depending on their functional community structure.

4.3. General Conclusions

When taking into consideration the poor repeatability of 3D photogrammetry at measuring surface complexity over highly complex reef surfaces the true variability of the negative relationships between Rao's Q and SAPA is likely amplified. This is a problem since our analysis suggests that the SAPA ratio is a potentially important driver of invertebrate community structure and that the community structure on our three surveyed reefs in driven by invertebrate abundances. Therefore, conclusions about the relationships of functional diversity and functional community composition with surface complexity cannot be made with certainty. Since biodiversity is generally positively correlated with functional diversity (Stuart-Smith et al. 2013), the relationship between biodiversity and surface complexity in our study is also inconclusive and corresponds to previously published data (Cook, Conway, and Burd 2008; Chu and Leys 2010; Dunham, Archer, et al. 2018). However 3D photogrammetry allows for the use of more than one quantifiable metric of habitat complexity. In our case, slope and relief may plays an equally important if not more important role in driving functional diversity and community structure than surface complexity.

4.4. Management and Monitoring Implications

To date, all known glass sponge reefs are formally protected either as MPAs or with imposed fisheries closures. While protection is an important step towards conserving these unique and fragile ecosystems, evaluating which conservation measures are meeting their targeted outcomes and which are not, is just as important for long-term ecosystem-based management (Tallis et al. 2010). However, identifying the best practices for long-term monitoring has been challenging since the majority of glass sponge reefs are only accessible by remotely or human operated submersibles, limiting our ability to consistently track changes over time and evaluate the best practices (Loh, Archer, and Dunham 2019). Despite these

challenges, key indicator species of reef health have been identified and 2D photogrammetric ROV based protocols for evaluating reef condition have been established. However, these practices may not always be the most cost effective or practical options for some reefs. Reefs in Howe Sound that are accessible to SCUBA divers present a unique opportunity for the collection of large amounts of data on the reefs through citizen science initiatives. This thesis explored a cheaper alternative for monitoring reef status than using an ROV. With access to an underwater digital camera and 3D reconstruction software, citizen scientists can gather meaningful information about the reefs' physical 3D habitat complexity and participate in long-term monitoring frameworks that utilize different tools appropriate for the location and depths of the reefs.

While further research is needed to develop more robust 3D modelling workflows that can measure reef 3D structure with higher precision and certainty, this thesis provides a foundation from which others can build more robust workflows. For instance, 3D measurements of surface complexity need to be improved, however, measurements of slope and relief can be applied immediately following the outlined protocols in this thesis. Subsequently, reef patches with high slopes would likely harbor schooling and bentho - pelagic fish that feed on benthic crustaceans. Knowing that species occupy different functional roles within a marine ecosystem, this thesis also provides a basis for identifying key indicator functional traits of reef status which can then be used to 1) infer underlying mechanisms behind the interactions between species and their sponge reef habitat and 2) be used to predict the consequences to ecosystem services from changes in functional community structure. In our case, by tracking the abundances of benthivorous fish, we can infer whether or not a reef community has a high abundance of small benthic crustaceans which would in turn provide an indication of whether the reef patch's surface is highly heterogeneous or not. This thesis has demonstrated how glass sponge reefs along the BC coast can be effectively monitored using 3D habitat complexity metrics and functional trait abundances by a range of stakeholders, including government entities, NGOs, indigenous peoples, and citizen scientists.

References

AgiSoft Metashape Professional (Version 1.6.5) (Software). (2020*). Retrieved from http://www.agisoft.com/downloads/installer/.

Albright LJ, McCrae SK. 1987. "Annual Bacterioplankton Biomasses and Productivities in a Temperate West Coast Canadian Fjord." Applied and Environmental Microbiology. 53:1277.

Archer SK, Kahn AS, Thiess M, Law L, Leys SP, Johannessen SC, Layman CA, Burke L, Dunham A. 2020. "Foundation Species Abundance Influences Food Web Topology on Glass Sponge Reefs." Frontiers in Marine Science. 7:799.

Austin WC, Conway KW, Barrie J, Krautter M. 2007. "Growth and morphology of a reef-forming glass sponge, *Aphrocallistes vastus* (Hexactinellida), and implications for recovery from widespread trawl damage." Porifera Research: Biodiversity, Innovation & Sustainability, Serie Livros. 28:139–45.

Barthel D. 1992. "Do hexactinellids structure antarctic sponge associations?" Ophelia. 36(2):111–118.

Barthel D, Wolfrath B. 1989. "Tissue sloughing in the sponge *Halichondria panicea*: a fouling organism prevents being fouled." Oecologia. 78:357–60.

Bates D, Maechler M, Bolker B, Walker S. 2015. "Fitting Linear Mixed-Effects Models Using lme4." Journal of Statistical Software. 67(1):1–48.

Bayley DTI, Mogg AOM, Purvis A, Koldewey HJ. 2019. "Evaluating the efficacy of small-scale marine protected areas for preserving reef health: A case study applying emerging monitoring technology." Aquatic Conservation: Marine and Freshwater Ecosystems. 29:2026–44.

Beaulieu S. 2001a. "Colonization of habitat islands in the deep sea: Recruitment to glass sponge stalks." Deep Sea Research I. 48:1121–37.

Beaulieu SE. 2001b. "Life on glass houses: sponge stalk communities in the deep sea." Marine Biology. 138:803–17.

Beck MW. 1998. "Comparison of the measurement and effects of habitat structure on gastropods in rocky intertidal and mangrove habitats." Marine Ecology Progress Series 169:165-178

Bell JJ. 2008. "The functional roles of marine sponges." Estuarine, Coastal and Shelf Science. 79:341–53.

Bell SS, McCoy ED, Mushinsky HR, editors. 1991. "Habitat structure: The physical arrangement of objects in space." London, England: Chapman and Hall.

Ben Lamine E, Di Franco A, Romdhane MS, Francour P. 2018. "Can citizen science contribute to fish assemblages monitoring in understudied areas? The case study of Tunisian marine protected areas." Estuarine, Coastal and Sh. 200:420–427.

Bett B, Rice AL. 1992. "The influence of hexactinellid sponge (*Pheronema carpenteri*) spicules on the patchy distribution of macrobenthos in the Porcupine Seabight (Bathyal NE Atlantic)." Ophelia. 36:217–26.

Bonuso N, Stone T, Williamson K. 2020. "Upper Triassic (Carnian) sponge reef mounds from South Canyon, central Nevada." Facies. 66(3).

Botta-Dukát Z. 2005. "Rao's quadratic entropy as a measure of functional diversity based on multiple traits." Journal of Vegetation Science. 16:533–540.

Botting JP, Muir LA. 2018. "Early sponge evolution: A review and phylogenetic framework." Palaeoworld. 27:1–29.

Bowerbank JS. 1862. "On the Anatomy and Physiology of the Spongiadae. Part III On the Generic Characters, the Specific Characters, and on the Method of Examination." Philosophical Transactions of the Royal Society. 152(2):1087–1135, pls LXXII–LXXIV.

Bracewell SA, Clark GF, Johnston EL. 2018. "Habitat complexity effects on diversity and abundance differ with latitude: an experimental study over 20 degrees." Ecology. 99:1964–74.

Bryson M, Ferrari R, Figueira W, Pizarro O, Madin J, Williams S, Byrne M. 2017. "Characterization of measurement errors using structure-from-motion and photogrammetry to measure marine habitat structural complexity." Ecology and Evolution. 7(15):5669–5681.

Burns JHR, Alexandrov T, Ovchinnikova E, Gates RD, Takabayashi M. 2016. "Investigating the spatial distribution of growth anomalies affecting *Montipora capitata* corals in a 3-dimensional framework." Journal of Invertebrate Pathology. 140:51–57.

Burns JHR, Delparte D, Gates RD, Takabayashi M. 2015. "Integrating structure-from-motion photogrammetry with geospatial software as a novel technique for quantifying 3D ecological characteristics of coral reefs." PeerJ. 3:1077.

Caceres I, Ibarra-Garcia EC, Ortiz M, Ayon-Parente M, Rodriguez-Zaragoza FA. 2020. "Effect of fisheries and benthic habitat on the ecological and functional diversity of fish at the Cayos Cochinos coral reefs (Honduras)." Marine Biodiversity. 50:9

Canterle AM, Nunes LT, Fontoura L, Maia HA, Floeter SR. 2020. "Reef microhabitats mediate fish feeding intensity and agonistic interactions at Príncipe Island Biosphere Reserve, Tropical Eastern Atlantic." Marine Ecology. 41:12609.

Carvalho LRS, Barros F. 2017. "Physical habitat structure in marine ecosystems: the meaning of complexity and heterogeneity." Hydrobiologia. 797:1–9.

Chapman A, Tunnicliffe V, Bates A. 2018. "Both rare and common species make unique contributions to functional diversity in an ecosystem unaffected by human activities." Diversity and Distributions. 24:568-578.

Chew KK, Holland D, Wells JW, McKenzie DH, Harris CK. 1973. "Depth, Distribution, and Size of Spot Shrimp *Pandalus platyceros* Trawled in Dabob Bay of Hood Canal." Vol. 64. Washington, USA. p. 28–32.

Chu JWF, Leys SP. 2010. "High resolution mapping of community structure in three glass sponge reefs (Porifera, Hexactinellida)." Marine Ecology Progress Series. 417:97–113.

Chu JWF, Leys SP. 2012. "The dorid nudibranchs *Peltodoris lentiginosa* and *Archidoris odhneri* as predators of glass sponges." Invertebrate Biology. 131:75–81.

Chu JWF, Maldonado M, Yahel G, Leys SP. 2011. "Glass sponge reefs as a silicon sink." Marine Ecology Progress Series. 441:1–14.

Clayton L, Dennison G. 2017. "Inexpensive Video Drop-camera for Surveying Sensitive Benthic Habitats: Applications from Glass Sponge (Hexactinellida) Reefs in Howe Sound, British Columbia." The Canadian Field-Naturalist. 131(1).

Conway KW, Barrie JV, Austin WC, Luternauer JL. 1991. "Holocene sponge bioherms on the western Canadian continental shelf." Continental Shelf Research. 11:771–90.

Conway KW, Barrie JV, Krautter M. 2005. "Geomorphology of unique reefs on the western Canadian shelf: sponge reefs mapped by multibeam bathymetry." Geo-Marine Letters. 25:205–13.

Conway KW, Dunham A, Burke LA, Archer SK, Shaw J, Kung R. 2020. "Chapter 17 - Sponge reefs on the Northeast Pacific margin: geomorphic and biological variability." In: Harris PT, Baker E, editors. Seafloor Geomorphology as Benthic Habitat (Second Edition).

Conway KW, Manfred Krautter JVB, Neuweiler M. 2001. "Hexactinellid Sponge Reefs on the Canadian Continental Shelf: A Unique 'Living Fossil'." Geoscience Canada. 28.

Conway KW, Whitney F, Leys SP, Barrie JV, Krautter M. 2017. "Sponge Reefs of the British Columbia, Canada Coast: Impacts of Climate Change and Ocean Acidification." In: Carballo JL, Bell JJ, editors. Cham: Springer International Publishing.

Cook, S. E. 2005. "Ecology of the hexactinellid sponge reefs on the western Canadian continental Shelf." MSc thesis. University of Victoria, Victoria, British Columbia, Canada.

Cook SE, Conway KW, Burd B. 2008. "Status of the glass sponge reefs in the Georgia Basin." Marine Environmental Research. 66:80– 86.

De Cáceres M, Legendre P, He. F. 2013. "Dissimilarity measurements and the size structure of ecological communities" Methods in Ecology and Evolution, 4: 1167-77. Methods in Ecology and Evolution. 4:1167–1177.

Devine BM, Baker KD, Edinger EN, Fisher JAD. 2020. "Habitat associations and assemblage structure of demersal deep-sea fishes on the eastern Flemish Cap and Orphan Seamount." Deep Sea Research Part I: Oceanographic Research Papers. 157:103210.

DFO. 2018. "Glass sponge aggregations in Howe Sound: locations, reef status, and ecological significance assessment." DFO Canadian Science Advisory Secretariat Science Response. 2018/032.

DFO. 2020a. "Hecate Strait/Queen Charlotte Sound Glass Sponge Reefs Marine Protected Area (HS/QCS MPA)" Fisheries and Oceans Canada. [accessed 2020 Dec 30]. https://www.dfo-mpo.gc.ca/oceans/mpa-zpm/hecate-charlotte/index-eng.html.

DFO. 2020b. "Strait of Georgia and Howe Sound Glass Sponge Reef Conservation Initiative." Fisheries and Oceans Canada. [accessed 2020 Jun 26]. https://www.dfo-mpo.gc.ca/oceans/ceccsr-cerceef/closures-fermetures-eng.html.

Diaz S, Lavorel S, Bello F, Quétier F, Grigulis K, Robson. T. 2008. "Incorporating plant functional diversity effects in ecosystem service assessments." Proceedings of the National Academy of Sciences of the United States of America. 104:20684–29689.

Du Preez C, Tunnicliffe V. 2012. "A new video survey method of microtopographic laser scanning (MiLS) to measure small-scale seafloor bottom roughness." Limnology and Oceanography: Methods. 10:899–909.

Dunham A, Archer SK, Davies SC, Burke LA, Mossman J, Pegg JR, Archer E. 2018. "Assessing condition and ecological role of deep-water biogenic habitats: Glass sponge reefs in the Salish Sea." Marine Environmental Research. 141:88–99.

Dunham A, Mossman J, Archer SK, Davies SC, Pegg JR, Archer E. 2018. "Glass Sponge Reefs in the Strait of Georgia and Howe Sound: Status Assessment and Ecological Monitoring Advice". Fisheries and Oceans Canada. Canadian Science Advisory Secretariat Research Document 2018/010

Earp HS, Liconti A. 2020. "Science for the Future: The Use of Citizen Science in Marine Research and Conservation." In: Jungblut S, Liebich V, Bode-Dalby M (eds). YOUMARES 9 – The Oceans: Our Research, Our Future. Springer, Cham.

Fabri MC, Vinha B, Allais AG, Bouhier ME, Dugornay O, Gaillot A, Arnaubec. A. 2019.
"Evaluating the ecological status of cold-water coral habitats using non-invasive
methods: An example from Cassidaigne canyon, northwestern Mediterranean Sea."
Progress in Oceanography. 178(102172).

Ferrari R, Figueira WF, Pratchett MS, Boube T, Adam A, Kobelkowsky-Vidrio T, Doo SS,
Atwood TB, Byrne M. 2017. "3D photogrammetry quantifies growth and external erosion
of individual coral colonies and skeletons." Scientific Reports. 7:16737.

Ferrari R, Malcolm HA, Byrne M, Friedman A, Williams SB, Schultz A, Jordan AR, Figueira WF.
2018. "Habitat structural complexity metrics improve predictions of fish abundance and
distribution." Ecography. 41:1077–91.

Fitt W. 2020. "Florida manatees *Trichechus manatus latirostric* actively consume the sponge
Chondrilla caribensis." PeerJ. 8:8443.

Floyd M, Mizuyama M, Obuchi M, Sommer B, Miller M, Kawamura I, Kise H, Reimer J, Beger
M. 2020. "Functional diversity of reef molluscs along a tropical-to-temperate gradient."
Coral Reefs. 39:1361-1376

Freiwald J, Meyer R, Caselle JE, Blanchette CA, Hovel K, Neilson D, Dugan J, Altstatt J, Nielsen
K, Bursek J. 2018. "Citizen science monitoring of marine protected areas: Case studies
and recommendations for integration into monitoring programs." Marine Ecology.
39:12470.

Froese R, Pauly D. (eds). 2019. "FishBase." World Wide Web electronic publication.
https://www.fishbase.org, version (12/2019).

Fukunaga A, Burns JHR, Craig BK, Kosaki RK. 2019. "Integrating Three-Dimensional Benthic
Habitat Characterization Techniques into Ecological Monitoring of Coral Reefs." Journal
of Marine Science and Engineering. 7.

Gerdes K, Arbizu PM, Schwarz-Schampera U, Schwentner M, Kihara TC. 2019. "Detailed
Mapping of Hydrothermal Vent Fauna: A 3D Reconstruction Approach Based on Video
Imagery." Frontiers in Marine Science. 6.

Gerovasileiou V, Dailianis T, Panteri E, Michalakis N, Gatti G, Sini M, Dimitriadis C, Issaris Y,
Salomidi M, Filiopoulou I, Doğan A, Thierry de Ville d'Avray L, David R, Çinar ME,
Koutsoubas D, Féral JP, Arvanitidis C. 2016. "CIGESMED for divers: Establishing a
citizen science initiative for the mapping and monitoring of coralligenous assemblages in
the Mediterranean Sea." Biodiversity Data Journal 4:e8692.
https://doi.org/10.3897/BDJ.4.e8692

González-Rivero M, Ereskovsky AV, Schönberg CHL, Ferrari R, Fromont J, Mumby PJ. 2013. "Life-history traits of a common Caribbean coral-excavating sponge, *Cliona tenuis* (Porifera: Hadromerida)." Journal of Natural History. 47:2815–34.

Gotelli NJ. 2000. "Null Model Analysis of Species Co-Occurrence Patterns". Ecology. 81:2606–21.

Gotelli NJ, McCabe DJ. 2002. "Species co-occurrence: A meta-analysis of J. M. Diamond's assembly rules model." Ecology. 83(8):2091.

Government of Canada. 2017. "Hecate Strait and Queen Charlotte Sound Glass Sponge Reefs Marine Protected Areas Regulations." Canada Gazette.

Granshaw SI. 2018. "Structure from motion: origins and originality." The Photogrammetric Record. 33:6–10.

Grant N, Matveev E, Kahn AS, Archer SK, Dunham A, Bannister RJ, Eerkes-Medrano D, Leys SP. 2019. "Effect of suspended sediments on the pumping rates of three species of glass sponge in situ." Marine Ecology Progress Series. 615:79–100.

Grant N, Matveev E, Kahn AS, Leys SP. 2018. "Suspended sediment causes feeding current arrests in situ in the glass sponge *Aphrocallistes vastus*." Marine Environmental Research. 137:111–20.

Gratwicke B, Speight MR. 2005. "Effects of habitat complexity on Caribbean marine fish assemblages." Marine Ecology Progress. 292:301–10.

Guillas KC, Kahn AS, Grant N, Archer SK, Dunham A, Leys SP. 2019. "Settlement of juvenile glass sponges and other invertebrate cryptofauna on the Hecate Strait glass sponge reefs." Invertebrate Biology. 138:12266.

Gutiérrez López M, de Leaniz MIG, Aza DT. 2020. "Do cryptic species of earthworms affect soil arthropods differently? The case of the *Carpetania elisae* complex in the center of the Iberian Peninsula." European Journal of Soil Biology. 96:103147.

Gutierrez-Heredia L, Benzoni F, Murphy E, Reynaud EG. 2016. "End to End Digitisation and Analysis of Three-Dimensional Coral Models, from Communities to Corallites." PLoS ONE. 11:0149641.

Gutt J, Boehmer A, Dimmler W. 2013. "Antarctic sponge spicule mats shape macrobenthic diversity and act as silicon trap." Marine Ecology. 480:57–71.

Hardin G. 1960. "The Competitive Exclusion Principle." Science. 131:1292.

Hawkes N, Korabik M, Beazley L, Rapp HT, Xavier JR, Kenchington E. 2019. "Glass sponge grounds on the Scotian Shelf and their associated biodiversity." Marine Ecology Progress Series. 614:91–109.

Hickin EJ. 1989. "Contemporary Squamish River sediment flux to Howe Sound, British Columbia." Canadian Journal of Earth Sciences. 26:1953–63.

House JE, Brambilla V, Bidaut LM, Christie AP, Pizarro O, Madin JS, Dornelas M. 2018. "Moving to 3D: relationships between coral planar area, surface area and volume." PeerJ. 6:4280.

Jamieson GS, Chew L. 2002. "Hexactinellid Sponge Reefs: Areas of Interest as Marine Protected Areas in the North and Central Coast Areas". Fisheries and Oceans Canada. Canadian Science Advisory Secretariat Research Document 2002/122

Jamieson GS, Pikitch EK. 1988. "Vertical distribution and mass mortality of prawns, *Pandalus platyceros*, in Saanich Inlet, British Columbia." U S Fish and Wildlife Service Fishery Bulletin. 86:601–08.

Johnson DW. 2007. "Habitat Complexity Modifies Post-Settlement Mortality and Recruitment Dynamics of a Marine Fish ". Ecology. 88:1716–25.

Kahn AS, Chu JWF, Leys SP. 2018. "Trophic ecology of glass sponge reefs in the Strait of Georgia, British Columbia." Scientific Reports. 8:756.

Kahn AS, Vehring LJ, Brown RR, Leys SP. 2016. "Dynamic change, recruitment and resilience in reef-forming glass sponges." Journal of the Marine Biological Association of the United Kingdom. 96:429–36.

Kahn AS, Yahel G, Chu JWF, Tunnicliffe V, Leys SP. 2015. "Benthic grazing and carbon sequestration by deep-water glass sponge reefs." Limnology and Oceanography. 60:78–88.

Kembel SW, Cowan PD, Helmus MR, Cornwell WK, Morlon H, Ackerly DD, Blomberg SP, Webb CO. 2010. Picante: R tools for integrating phylogenies and ecology. Bioinformatics. 26(11):1463–1464.

Konstantinou D, Kakakiou RV, Panteris E, Voultsiadou E, Gkelis S. 2020. "Photosynthetic Sponge-associated Eukaryotes in the Aegean Sea: A Culture-dependent Approach." Journal of Eukaryotic Microbiology. 67:660–70.

Kostylev V, Erlandsson J, Ming M, Williams. G. 2005. "The relative importance of habitat complexity and surface area in assessing biodiversity: Fractal application on rocky shores." Ecological Complexity. 2(3):272–286.

Krautter M, Conway KW, Barrie JV. 2006. "Recent hexactinosidan sponge reefs (silicate mounds) off British Columbia, Canada: Frame-building processes." Journal of Paleontology. 80:38–48.

Krautter M, Conway KW, Barrie JV, Neuweiler M. 2001. "Discovery of a 'Living Dinosaur': Globally unique modern hexactinellid sponge reefs off British Columbia, Canada." Facies. 44:265–82.

Laliberté E, Legendre P. 2010. "A distance-based framework for measuring functional diversity from multiple traits." Ecology. 91:299–305.

Laliberté E, Legendre P, Shipley B. 2014. FD: measuring functional diversity from multiple traits, and other tools for functional ecology. R package version. 1:0–12.

Lamb A, Hanby BP. 2005. "Marine life of the pacific northwest: A photographic encyclopedia of invertebrates, seaweeds and selected fishes." Harbour Publishing.

Law LK. 2018. "Distribution, biodiversity, and function of glass sponge reefs in the Hecate Strait, British Columbia, Canada." MSc thesis. University of Alberta, Edmonton, Alberta, Canada.

Law LK, Reiswig HM, Ott BS, McDaniel N, Kahn AS, Guillas KC, Dinn C, Leys SP. 2020. "Description and distribution of *Desmacella hyalina sp.* nov. (Porifera, Desmacellidae), a new cryptic demosponge in glass sponge reefs from the western coast of Canada." Marine Biodiversity. 50:55.

Leys S, Cheung E, Boury-Esnault N. 2006. "Embryogenesis in the glass sponge *Oopsacas minuta*: Formation of syncytia by fusion of blastomeres." Integrative and Comparative Biology. 46:104–17.

Leys SP, Hill A. 2012. "Chapter one - The Physiology and Molecular Biology of Sponge Tissues." In: Becerro MA, Uriz MJ, Maldonado M, Turon X, editors. Advances in Marine Biology. 62.

Leys SP, Lauzon NRJ. 1998. "Hexactinellid sponge ecology: growth rates and seasonality in deep water sponges." Journal of Experimental Marine Biology and Ecology. 230:111–29.

Leys SP, Mackie GO. 1997. "Electrical recording from a glass sponge." Nature. 387:29–30.

Leys SP, Mackie GO, Meech RW. 1999. "Impulse conduction in a sponge." Journal of Experimental Biology. 202:1139.

Leys SP, Mackie GO, Reiswig HM. 2007. "The biology of glass sponges." Advances in Marine Biology. 52:1–145.

Leys SP, Meech RW. 2006. "Physiology of coordination in sponges." Canadian Journal of Zoology. 84:288–306.

Leys SP, Wilson K, Holeton C, Reiswig HM, Austin WC, Tunnicliffe V. 2004. "Patterns of glass sponge (Porifera, Hexactinellida) distribution in coastal waters of British Columbia, Canada." Marine Ecology Progress Series. 283:133–49.

Leys SP, Yahel G, Reidenbach MA, Tunnicliffe V, Shavit U, Reiswig HM. 2011. "The Sponge Pump: The Role of Current Induced Flow in the Design of the Sponge Body Plan." PLoS ONE. 6:27787.

Lochhead I, Hedley. N. 2020. "3D Modelling in Temperate Water: Building Rigs and Data Science to Support Glass Sponge Monitoring Efforts in Coastal British Columbia." ISPRS - International Archives of the Photogrammetry, Remote Sensing and Spatial Information Sciences. 43(2):969–976.

Loh TL, Archer SK, Dunham A. 2019. "Monitoring program design for data-limited marine biogenic habitats: A structured approach." Ecology and Evolution. 9:7346–59.

López-Pérez A, Ballesteros. LM. 2004. "Coral Community Structure and Dynamics in the Huatulco Area, Western Mexico." Bulletin of Marine Science. 75:453–472.

Macarthur R, Levins. R. 1967. "The Limiting Similarity, Convergence, and Divergence of Coexisting Species." The American Naturalist. 101:377–385.

MacArthur RH, MacArthur JW, MacArthur RH, MacArthur JW. 1961. "On Bird Species Diversity." Ecology. 42:594–98.

Madduppa H. 2012. "Fish biodiversity in coral reefs and lagoon at the Maratua Island, East Kalimantan." Journal of Biological Diversity. 13:145–150.

Magurran AE. 2004. "Measuring Biological Diversity" Blackwell Publishing, Oxford.

Marliave JB, Borden LA. 2020. "Climate and weather factors affecting winter sheltering by shoreline Copper Rockfish *Sebastes caurinus* in Howe Sound, British Columbia." Scientific Reports. 10:14277.

Marliave JB, Borden LA, Schultz JA, Gibbs DM, Dennison GJ. 2020. "Formation, Persistence, and Recovery of Glass Sponge Reefs: A Case Study." In: Invertebrates - Ecophysiology and Management.

Marliave JB, Conway KW, Gibbs DM, Lamb A, Gibbs C. 2009. "Biodiversity and rockfish recruitment in sponge gardens and bioherms of southern British Columbia, Canada." Marine biology. 156:2247–54.

Marre G, Holon F, Luque S, Boissery P, Deter. J. 2019. "Monitoring Marine Habitats With Photogrammetry: A Cost-Effective, Accurate, Precise and High-Resolution Reconstruction Method." Frontiers in Marine Science. 6:276.

Mason NWH, Bello F, Mouillot D, Pavoine S, Dray S. 2013. "A guide for using functional diversity indices to reveal changes in assembly processes along ecological gradients." Journal of Vegetation Science. 24:794–806.

Mason NWH, Lanoiselée C, David Mouillot JBW, Argillier C. 2008. "Does Niche Overlap Control Relative Abundance in French Lacustrine Fish Communities? A New Method Incorporating Functional Traits." Journal of Animal Ecology. 77:661–69.

Mason NWH, Lanoiselée C, Mouillot D, Irz P, Argillier C. 2007. "Functional characters combined with null models reveal inconsistency in mechanisms of species turnover in lacustrine fish communities." Oecologia. 153:441–52.

McIntyre S, Lavorel S, Landsberg J, Forbes T. 1999. "Disturbance response in vegetation – towards a global perspective on functional traits." Journal of Vegetation Science. 10:621-630

McNeely D, Bertness M, Gaines S, Hay M. 2001. "Marine Community Ecology." Ecology. 82.

Medjkane M, Maquaire O, Costa S, Th Roulland PL, Fauchard C, Antoine R, Davidson R. 2018. "High-resolution monitoring of complex coastal morphology changes: cross-efficiency of SfM and TLS-based survey (Vaches-Noires cliffs, Normandy, France)." Landslides. 15:1097–108.

Micheletti N, Chandler J, Lane SN. 2015. "Structure from motion (SFM) photogrammetry." Loughborough University Journal contribution.

Moberg F, Folke C. 1999. "Ecological goods and services of coral reef ecosystems." Ecological Economics. 29:215–233.

Mouchet MA, Villéger S, Mason NWH, Mouillot D. 2010. "Functional diversity measures: an overview of their redundancy and their ability to discriminate community assembly rules." Functional Ecology. 24:867–76.

Mouillot D, Dumay O, Tomasini. JA. 2007. "Limiting similarity, niche filtering and functional diversity in coastal lagoon fish communities." Estuarine, Coastal and Shelf Science. 71:443–456.

Mouillot D, Graham NAJ, Villéger S, Mason NWH, Bellwood DR. 2013. "A functional approach reveals community responses to disturbances." Trends in Ecology & Evolution. 28:167–77.

Narbonne GM, Dixon OA. 1984. "Upper Silurian lithistid sponge reefs on Somerset Island, Arctic Canada." Sedimentology. 31:25–50.

Neuweiler F, Mehdi M, Wilmsen. M. 2001. "Facies of Liassic sponge mounds, central High Atlas, Morocco." Facies. 44:243–264.

Nooten S, Schultheiss P, Facey S, Rowe R, Cook. J. 2019. "Habitat complexity affects functional traits and diversity of ant assemblages in urban green spaces (Hymenoptera: Formicidae)." Myrmecological News. 29:67–77.

Olinger LK, Scott AR, McMurray SE, Pawlik JR. 2019. "Growth estimates of Caribbean reef sponges on a shipwreck using 3D photogrammetry." Scientific Reports. 9:18398.

Orland C, Queirós AM, Spicer JI, McNeill CL, Higgins S, Goldworthy S, Zananiri T, Archer L, Widdicombe S. 2016. "Application of computer-aided tomography techniques to visualize kelp holdfast structure reveals the importance of habitat complexity for supporting marine biodiversity." Journal of Experimental Marine Biology and Ecology. 477:47–56.

Pailhas, Y., Petillot, Y. & Capus, C. 2010. "High-Resolution Sonars: What Resolution Do We Need for Target Recognition?" EURASIP Journal on Advances in Signal Processing. 205095.

Pandolfi JM, Minchin PR. 1996. "A comparison of taxonomic composition and diversity between reef coral life and death assemblages in Madang Lagoon, Papua New Guinea." Palaeogeography, Palaeoclimatology, Palaeoecology. 119:321–41.

Paradis E, Schliep K. 2019. "ape 5. 0: an environment for modern phylogenetics and evolutionary analyses in R". Bioinformatics. 35(3):526–528.

Pavoine S, Vallet J, Dufour A, Gachet S, Daniel H. 2009. "On the challenge of treating various types of variables: application for improving the measurement of functional diversity." Oikos. 118:391–402.

Pertierra LR, Segovia NI, Noll D, Martinez PA, Pliscoff P, Barbosa A, Aragón P, Rey AR, Pistorius P, Trathan P, et al. 2020. "Cryptic speciation in gentoo penguins is driven by geographic isolation and regional marine conditions: Unforeseen vulnerabilities to global change." Diversity and Distributions. 26:958–75.

Piazza P, Cummings V, Guzzi A, Hawes I, Lohrer A, Marini S, Marriott P, Menna F, Nocerino E, Peirano A, et al. 2019. "Underwater photogrammetry in Antarctica: long-term observations in benthic ecosystems and legacy data rescue." Polar Biology. 42:1061–1079.

Planes S, Lecchini D, Mellin C, Charton JG, Harmelin-Vivien M, Kulbicki M, Mou-Tham G, Galzin AR. 2012. "Environmental determinants of coral reef fish diversity across several French Polynesian atolls." Comptes Rendus Biologies. 335:417–423.

Plass-Johnson JG, Taylor MH, Husain AAA, Teichberg MC, Ferse SCA. 2016. "Non-Random Variability in Functional Composition of Coral Reef Fish Communities along an Environmental Gradient." PLoS ONE. 11:0154014.

Prado E, Sánchez F, Rodríguez-Basalo A, Altuna Á, Cobo. A. 2019. "Analysis of the population structure of a gorgonian forest (*Placogorgia sp.*) using a photogrammetric 3D modeling

approach at Le Danois Bank, Cantabrian Sea." Deep Sea Research Part I: Oceanographic Research Papers. 153(103124).

Price DM, Robert K, Callaway A, Lacono CL, Hall RA, Huvenne VAI. 2019. "Using 3D photogrammetry from ROV video to quantify cold-water coral reef structural complexity and investigate its influence on biodiversity and community assemblage." Coral Reefs. 38:1007–21.

Pygas DR, Ferrari R, Figueira WF. 2020. "Review and meta-analysis of the importance of remotely sensed habitat structural complexity in marine ecology." Estuarine, Coastal and Shelf Science. 235:106468.

Rao CR. 1982. "Diversity and dissimilarity coefficients: A unified approach." Theoretical Population Biology. 21:24–43.

Raoult V, David PA, Dupont SF, Mathewson CP, O'Neill SJ, Powell NN, Williamson JE. 2016. "GoProsTM as an underwater photogrammetry tool for citizen science." PeerJ. 4:1960.

Raoult V, Reid-Anderson S, Ferri A, Williamson JE. 2017. "How Reliable Is Structure from Motion (SfM) over Time and between Observers? A Case Study Using Coral Reef Bommies." Remote Sensing. 9.

ReefLifeSurvey [Internet]. 2021. [accessed 2020 Jan 1]. https://www.reeflifesurvey.com/methods/.

Riemann JC, Ndriantsoa SH, Rödel M-O, Glos. J. 2017. "Functional diversity in a fragmented landscape — Habitat alterations affect functional trait composition of frog assemblages in Madagascar." Global Ecology and Conservation. 10:173–183.

Rojas-Montiel B, Reyes-Bonilla H, Calderon-Aguilera LE, Ramirez-Ortiz G, Lopez-Perez A, Hernandez L, Fernandez Rivera-Melo FJ. 2020. "Echinoderm functional diversity does not correlate with protection level of marine protected areas in the Mexican Pacific." Biodiversity and Conservation. 29:1871-1896.

Sacristán-Soriano O, Turon X, Hill. M. 2020. "Microbiome structure of ecologically important bioeroding sponges (family Clionaidae): the role of host phylogeny and environmental plasticity." Coral Re. 39:1285–1298.

Sakamoto Y, Ishiguro M, Kitagawa G. 1986. "Akaike information criterion statistics."

Schulze FE, Shumway CA, Hofmann HA, Dobberfuhl AP. 1886. "Über den Bau und das System der Hexactinelliden", Abhandlungen der Königlichen Akademie der Wissenschaften zu Berlin (Physikalisch-Mathematisch Classe. Freshwater Biology. 52:1–97.

Smith RS, Johnston EL, Clark GF. 2014. "The Role of Habitat Complexity in Community Development Is Mediated by Resource Availability." PLoS ONE. 9:102920.

Soest V, M. RW, Boury-Esnault N, Vacelet J, Dohrmann M, Erpenbeck D, Voogd NJD, Santodomingo N, Vanhoorne B, Kelly M, et al. 2012. "Global Diversity of Sponges (Porifera)." PLoS ONE. 7:35105.

Stevenson A, Archer SK, Schultz JA, Dunham A, Marliave JB, Martone P, Harley CDG. 2020. "Warming and acidification threaten glass sponge *Aphrocallistes vastus* pumping and reef formation." Scientific Reports. 10:8176.

Stone RP, Conway KW, Csepp DJ, Barrie JV. 2014. "The boundary reefs : Glass sponge (Porifera: Hexactinellidae) reefs on the international border between Canada and the United States." In: Center Alaska Fisheries Science, editor.

Stronach JA, Webb AJ, Murty TS, Cretney WJ. 1993. "A three-dimensional numerical model of suspended sediment transport in Howe sound, British Columbia." Atmosphere-Ocean. 31:73–97.

Stuart-Smith RD, Bates AE, Lefcheck JS, Duffy JE, Baker SC, Thomson RJ, Stuart-Smith JF, Hill NA, Kininmonth SJ, Airoldi L, et al. 2013. "Integrating abundance and functional traits reveals new global hotspots of fish diversity." Nature. 501:539–42.

Sueiro MC, Bortolus A, Schwindt E, Telford MJ, Moroz LL, Halanych KM. 2011. "Habitat complexity and community composition: relationships between different ecosystem engineers and the associated macroinvertebrate assemblages." Helgoland Marine Research. 65:467–77.

Syvitski JPM, Macdonald RD. 1982. "Sediment character and provenance in a complex fjord; Howe Sound, British Columbia." Canadian Journal of Earth Sciences. 19:1025–44.

Tallis H, Levin PS, Ruckelshaus M, Lester SE, McLeod KL, Fluharty DL, Halpern BS. 2010. "The many faces of ecosystem-based management: Making the process work today in the real places." Marine Policy 34(2): 340-348

Telford MJ, Moroz LL, Halanych KM. 2016. "A sisterly dispute." Nature. 529:286–87.

Thomson RE. 1981. Oceanography of the British Columbia coast. Ottawa, ON, Canada: Canadian Government Publishing Centre.

Tian X, Wang Y. 2020. "Palaeontological and sedimentological characteristics of the Changhsingian (Late Permian) platform–margin sponge reef and intraplatform skeletal mound in NE Sichuan Basin, South China: their palaeoenvironmental implications." Carbonates and Evaporites. 36(9).

Tokeshi M, Arakaki S. 2012. "Habitat complexity in aquatic systems: fractals and beyond." Hydrobiologia. 685:27–47.

Tompkins-MacDonald GJ, Leys SP. 2008. "Glass sponges arrest pumping in response to sediment: implications for the physiology of the hexactinellid conduction system." Marine Biology. 154:973–84.

Vegan: Community ecology package. R-project.org. [accessed 2020c Dec 22]. https://CRAN.R-project.org/package=vegan.

Verdonschot RCM, Didderen K, Verdonschot PFM. 2012. "Importance of habitat structure as a determinant of the taxonomic and functional composition of lentic macroinvertebrate assemblages." Limnologica. 42:31–42.

Villar N, Siqueira T, Zipparro V, Farah F, Schmaedecke G, Hortenci L, Brocardo CR, Jordano P, Galetti M. 2020. "The cryptic regulation of diversity by functionally complementary large tropical forest herbivores." Journal of Ecology. 108:279–290.

Villéger S, Miranda JR, Hernández DF, Mouillot. D. 2010. "Contrasting changes in taxonomic vs. functional diversity of tropical fish communities after habitat degradation." Ecological Applications. 20:1512–1522.

Villéger S, Miranda JR, Hernandez DF, Mouillot D. 2012. "Low Functional β-Diversity Despite High Taxonomic β-Diversity among Tropical Estuarine Fish Communities." PLoS ONE. 7:40679.

Violle C, Navas M-L, Vile D, Kazakou E, Fortunel C, Hummel I, Garnier. E. 2007. "Let the concept of trait be functional!" Oikos. 116:882–892.

Walbridge S, Slocum N, Pobuda M, Wright DJ. 2018. "Unified Geomorphological Analysis Workflows with Benthic Terrain Modeler." Geosciences. 8(3):94.

Whitney F, Conway K, Thomson R, Barrie V, Krautter M, Mungov G. 2005. "Oceanographic habitat of sponge reefs on the Western Canadian Continental Shelf." Continental Shelf Research. 25:211–226.

Wörheide G, Dohrmann M, Erpenbeck D, Larroux C, Maldonado M, Voigt O, Borchiellini C, Lavrov DV. 2012. "Chapter One - Deep Phylogeny and Evolution of Sponges (Phylum Porifera)." In: Mikel A. Becerro, Maria J. Uriz, Manuel Maldonado and Xavier Turon, editor. Advances in Marine Biology.

Yahel G, Eerkes-Medrano DI, Leys SP. 2006. "Size independent selective filtration of ultraplankton by hexactinellid glass sponges." Aquatic Microbial Ecology. 45:181–94.

Yahel G, Whitney F, Reiswig HM, Eerkes-Medrano DI, Leys SP. 2007. "In situ feeding and metabolism of glass sponges (Hexactinellida, Porifera) studied in a deep temperate fjord with a remotely operated submersible." Limnology and Oceanography. 52:428–40.

Zobel M. 1997. "The relative of species pools in determining plant species richness: an alternative explanation of species coexistence?" Trends in Ecology & Evolution. 12:266–269.

Appendix 1

Table S.1.1. Functional Traits Assignment. Traits were assigned to taxonomic groups based on dietary preference. Filter feeders, those animals that trap food particles or prey from the ambient water, were considered sessile organisms such as sponges and anemones. Detritivores were organisms, such as crabs and shrimp, which feed primary on detritus. Planktivores were animals that feed on plankton (phytoplankton and zooplankton). Zooplanktivores were animals who feed primarily on zooplankton in the water column. Piscivores were organisms which prey on fish. Benthivores were animals that feed on benthic prey. These animals could eat crustaceans or soft bodied invertebrates, such as seastars. Crustaceavores were animals who feed primarily on crustaceans, such as crabs and shrimp. We also included habitat use traits as a proxy for where the animals were commonly found on a glass sponge reef. For instance, schooling organisms, including shiner perch (*Cymatogaster aggregata*), were often seen swimming in schools over reef plots. Strictly benthic animals, such as squat lobsters (*Munida quadrispina*) were found on the reef building sponges. Benthopelagic animals were often found near the bottom of the reef but could also swim above it. Rockfishes and lingcod (Ophiodon elongatus) were classified as benthopelagic organisms. Lastly, crevice-dwelling organisms were those found inside and in between reef sponge oscula and mittens or at the bases of reef glass sponges. Information and data on the functional traits of taxonomic groups present in this study was derived from online resources and books, including http://www.fishbase.org and Lamb and Hanby (2005). Since we did not distinguish various life-stages of our observed species, nor did we collect any size measurements of the animals, no ontogenetic changes in traits were not included in the analysis. Traits were assigned to animals under the assumption that all observed animals were in their adult life stage.

Taxonomic Group/Trait	Filter feeder	Detritivore	Planktivore	Zooplanktivore	Piscivore	Benthivore	Spongivore	Crustaceavore	Schooling	Benthic	Bentho-pelagic	Crevice dwelling
Platichthys.stellatus	0	0	1	1	1	1	0	1	0	1	0	0
Cymatogaster.aggregata	0	0	1	1	0	1	0	1	1	0	1	0
Ophiodon.elongatus	0	0	0	0	1	1	0	1	0	0	1	1
Hexagrammos.decagrammus	0	0	0	0	1	1	0	1	0	0	1	0
Sebastes.ruberrimus	0	0	1	1	1	1	0	1	1	0	1	1
Sebastes.caurinus	0	0	0	1	1	0	0	0	0	0	1	1
Sebastes.emphaeus	0	0	1	1	0	1	0	0	1	0	1	1
Sebastes.flavidus	0	0	1	1	1	1	0	1	1	0	1	1

Species												
Sebastes.maliger	O	O	1	1	1	1	O	1	O	O	1	1
Ronquilus.jordani	O	O	1	1	O	1	O	1	O	1	O	1
Rhinogobiops.nicholsii	O	O	1	1	O	1	O	1	O	1	O	1
Munida.quadrispina	O	1	1	1	O	O	O	O	O	1	O	1
Pandalus.danae	O	1	O	O	O	1	O	1	O	1	O	O
Pandalus.platyceros	O	1	O	O	O	1	O	1	O	1	O	O
Pandalus.borealis	O	1	O	O	O	1	O	1	O	O	1	O
Chorilia.longipes	O	1	O	O	O	1	O	O	O	1	O	O
Heptacarpus.spp	O	1	O	O	O	1	O	O	O	1	O	O
Pagurus.spp	O	1	O	O	O	1	O	1	O	1	O	O
Eualus.spp	O	1	O	O	O	O	O	O	O	1	O	1
Caridea	O	1	O	O	O	O	O	O	O	1	O	1
Gammaridae	O	1	1	O	O	1	O	O	O	O	1	O
Oregonia.gracilis	O	1	O	O	O	1	O	O	O	1	O	O
Henricia.leviuscula	O	O	O	O	O	1	1	O	O	1	O	O
Styela.gibbsii	1	O	1	O	O	O	O	O	O	1	O	O
Orthasterias.koehleri	O	1	O	O	O	1	O	1	O	1	O	O
Mediaster.aequalis	O	1	O	O	O	1	1	O	O	1	O	O
Pteraster.tesselatus	O	O	O	O	O	1	1	O	O	1	O	O
Ceramaster.patagonicus	O	O	O	O	O	1	1	O	O	1	O	O
Cirolana.harfordi	O	1	O	O	O	1	O	O	O	1	O	O
Terebellida	1	1	1	1	O	1	O	O	O	1	O	O
Myxicola.infundibulum	1	O	1	O	O	O	O	O	O	1	O	1
Serpula.columbiana	1	O	1	O	O	O	O	O	O	1	O	1
Ophiopholis.aculeata	1	1	1	1	O	O	O	O	O	1	O	1
Parastichopus.californicus	O	1	O	O	O	1	O	O	O	1	O	O
Hydrozoa	1	O	1	O	O	O	O	O	O	1	O	O
Porifera	1	O	1	O	O	O	O	O	O	1	O	O
Demospongiae	1	O	1	O	O	O	O	O	O	1	O	O
Asbestopluma.occidentalis	1	O	1	O	O	O	O	O	O	1	O	O
Metridium.farcimen	1	O	1	1	O	O	O	O	O	1	O	O
Triopha.catalinae	O	O	O	O	O	1	O	O	O	1	O	O
Diaulula.sandiegensis	O	O	O	O	O	O	1	O	O	1	O	O

Table S.1.2. Species Counts. Abundances of species and other taxonomic groups at each of the survey sites 1 – 15.

Taxonomic Group/Plot #	1	2	3	4	5	6	7	8	9	10	11	12	13	14	15
Platichthys stellatus	0	0	0	0	0	0	0	0	0	0	0	0	1	0	0
Cymatogaster aggregata	0	0	0	0	0	0	0	0	0	0	3	0	5	20	0
Ophiodon elongatus	0	0	0	0	0	0	1	1	0	0	0	0	0	0	0
Hexagrammos decagrammus	0	0	0	0	1	0	0	0	0	0	0	0	0	0	0
Sebastes ruberrimus	0	0	0	0	0	0	0	0	0	0	0	1	0	0	0
Sebastes caurinus	0	0	0	0	0	0	0	0	0	0	0	1	0	0	0
Sebastes emphaeus	0	0	0	0	0	0	0	0	0	0	0	11	0	14	7
Sebastes flavidus	0	0	0	1	2	0	0	0	0	0	0	0	0	5	3
Sebastes maliger	2	0	0	5	2	1	0	1	0	0	0	4	0	3	3
Ronquilus jordani	0	1	0	0	0	1	0	0	0	0	0	0	0	0	0
Rhinogobiops nicholsii	0	0	0	0	0	2	0	0	2	3	2	0	0	0	1
Munida quadrispina	18	19	14	9	43	2	52	63	7	13	32	37	1	68	43
Pandalus danae	5	9	9	0	23	8	7	1	8	12	27	23	14	0	52
Pandalus platyceros	0	0	0	1	0	0	0	0	0	0	0	0	0	0	0
Pandalus borealis	0	0	0	0	5	0	0	0	0	0	0	0	0	1	9
Chorilia longipes	2	0	1	0	1	1	1	0	0	0	0	0	0	0	0
Heptacarpus spp.	0	1	0	0	0	0	0	0	0	3	0	0	0	0	0
Pagurus spp.	3	2	0	0	0	0	0	0	0	0	0	0	0	0	0
Eualus spp.	215	1	2	210	420	100	500	55	0	50	35	30	0	33	45
Caridea	0	0	0	0	0	1	0	0	0	0	0	0	0	0	0
Gammaridae	25	0	0	0	0	0	600	0	0	3	0	0	0	0	0
Oregonia gracilis	5	0	0	1	1	0	0	0	0	0	0	0	0	0	0
Henricia leviuscula	1	0	0	0	0	0	0	0	0	0	0	0	0	0	0
Styela gibbsii	0	0	1	0	0	0	0	0	3	2	0	0	1	0	0
Orthasterias koehleri	0	0	1	0	0	0	0	0	0	0	0	0	0	0	0
Mediaster aequalis	0	0	0	0	0	0	0	0	0	0	0	2	0	1	0
Pteraster tesselatus	0	0	0	2	1	0	0	0	0	0	0	0	0	0	0
Ceramaster patagonicus	0	0	0	0	1	0	0	0	0	0	0	0	0	0	0
Cirolana harfordi	0	0	0	0	2	1	0	0	0	0	0	0	0	0	0
Terebellida	0	2	0	0	2	0	2	4	4	3	1	2	0	0	0
Myxicola infundibulum	0	0	0	0	0	3	1	0	7	4	0	0	10	0	0
Serpula columbiana	0	0	0	0	0	0	0	0	0	0	0	0	4	0	0
Ophiopholis aculeata	0	0	2	0	0	0	0	0	6	1	0	1	0	2	1
Parastichopus californicus	0	0	1	0	0	0	0	0	0	0	0	0	1	1	2
Hydrozoa	0	0	1	0	0	0	0	0	0	0	0	0	0	0	0
Porifera	0	1	1	1	1	0	2	2	0	3	0	0	0	0	0
Demospongiae	0	1	0	0	0	0	0	0	0	0	0	0	0	0	0

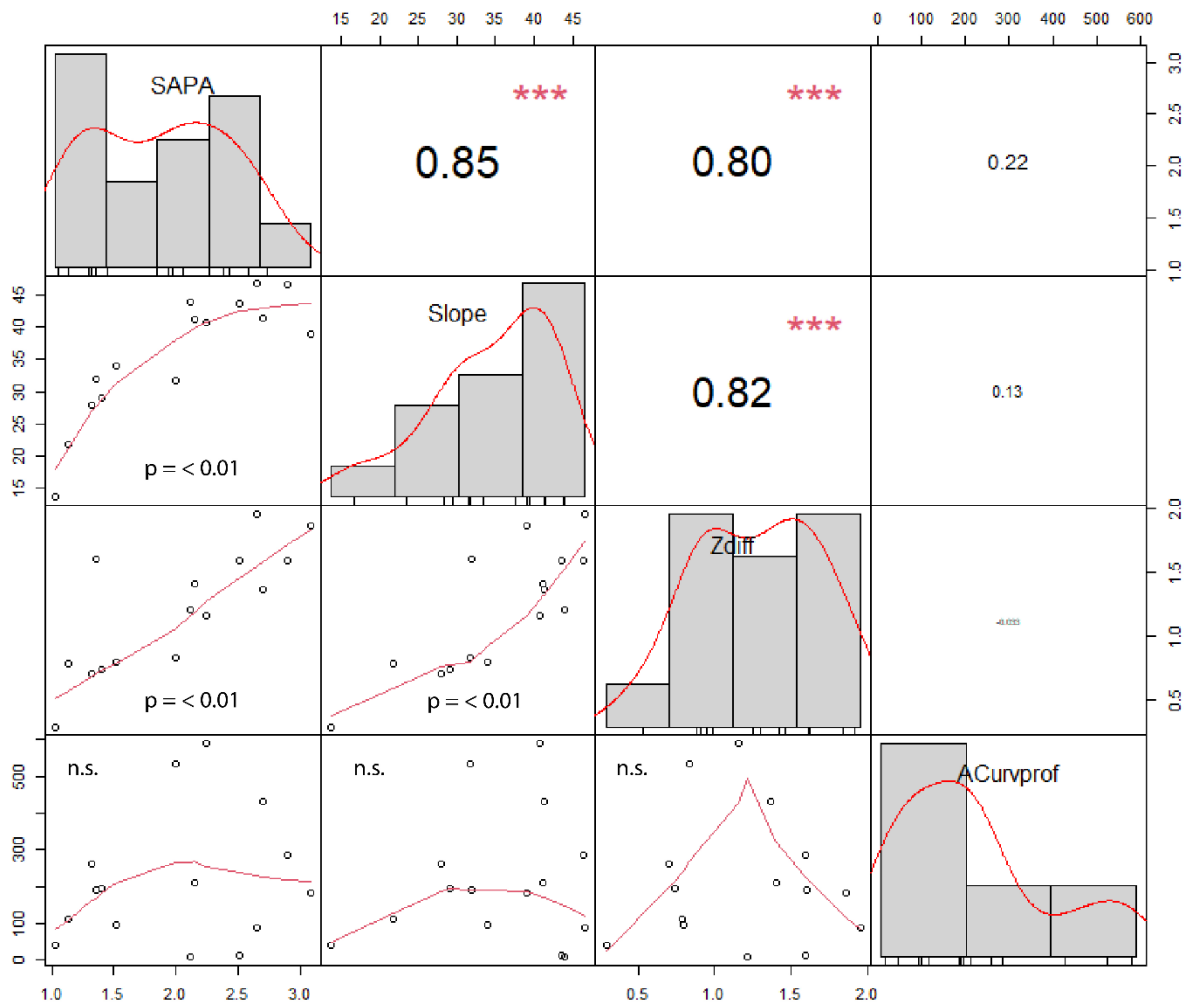|															
Asbestopluma occidentalis	0	1	0	0	3	0	0	0	0	0	0	0	0	0	0
Metridium farcimen	0	0	0	0	0	0	0	0	2	0	0	0	0	0	0
Triopha catalinae	0	0	0	0	0	0	0	0	0	0	0	0	2	0	0
Diaulula sandiegensis	0	0	0	0	0	0	0	0	0	0	1	0	0	0	0

Figure S.1.1. 3D Metric Correlation Matrix. Surface complexity (SAPA), slope (Slope), relief (Zdiff), and curvature (ACurvprof) were assessed for correlation. Scatterplots show the correlations between each pair of metrics. n.s. indicates a non-significant relationship. Histograms display the distribution of values of each of the four metrics from the 15 survey sites. Numbers in the top and right panels represent the r^2 values of each correlation and the number of red stars indicates the significance. While surface complexity had a strong correlation with slope and relief, the variance inflation factors (VIF) for surface complexity, slope, and relief were all less than 5 which indicated that the collinearity among these three predictors in our regression models was minimal and did not warrant further investigation.